

**EFFECTS OF IRRIGATION AND NITROGEN ADDITION ON THE
COMPONENTS OF NET ECOSYSTEM CARBON BALANCE IN
NEW ZEALAND GRAZED GRASSLANDS**

THESIS

Submitted in partial fulfilment of the requirements
for the degree of Doctor of Philosophy in Ecology
at the University of Canterbury

by

Gabriel Moinet

2016

A mes grands-pères, René Hédin et Philippe Moinet.

ACKNOWLEDGEMENTS

I would like to thank my advisors, David Whitehead from Landcare Research and Matthew Turnbull from University of Canterbury, who invited me to New Zealand and offered their time to guide me through this PhD project. David followed my progress closely and offered his mentorship and friendship. I am very grateful to him. I also thank Ellen Cieraad, who was made an official part of the supervisory team for the numerous hours she gave to support and advise me. Ellen took on the tedious task of teaching me what I needed to know about statistical analysis.

I would also like to thank Landcare Research for hosting me during the last three years. I am particularly thankful to John Hunt, Graeme Rogers and Anitra Fraser, who offered valuable technical expertise and mountains of funny and interesting information about New Zealand, as well as Pete Millard, who offered his expertise and advice in the use of stable isotopes of carbon. I also thank Matti Barthel, Sam Murray and Anna Zakharova who helped in the early stages of my project before leaving Landcare Research.

I am also grateful to Denis Curtin, Weiwen Qiu and Chris Dunlop, from Plant and Food Research, for hosting me in their laboratory and helping me with soil measurements and interpretation. For help with field and laboratory measurements, I also thank Benoit and Mary Gambier, Benoit Wagler, Jeanne Louis and Horacio Bown.

I want to thank my dearest friends in New Zealand, who gave their support when needed and took me through the difficult times. Thank you Marjon, and thank you Mariona, Marta, Javi, Carla, Camille, Ursula, Audrey, Mica, Sam, Damia, Bruno, Simon, Kooki, Maud and all the others who made my life in New Zealand so enjoyable.

Most importantly, I thank my family, especially my parents, Véronique and Laurent, who patiently helped me making the right decisions and pushed me to keep going in my studies, and my grand-parents, Odile and René, without whose moral and financial support none of this would have been possible. The last three years were marked by the loss of my two-grand-fathers, Philippe and

René, who both gave all they had to bring up and cherish the wonderful and loving members of this family. My kindest thoughts go to my grand-mothers, Odile and Josette, and to Max, and all the others. For their love, I am infinitely grateful to each one of them.

TABLE OF CONTENTS

LIST OF TABLES	ix
LIST OF FIGURES.....	xi
LIST OF ABBREVIATIONS.....	xv
ABSTRACT.....	xviii
CHAPTER 1 Introduction	1
1.1 Terrestrial ecosystems and global change.....	2
1.2 The terrestrial carbon cycle	3
1.3 The New Zealand context	5
1.4 Thesis objectives	6
1.5 Study sites	7
1.6 Thesis outline	9
1.7 Thesis contribution	11
CHAPTER 2 Addition of nitrogen fertiliser increases net ecosystem carbon dioxide uptake and the loss of soil organic carbon in grassland growing in mesocosms	12
2.1 Introduction	13
2.2 Materials and methods.....	16
2.2.1 Preparation of the mesocosms	16
2.2.2 Measurements of net ecosystem carbon dioxide exchange and soil respiration	18
2.2.3 Partitioning soil respiration.....	19
2.2.4 Experimental design.....	20

2.2.5	Statistical analyses	21
2.3	Results.....	23
2.3.1	Soil temperature and soil water content.....	23
2.3.2	Soil, root and leaf properties	23
2.3.3	Net ecosystem carbon dioxide exchange and light use efficiency	25
2.4	Ecosystem respiration and soil respiration.....	26
2.5	Partitioning soil respiration using the natural abundance $\delta^{13}\text{C}$ technique.....	30
2.5.1	Root exclusion technique and method comparison	30
2.6	Discussion.....	31
2.6.1	Net ecosystem CO_2 exchange	32
2.6.2	Components of soil respiration.....	33
2.7	Conclusions	35
CHAPTER 3 Phytomass index improves estimates of net ecosystem carbon dioxide exchange in intensively grazed grassland.....		36
3.1	Introduction	37
3.2	Materials and methods.....	38
3.2.1	Site description	38
3.2.2	Measurements of carbon dioxide exchange.....	39
3.2.3	Experimental design.....	40
3.2.4	Phytomass index	41
3.3	Results.....	45
3.3.1	Growing conditions and seasonal variations	45

3.3.2	Effect of simulated grazing on F_N and phytomass index.....	45
3.3.3	Model performances.....	47
3.3.4	Cumulative net ecosystem CO_2 exchange and net ecosystem carbon balance.....	53
3.4	Discussion.....	55
3.4.1	Phytomass index and components of net ecosystem CO_2 exchange	56
3.4.2	Grazing effects on the net ecosystem CO_2 exchange	57
3.5	Conclusions	58
CHAPTER 4 Soil heterotrophic respiration is insensitive to changes in soil water content but related to microbial access to organic matter		59
4.1	Introduction	60
4.2	Materials and methods.....	63
4.2.1	Site description	63
4.2.2	Experimental design.....	64
4.2.3	Natural abundance carbon isotope technique	65
4.2.4	Measurements of $\delta^{13}CR_S$	65
4.2.5	Measurements of $\delta^{13}CR_H$ and $\delta^{13}CR_A$	67
4.2.6	Soil analyses	68
4.2.7	Statistical analyses	69
4.3	Results.....	71
4.3.1	Climate and control plots during the two campaigns.....	71
4.3.2	Differences between the treatments	71
4.3.3	Environmental and soil property drivers of respiration rates	78

4.4	Discussion.....	80
4.4.1	Contribution of R_H to R_S	81
4.4.2	Response to nitrogen addition.....	81
4.4.3	Response to irrigation.....	82
4.4.4	Drivers of heterotrophic respiration, R_H	82
4.4.5	Drivers of autotrophic respiration, R_A	84
4.5	Conclusions	85
CHAPTER 5 Effects of irrigation and addition of nitrogen fertiliser on net ecosystem carbon		
balance in a New Zealand grazed grassland		
87		
5.1	Introduction	88
5.2	Materials and methods.....	90
5.2.1	Site description	90
5.2.2	Experimental design.....	90
5.2.3	Measurements of CO_2 exchange and biomass	92
5.2.4	Responses of CO_2 exchange to environmental variables.....	93
5.2.5	Phytomass index	94
5.2.6	Statistical analyses	95
5.3	Results.....	97
5.3.1	Growing conditions.....	97
5.3.2	Seasonal measurements of the components of ecosystem CO_2 exchange.....	97
5.3.3	Cumulative biomass and canopy nitrogen content	102
5.3.4	Models of net ecosystem CO_2 exchange and its components.....	103

5.3.5	Cumulative F_N and annual estimates of the components of carbon balance.....	105
5.4	Discussion.....	108
5.4.1	Effects of irrigation and nitrogen on seasonal measurements.....	109
5.4.2	Annual estimates and net ecosystem carbon balance	111
5.4.3	Implications for changes to soil carbon stocks	112
CHAPTER 6	General discussion	115
6.1	General results.....	116
6.2	Drivers of carbon balance components.....	117
6.2.1	Ecosystem carbon uptake	117
6.2.2	Soil organic matter decomposition, R_H	118
6.3	Soil carbon stocks under intensive management.....	119
6.4	Conclusions and future research	121
REFERENCES	124
APPENDIX A	Back extrapolation approach to estimate $\delta^{13}C_{R_H}$.....	138

LIST OF TABLES

Table 2.1: Soil and root carbon and nitrogen concentrations and C:N ratios at the end of the experiment for the low, N_0 , and high nitrogen, N_1 , treatments. All values shown are mean \pm standard error.	24
Table 2.2: Leaf nitrogen concentration and specific leaf area at different times throughout the measurement period when the grass was clipped. The mention 'NA' indicates non available data. All values shown are mean \pm standards error.	24
Table 2.3: Estimated values of the parameters of modelled net ecosystem CO_2 exchange, F_N (a , b and c), and light use efficiency, α (p and q) for the low (N_0) and high nitrogen (N_1) treatments, after concurrent addition of nitrogen and clipping, clipping alone and addition of nitrogen alone. Values of parameters centred are not significantly different between the nitrogen treatments. All values shown are mean \pm standards error.	27
Table 2.4: Carbon isotopic signatures for air collected from soil respiration ($\delta^{13}CR_S$) incubation of root-free soil ($\delta^{13}CR_H$) and incubation of roots ($\delta^{13}CR_A$) and calculated values of the proportion of soil respiration resulting from heterotrophic respiration (fR_H) for the low (N_0) and high nitrogen (N_1) treatments. The asterisk indicates a significant difference in values between nitrogen treatments. All values shown are mean \pm standard error.	31
Table 3.1: Seasonal variations in the components of net ecosystem CO_2 exchange. Mean values of soil respiration (R_S), night time ecosystem respiration (R_E), and leaf respiration (R_L) calculated as the difference between hourly means of R_E and R_S are represented for the two measurement periods (spring and summer, 89 days, and late summer to early autumn, 62 days). Values are mean \pm standard errors.	46
Table 3.2: Summary results from the cross validations realised for models of ecosystem respiration (R_E), soil respiration (R_S), and leaf respiration (R_L) using the hold-out method. Root mean square errors (RMSE) and adjusted coefficient of determination (R^2) are given for values calculated on half the data set (testing set) using Equations 3.3 (R_E and R_S) and 3.4 (R_L), with no phytomass index, including calculated P_i and including modelled P_i'	47
Table 3.3: Cumulated net ecosystem CO_2 exchange (F_N) during the two measurement periods (spring and summer, and late summer to early autumn). Cumulative F_N values are calculated from hourly measured and modelled values of F_N . Estimates from the model not including the phytomass index (Equation 3.5), the model including modelled phytomass index (Equation 3.6) and the model including calculated phytomass index (Equation 3.7) are shown. Values shown are mean (\pm standard error, $n=4$) from the four clear top chambers for the measured values. For the modelled estimates, the upper and lower limits of 95% intervals from the Monte Carlo simulations (1 000 runs) are included.....	54

Table 4.1: Environmental variables during the campaigns in spring, one month after treatments started and in summer, six months after the treatments started. Soil temperature and soil volumetric water content were measured in the control, non-irrigated and non-fertilised plots. Only soil temperature measured at a depth of 50 mm is represented. The P-values are from Student *t*-tests comparing means between the two campaigns. Values for each campaign are means of half-hourly values recorded on each day when measurements for partitioning were made. All values shown are mean \pm standard error. 72

Table 4.2: Environmental variables for the spring campaign, one month after treatments started and the summer campaign, six months after treatments started. The variables shown are soil temperature measured at a depth of 50 mm (T_S), soil gravimetric water content (W_S), total carbon concentration (C_{tot}), total nitrogen concentration (N_{tot}), specific surface area (S_A), hot water extractable carbon (C_{HW}) dissolved organic carbon (C_D), macro-organic matter carbon (C_{MOM}), particulate organic matter carbon (C_{POM}). Also shown are isotopic signatures of CO_2 respired by the root-free soil ($\delta^{13}CR_H$), autotrophic component ($\delta^{13}CR_A$), and the soil ($\delta^{13}CR_S$), the proportion of heterotrophic respiration from soil respiration (fR_H), soil respiration (R_S), autotrophic respiration (R_A) and heterotrophic respiration (R_H). Values are means \pm standard error for *n* replicate measurements in each treatment: control (I_0N_0), non-irrigated fertilised (I_0N_1), irrigated non-fertilised (I_1N_0) and irrigated fertilised (I_1N_1). The P-values are the results of linear models testing for the effects of irrigation and nitrogen addition treatments and their interactions. When significant ($P < 0.05$) or marginally significant ($P < 0.1$), the significant term (Signif.) is represented by I for irrigation treatment, N for nitrogen treatment and I*N for the interaction. When the interaction is significant, letters represent homogeneous Tukey groups. 76

Table 4.3: Summary of selected best models fitted with environmental variables and soil properties to explain variations in soil respiration (R_S) autotrophic respiration, (R_A) and heterotrophic respiration (R_H). AICc is the Akaike's information criterion corrected for small sample size; $\Delta AICc = AICc - AICc_{min}$, where $AICc_{min}$ is the smallest AICc, representing the best model; A_w , Akaike's weight; cum. A_w , sum of A_w ; LogLik, Log likelihood ratio. 79

Table 5.1: Parameters for the models of soil respiration (R_S), leaf respiration (R_L) and gross canopy photosynthesis (A), including and not including the phytomass index (P_i). When significant ($P < 0.05$), different parameters are shown for the four treatments: non-irrigated with no nitrogen addition (I_0N_0), irrigated with no nitrogen addition (I_1N_0), non-irrigated with nitrogen addition (I_0N_1) and irrigated with nitrogen addition (I_1N_1). R_{10} is the respiration rate at a basal temperature of 10 °C, E_0 is the activation energy of the enzymatic reaction, g and f are the parameters describing the response of respiration to soil volumetric water content, α is the light use efficiency and A_{max} is the rate of gross photosynthesis under saturating irradiance. . 101

LIST OF FIGURES

Figure 1.1: Conceptual diagram depicting the ecosystem CO ₂ exchanges as well as transfers of carbon from leaves to roots to soil.....	5
Figure 1.2: High stock numbers and the pivot irrigator at Beacon Farm	8
Figure 1.3: The experimental set up at Ashely Dene Farm.....	9
Figure 2.1: Cumulative leaf dry mass with time throughout the experiment for the low (N ₀) and high (N ₁) nitrogen treatments. The vertical bars show standard errors of the mean.....	25
Figure 2.2: Net ecosystem CO ₂ exchange (F _N) and light use efficiency (α) modelled as a function of number of days after (A) clipping and addition of nitrogen, (B) clipping only and (C) addition of nitrogen only for the low (N ₀) and high (N ₁) nitrogen treatments. The vertical bars show standard errors of the mean. A single solid line is used when the model does not differ significantly between the nitrogen treatments.....	28
Figure 2.3: Soil respiration (R _S) and ecosystem respiration (R _E) modelled as a function of number of days after (A) concurrent clipping and addition of nitrogen, (B) clipping alone and (C) addition of nitrogen alone, for the low (N ₀) and high nitrogen (N ₁) treatments. The vertical bars show standard errors of the mean. A single solid line is used when the model does not differ significantly between nitrogen treatments.	29
Figure 2.4: Rates of soil heterotrophic respiration (R _H) on day 7 after concurrent clipping and addition of nitrogen using two partitioning techniques, for the low (N ₀) and high (N ₁) nitrogen treatments. The vertical bars represent standard errors of the mean. The asterisk indicates a significant difference in values between nitrogen treatments.....	31
Figure 3.1: Variations in environmental variables at the Beacon Farm site for the two measurement periods (spring and early summer, and late summer to early autumn): (A and A') daily mean of soil temperature (T _S) at 100 mm depth (black line) and air temperature (T _a , grey line); (B and B') daily mean soil volumetric water content at 100 cm depth (θ _S); (C and C') daily total irradiance (Q) and (D and D') hourly values of F _N for each of the four clear chambers (grey points) and daily mean (black line). The vertical dashed lines show the timings of simulated grazing events.	44
Figure 3.2: Calculated (P _i , grey symbols) and modelled (P _i ', black symbols) phytomass index for the site at Beacon Farm for the first measurement period (A, spring and early summer) and the second period (A', late summer to early autumn) and; (B) cross-validation for the model for the phytomass index. Parameters were derived from the model fitted on half the data set (training set) and the model cross-validation shown in (B) was performed on the other half (testing set)	

consisting of alternate days. The vertical dashed lines show the timings of simulated grazing events..... 49

Figure 3.3: Response of: (A) leaf respiration (R_L) to air temperature (T_a), (B) soil respiration (R_S) to soil temperature (T_s), and (C) ecosystem respiration (R_E) to T_s . The symbols are hourly values of: (A) calculated R_L from the difference between hourly means of R_E and R_S , (B) the three dark chambers at night and day for R_S and (C) the four clear chambers at night for R_E . All data points are coloured according to the calculated phytomass index (P_i)..... 50

Figure 3.4: (A) Light response of measured day time gross photosynthesis (A_{meas}) to photosynthetically active radiation (Q), and hold-out cross validation of models fit with (B) standard light response model (Equation 3.2); (C) light response model including the calculated phytomass index (Equation 3.2 including P_i) and; (D) light response model including the modelled phytomass index (Equation 3.2 including P_i'). Model parameters were derived from models fitted on half the data set (training set) and the model cross-validations shown in (B), (C) and (D) were performed on the other half (testing set) consisting of alternate hours. The data are classified in relation to P_i as shown by the colours. 51

Figure 3.5: Cross-validations of models using the hold-out method for net ecosystem CO_2 exchange (F_N) fitted with the combination of models for soil respiration, leaf respiration and net photosynthesis: (A) without the phytomass index (Equation 3.5), (B) incorporating the calculated phytomass index (P_i , Equation 3.6) and (C) incorporating the modelled phytomass index (P_i' , Equation 3.7). The parameters were derived from models fitted on half the data set (training set) and the model cross-validations shown were performed on the other half (testing set) consisting of alternate hours. The data for F_N are classified in relation to P_i as shown by the colours..... 52

Figure 3.6: Cumulative net ecosystem CO_2 exchange (F_N) for the two measurement periods in spring and early summer (left panel), and late summer to early autumn (right panel) at the Beacon Farm site. Black lines represent measured values of F_N (mean of the four clear chambers). The green, pink and orange lines represent modelled values of F_N without the phytomass index (Equation 3.5), incorporating the calculated phytomass index (P_i , Equation 3.6), and incorporating the modelled phytomass index (P_i' , Equation 3.7), respectively. 55

Figure 4.1: Rates of (A) soil respiration, R_S , (B) autotrophic respiration, R_A , and (C) heterotrophic respiration, R_H , for the control, I_0N_0 , non-irrigated fertilised, I_0N_1 , irrigated non-fertilised, I_1N_0 , and irrigated fertilised, I_1N_1 treatment for the spring campaign, one month after treatments started and the summer campaign, six months after the treatments started. The letters represent significant differences between irrigation treatments. The vertical bars indicate standard errors of the mean..... 73

Figure 4.2: Relationship between rates of soil respiration (R_S) and (A) autotrophic respiration (R_A) and (B) heterotrophic respiration (R_H) combined for both measurement campaigns. The solid line represent a significant relationship ($P < 0.0001$) and the dashed line a non-significant relationship ($P = 0.2$)..... 75

Figure 4.3: Rates of (A) soil respiration (R_S), (B) autotrophic respiration (R_A), and (C) heterotrophic respiration (R_H) in response to soil gravimetric water content (W_S). The lines are linear relationships fitted to the data with a solid line representing a significant relationship ($P < 0.0001$) and the dashed line a non-significant relationship ($P = 0.7$). Open and closed symbols represent replicates measurements for the irrigated and non-irrigated plots, respectively..... 80

Figure 5.1: Changes in daily mean environmental variables for the measurement period from October 2014 to September 2015. (A) Air temperature (T_a , dashed grey line), and soil temperature (T_s) for the irrigated plots (treatment I_1 , continuous grey line) and the non-irrigated treatment (I_0 , continuous black line). (B) Soil volumetric water content (θ_s) for the treatments I_1 (grey line) and I_0 (black line). (C) Photosynthetically active irradiance (Q). 99

Figure 5.2: Variations in seasonal measurements of (A) net ecosystem CO_2 exchange (F_N), (B) ecosystem respiration (R_E) and (C) soil respiration (R_S) for the four treatments: non-irrigated with no nitrogen addition (I_0N_0 , filled squares), irrigated with no nitrogen addition (I_1N_0 , open squares), non-irrigated with nitrogen addition (I_0N_1 , filled triangles) and irrigated with nitrogen addition (I_1N_1 , open triangles). The vertical bars represent standard error of the mean ($n = 6$). 100

Figure 5.3: Cumulative (A) leaf dry mass and (B) canopy nitrogen content for the four treatments: : non-irrigated with no nitrogen addition (I_0N_0 , filled squares), irrigated with no nitrogen addition (I_1N_0 , open squares), non-irrigated with nitrogen addition (I_0N_1 , filled triangles) and irrigated with nitrogen addition (I_1N_1 , open triangles). The vertical bars represent standard error of the mean ($n = 6$). 104

Figure 5.4: Cross-validations, using the hold-out method, of models for net ecosystem CO_2 exchange (F_N) (A) not including the phytomass index, and (B) and including the phytomass index. Model parameters were derived from models fitted using half the data set (training set) and the model cross-validations shown were performed on the other half (testing set). R^2 is the coefficient of determination, RMSE is the root mean square error, and $F_{N\text{ meas}}$ and $F_N\text{ model}$ are measured and modelled F_N , respectively. 105

Figure 5.5: Cumulative net ecosystem CO_2 exchange (F_N) for the measurement period from October 2014 to September 2015, for the four treatments: non-irrigated with no nitrogen addition (I_0N_0 , continuous black line), irrigated with no nitrogen addition (I_1N_0 , dashed black line), non-irrigated with added nitrogen (I_0N_1 , continuous grey line) and irrigated with added nitrogen (I_1N_1 , dashed grey line)..... 107

Figure 5.6: Annual estimates of gross canopy photosynthesis (A, white bars), soil respiration (R_S , black bars), leaf respiration (R_L , dark-grey bars) and biomass exported via grazing (F_{export} , light-grey bars), for the four treatments: non-irrigated with no nitrogen addition (I_0N_0), irrigated with no nitrogen addition (I_1N_0), non-irrigated with added nitrogen (I_0N_1) and irrigated with nitrogen addition (I_1N_1). Vertical bars indicate uncertainties calculated as 95% confidence intervals of 1000 Monte Carlo simulations..... 107

Figure 5.7: Annual estimates of net ecosystem carbon balance (N_b) for the four treatments: non-irrigated with no nitrogen addition (I_0N_0), irrigated with no nitrogen addition (I_1N_0), non-irrigated with nitrogen addition (I_0N_1) and irrigated with nitrogen addition (I_1N_1). Vertical bars indicate uncertainties calculated as 95% confidence intervals of 1000 Monte Carlo simulations. 108

Figure A: Isotopic signature of respired CO_2 from root-free soil, $\delta^{13}CR_H$, in response to time for root-free soils incubated at 4, 7.5 and 10 min and at 5, 7.5 and 10 min. The vertical bars indicate standard errors of the mean. 140

LIST OF ABBREVIATIONS

α	light use efficiency
$\delta^{13}\text{C}$	^{13}C isotopic signature
$\delta^{13}\text{C}_{\text{R}_A}$	^{13}C isotopic signature of the CO_2 emitted from soil autotrophic respiration
$\delta^{13}\text{C}_{\text{R}_H}$	^{13}C isotopic signature of the CO_2 emitted from soil heterotrophic respiration
$\delta^{13}\text{C}_{\text{R}_S}$	^{13}C isotopic signature of the CO_2 emitted from soil respiration
θ_s	soil volumetric water content
a	parameter for the exponential decay function of F_N with time after grazing: steady-state value
A	gross canopy photosynthesis
A_{max}	rate of gross photosynthesis under saturating irradiance
b	parameter for the exponential decay function of F_N with time after grazing: defines the initial value.
c	parameter for the exponential decay function of F_N with time after grazing: defines the shape of the curve
C_D	dissolved organic carbon
C_{HW}	hot water extractable carbon
C_{MOM}	macro-organic matter carbon
C_{POM}	particulate organic matter carbon
C_{tot}	total carbon concentration
E_0	parameter related to the activation energy of enzymatic reactions
f	parameter for the Gompertz function defining the response of respiration to water content
fR_H	proportion of soil respiration contributed by heterotrophic respiration

fR_A	proportion of soil respiration contributed by autotrophic respiration
F_N	net ecosystem CO ₂ exchange
g	parameter for the Gompertz function defining the response of respiration to water content
G_{DC}	cumulative growing degree day
G_{DC95}	parameter for the asymptotic exponential function of P_i with G_{DC} after grazing: value of G_{DC} when P_i equals 95 % of P_{imax}
G_{DCmax}	parameter for the asymptotic exponential function of P_i with G_{DC} after grazing: value of G_{DC} when P_i equals P_{imax}
I_0	control irrigation treatment
I_1	irrigation treatment
n_{95}	time to reach 95% of the changes in exponential functions of F_N and α after grazing
N_0	control addition of nitrogen fertiliser treatment
N_1	addition of nitrogen fertiliser treatment
N_B	net ecosystem carbon balance
N_{tot}	total nitrogen concentration
p	parameter for the asymptotic exponential function of α with time after grazing: defines the initial value
P_i	phytomass index
P_{imax}	values of the phytomass index on the last day before grazing
q	parameter for the asymptotic exponential function of α with time after grazing: defines the shape of the curve
Q	irradiance
Q_C	cumulative irradiance
R_{10}	respiration rate at a basal temperature of 10 °C
R_A	soil autotrophic respiration

R_E	ecosystem respiration
R_L	leaf respiration
R_H	soil heterotrophic respiration
R_S	soil respiration
S_A	soil specific surface area
S_θ	water stress integral
T_a	air temperature
T_s	soil temperature
W_s	soil gravimetric water content
z	parameter for the asymptotic exponential function of P_i with G_{DC} after grazing: defines the shape of the curve

ABSTRACT

There is growing evidence that continued emissions of greenhouse gases from anthropogenic activities associated with climate warming are responsible for widespread, severe and irreversible impacts leading to insecurity of food supply to support the needs of increasing population growth. Improved use of agricultural land and management practices can result in increased soil carbon sequestration and are critically important to maintain productivity and mitigate the effects of anthropogenic carbon dioxide emissions. Globally, there is a trend towards intensification of grassland systems to increase agricultural productivity. While this ensures increased pasture growth, and supports higher number of grazing animals per unit area, the impacts on ecosystem carbon dynamics remain largely unknown. This is of particular importance in New Zealand, where grasslands occupy large areas and where there is rapid and widespread expansion of intensification using irrigation and nitrogen fertilisers to convert traditional extensively grazed sheep and beef pastoral systems to dairy farming. The research in this thesis investigates the following question: *Will the conversion to intensive dairy farm management result in soil carbon sequestration in New Zealand managed grasslands?*

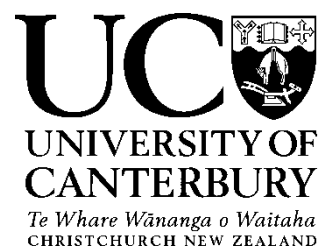
The ability to quantify and predict the impacts of changing management practices on soil carbon stocks and their potential feedbacks on atmospheric CO₂ concentration largely depends on our ability to understand the mechanisms regulating changes in the components of the net ecosystem carbon balance: gross photosynthesis, ecosystem respiration, and the autotrophic and heterotrophic components of soil respiration. To investigate the impacts of management practices on these components, I designed a series of laboratory and field experiments on shallow, stony soils in Canterbury, New Zealand, that are characteristic of sites where widespread conversion to dairy farming is occurring. The experimental treatments allowed measurement and modelling of the effects of irrigation, addition of nitrogen fertiliser and intensive grazing management. To account for variations in above-ground biomass through seasons and grazing cycles, I developed a phytomass

index and used this in models to interpret changes in the components of carbon balance. Changes in carbon dynamics under irrigation and nitrogen addition were dominated by above-ground processes and consistently resulted in increased net ecosystem productivity. Measuring the effects of the treatments during the first year after a simulated conversion of dryland to dairy farming, I showed net losses of carbon from the ecosystem, ranging from $284 \text{ gC m}^{-2} \text{ y}^{-1}$ to $540 \text{ gC m}^{-2} \text{ y}^{-1}$ across combinations of irrigation and nitrogen addition treatments, although uncertainties were large, so that differences were not significant. From the findings, I hypothesise that losses of carbon from the grassland soil at this study site will continue to exceed ecosystem carbon inputs, despite increased above-ground productivity. To explore this further, I adopted and improved techniques using stable isotopes of carbon to measure rates of soil organic matter decomposition in the field, while avoiding disturbance to the soil environment. The findings showed no effects of irrigation and addition of nitrogen fertiliser on the rates of soil organic matter decomposition. I used indices of soil physical protection of organic matter to interpret differences in the rates of decomposition and provided direct evidence to support the emerging theory that soil organic matter decomposition is predominantly regulated by microbial access to the carbon substrate.

From earlier studies on long-term changes in soil carbon stocks and the new insights from my research, I conclude that there is no evidence that conversion to intensive dairy farming on shallow, stony soils in New Zealand leads to beneficial effects for soil carbon stocks. The effects are likely to depend on soil type and management practices that determine the level of organic matter protection and its stability and more research is needed to identify mechanistic linkages between soil organic matter dynamics and soil structure.

The new insights from my findings have important implications for our ability to model and predict future changes in carbon stocks for grasslands globally, in relation to changing climate and management practices.

Deputy Vice-Chancellor's Office
Postgraduate Office



Co-Authorship Form

This form is to accompany the submission of any thesis that contains research reported in co-authored work that has been published, accepted for publication, or submitted for publication. A copy of this form should be included for each co-authored work that is included in the thesis. Completed forms should be included at the front (after the thesis abstract) of each copy of the thesis submitted for examination and library deposit.

Please indicate the chapter/section/pages of this thesis that are extracted from co-authored work and provide details of the publication or submission from the extract comes:

Chapter 2: published in *Geoderma*.

Chapter 3: Under review in *Agriculture, Ecosystems & Environment*.

Chapter 4: In press in *Geoderma*.

Chapter 5: Under review in *Agriculture, Ecosystems & Environment*.

Please detail the nature and extent (%) of contribution by the candidate:

Chapter 2 (90% contribution)

Authors: Gabriel Y. K. Moinet, Ellen Cieraad, Graeme N. D. Rogers^a, John E. Hunt, Peter Millard, Matthew H. Turnbull, David Whitehead.

GYKM co-designed the experiment with MHT, JEH and DW, collected and analysed the data and wrote the manuscript. EC was critical in the data analysis and provided reviews for the drafts. DW and MH critically reviewed all drafts. GNR helped with experimental set up and instrumentation. PM was indispensable in interpreting and presenting the results.

Chapter 3 (90% contribution)

Authors: Gabriel Y. K. Moinet, Ellen Cieraad, John E. Hunt, Matthew H. Turnbull, David Whitehead
GYKM co-designed the experiment with DW, JEH and MHT, collected and analysed the data and wrote the manuscript. DW, EC and MH reviewed all drafts. JEH helped with field measurements and instrumentation. EC helped with data analysis.

Chapter 4 (90% contribution)

Authors: Gabriel Y. K. Moinet, Ellen Cieraad, John E. Hunt, Anitra Fraser, Matthew H. Turnbull, David Whitehead
GYKM co-designed the experiment with DW, EC and MHT, collected and analysed the data and wrote the manuscript. DW, EC and MH reviewed all drafts. JEH and AF helped with field measurements and instrumentation. EC helped with data analysis.

Chapter 5 (90% contribution)

Authors: Gabriel Y. K. Moinet, Ellen Cieraad, Matthew H. Turnbull, David Whitehead
GYKM co-designed the experiment with DW, EC and MHT, collected and analysed the data and wrote the manuscript. DW, EC and MH reviewed all drafts.

Certification by Co-authors:

If there is more than one co-author then a single co-author can sign on behalf of all

The undersigned certifies that:

- The above statement correctly reflects the nature and extent of the PhD candidate's contribution to this co-authored work
- In cases where the candidate was the lead author of the co-authored work he or she wrote the text

Name: *Professor Matthew Turnbull*



Signature:

Date: *6/4/16*

CHAPTER 1 Introduction

1.1 Terrestrial ecosystems and global change

Climate change is one of the greatest global issues of the 21st century. Anthropogenic emissions of greenhouse gases have grown since pre-industrial times, increasing by 80% between 1970 and 2010, with an acceleration in the last decade to reach 8.7 Pg C y⁻¹ in 2010 (IPCC, 2014). Continued emissions of greenhouse gases are very likely to cause further warming and other severe, widespread and irreversible impacts globally, including species extinction and food insecurity (IPCC, 2014).

The terrestrial biosphere absorbs approximately one third of anthropogenic carbon emissions (Schimel et al., 2001) and is crucial for mitigating the increase of carbon dioxide (CO₂) concentration in the atmosphere (Pachauri et al., 2014). With an estimated 2 344 Pg C, soils are the second largest pool of carbon on Earth (after the oceans, 38 400 Pg C) (Jobbagy and Jackson, 2000). Small changes in this reservoir could release a large amount of carbon to the atmosphere compared with anthropogenic emissions (Rustad et al., 2000). Conversely, land management practices that result in soil carbon sequestration represent an opportunity to partly offset these emissions (Paustian et al., 1997; Lal, 2004; Stockmann et al., 2013). Agricultural lands represent over 15% of global carbon emissions, reaching 1.5 Pg C y⁻¹ in 2012 (FAOSTAT, 2012). Historically, soil carbon stocks in these systems have been depleted severely due to poor management (Lal, 2004, 2009). Part of this carbon can be regained, and the mitigation potential for carbon sequestration in agricultural soils (not accounting for the potential reduced losses) was estimated to be around 1.3 Pg C y⁻¹ by 2030 (Smith et al., 2013). Globally, grasslands are a central element of the carbon cycle. Grazed grasslands cover 26% of the earth's ice free land surface (Steinfeld et al., 2006) and contain about 12% of global soil organic carbon (Schlesinger, 1977). They represent 70% of agriculture lands (FAOSTAT 2012) and are estimated to account for up to 23% of the mitigation potential of total agriculture.

As well as addressing the issue of rising atmospheric CO₂ concentration, sequestering carbon in the soil can improve characteristics that support resilience and sustainability. Indeed, carbon constitutes 58% of soil organic matter (Stockmann et al., 2013), a key component involved in the

numerous terrestrial ecosystem services provided by soils. Lal (2009) summarised the benefits of soil organic matter in these terms: soil organic matter is necessary to maintain satisfactory soil structure, nutrient availability, biological activity, retention of water and support for biodiversity. It also decreases the risk of erosion, improves the use efficiency of inputs (nutrients, water) and increases ecosystem resilience. Particularly relevant in agricultural lands, soil organic matter enhances soil productive capacity, a necessary requisite to sustain food production on the long-term.

There is an urgent need to identify agricultural management practices that result in increased soil carbon sequestration as they represent an essential strategy in the context of global change to both significantly contribute to climate mitigation and to secure sustainable food production to tackle current and projected food insecurity.

1.2 The terrestrial carbon cycle

Terrestrial ecosystems may be sinks or sources of carbon to the atmosphere depending on the balance between carbon inputs (photosynthesis, imports of organic matter) and losses (ecosystem respiration, product exports, leaching) (Chapin et al., 2006; Paterson et al., 2009). The net ecosystem carbon balance (N_B) is defined as:

$$N_B = -F_N + F_{\text{import}} - F_{\text{export}} - F_{\text{leach}} - F_{\text{erosion}} \quad (1.1)$$

where F_N is the net ecosystem CO_2 exchange, F_{import} is the carbon imported in supplementary feed, animal excreta and manure, F_{export} is the carbon exported in harvested plant biomass for farm production, F_{leach} is the carbon lost via leaching through soil to groundwater and F_{erosion} is carbon lost or gained through erosion. Following the micrometeorological convention, a positive sign of N_B indicates a terrestrial sink of carbon and a positive sign of F_N indicates a terrestrial source of CO_2 .

For pastoral agriculture, the primary purpose of intensive grassland management is to maximise the exports through increased feed productivity to support number of grazing animals, with a direct effect on F_{export} and F_{import} . On the flat topography where most dairy farms occur in New Zealand, F_{erosion} can be considered negligible (Mudge et al., 2011). Furthermore, F_{leaching} is expected to be

reduced through enhancing organic carbon sequestration in the soil (Lal, 2009), so that overall, F_N appears to be the primary component of the carbon balance on which soil carbon sequestration depends.

The net ecosystem CO_2 exchange is the balance between CO_2 fluxes into the ecosystem (gross canopy photosynthesis, A , also referred to as gross primary production) and out of the ecosystem (ecosystem respiration, R_E). The input of carbon to terrestrial ecosystems is by photosynthesis and this removes approximately 120 Pg C y^{-1} from the atmosphere globally (Schlesinger, 1997). About two third of the carbon losses are derived from soil respiration (R_S), the rest being released by above-ground plant respiration, also referred to as leaf respiration (R_L) (Schlesinger and Andrews, 2000). Release of CO_2 from the soil (R_S) can be partitioned conceptually in varying number of sources (Kuzyakov, 2006). A common approach is to distinguish the CO_2 released from the soil as a consequence of root activity and their associated mycorrhizal fungi and rhizosphere microbes (autotrophic respiration, R_A) from CO_2 released from microbial degradation of soil organic matter (heterotrophic respiration, R_H). Thus, the net ecosystem CO_2 exchange is defined as:

$$F_N = R_L + R_A + R_H - A. \quad (1.2)$$

Partitioning soil respiration into its autotrophic and heterotrophic components is particularly important. The CO_2 released to the atmosphere as a consequence of R_A is derived from the rapid turnover of recently assimilated carbon and is believed to obscure the consequences of total soil respiration in soil carbon dynamics (Cheng and Kuzyakov, 2001). Only CO_2 derived from soil organic matter decay (R_H) contributes to changes in the long-term soil carbon profile and in atmospheric CO_2 concentrations (Kuzyakov, 2006). Therefore, the potential for soils to sequester carbon depends strongly on the relative responses of gross primary production and the components of ecosystem respiration, and particularly R_H , to environmental conditions and management practices (Grace and Rayment, 2000; Paterson et al., 2009).

The dynamics of the ecosystem carbon balance components under different environmental and management conditions are underpinned by complex and inter-related mechanisms. Further

detailed review of the current state of knowledge and formulation of hypotheses are presented in the body of the thesis in the introductions for the different chapters, as relevant to their content.

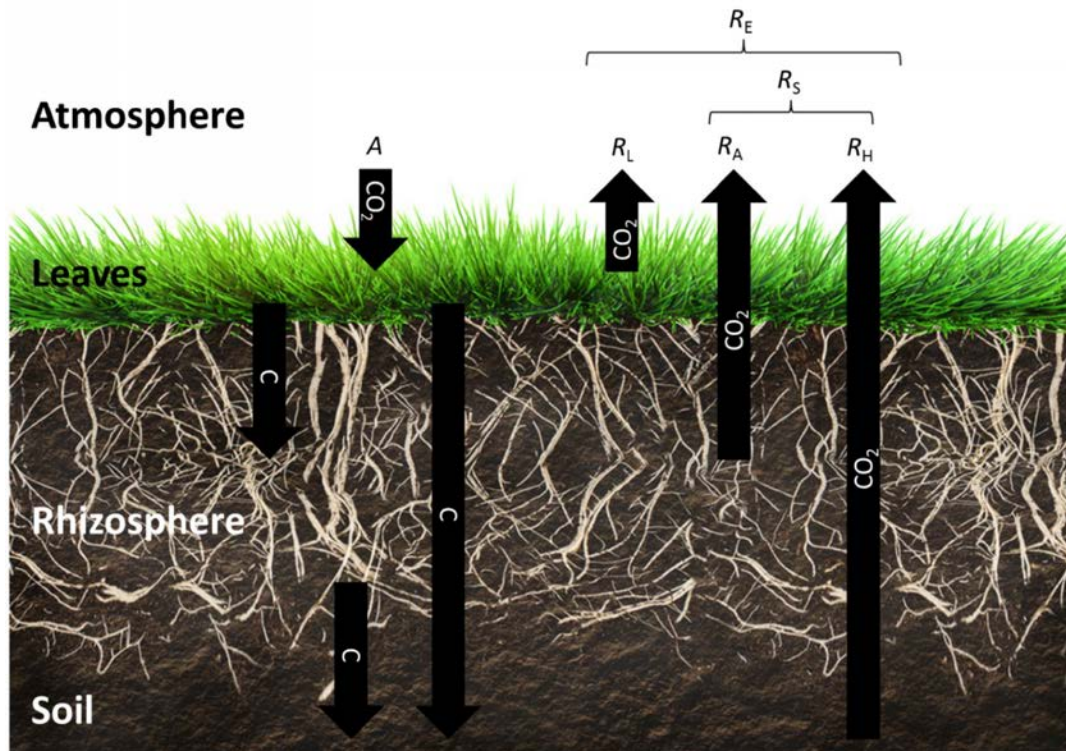


Figure 1.1: Conceptual diagram depicting the ecosystem CO₂ exchanges as well as transfers of carbon from leaves to roots to soil. The fluxes represented are: gross canopy photosynthesis (A), ecosystem respiration (R_E), above-ground plant respiration (R_L), soil respiration (R_S), soil autotrophic respiration (R_A) and soil heterotrophic respiration (R_H).

1.3 The New Zealand context

In New Zealand, grassland ecosystems cover 40% of the total land surface (MacLeod and Moller, 2006), and represent 50% of the national carbon stock inventory (Tate et al., 2005). They represent a critical focus for reducing the agricultural national carbon budget. Following global trends, New Zealand pastures are under rapid and widespread management intensification, with the conversion of traditional extensively grazed sheep and beef pastoral systems to dairy farming (MacLeod and Moller, 2006). In particular, intensification of farming practices with irrigation and addition of nitrogen fertiliser on the shallow, stony soils in eastern regions with low rainfall on the Canterbury

Plains, in Hawkes Bay, Otago and parts of Southland is expanding rapidly. Grazed grasslands used for dairy farming typically are intensively managed to support high stock numbers to maximise production and profitability. Dairy production now represents 25% of New Zealand's total exports and has positioned the country as the world's largest exporter of tradeable dairy products (FAOSTAT, 2014). While dairy farming ensures short-term productivity and rapid economic benefits, large uncertainties remain regarding its environmental and economical sustainability. New Zealand studies attempting to quantify the effects of such land use change on the soil carbon stocks and dynamics are scarce and show contradictory results. Evidence from the limited long-term data that are available suggests that soil carbon stocks decrease or remain unchanged decades after conversion to dairy farming (Schipper et al. 2013; 2014). Other studies have shown net ecosystem uptakes of carbon at intensively managed dairy farms which, if sustained over time, may result in increasing soil carbon stocks (Mudge et al., 2011; Rutledge et al., 2015; Hunt et al., 2016). Understanding the mechanisms leading to changes in grazed grassland ecosystems carbon dynamics under key management practices incorporating irrigation, addition of nitrogen fertiliser and grazing is needed urgently to determine whether intensive dairy grassland management represent a climate mitigation option and a sustainable production system.

1.4 Thesis objectives

This overall objective of this thesis is to provide new insights to our current state of knowledge of the components of grassland ecosystem carbon balance by testing hypotheses that address the processes regulating carbon exchange for each component In the context of pasture management intensification in New Zealand, and given the national- and global-scale implications for economic and environmental sustainability, this thesis sets out to address the following question: *Will the conversion from dryland to intensive dairy farm management result in increasing soil carbon sequestration in New Zealand's managed grasslands?* The approach is to study the effects of

irrigation, addition of nitrogen fertiliser and intensive grazing on the components of net ecosystem carbon balance, with a specific focus on the impacts on soil heterotrophic respiration.

The objectives to investigate the mechanisms underpinning changes in the components of the carbon balance were to:

1. Estimate the components of carbon balance in response to simulated grazing events and variability in environmental conditions (Chapter 2 and 3).
2. Measure and model seasonal changes in carbon balance components in response to irrigation and the addition of nitrogen fertiliser (Chapter 5)
3. Determine the response of soil organic matter decomposition to changes in environmental variables associated with conversion of dryland to irrigated, intensive farming practices by:
 - a. Developing and testing methodologies to partition rates of soil heterotrophic respiration in undisturbed soils using a natural abundance ^{13}C isotope approach (Chapter 2).
 - b. Determining the response of soil heterotrophic respiration to irrigation and addition of nitrogen fertiliser (Chapter 4).

1.5 Study sites

The thesis addresses the objectives in four experimental chapters describing research undertaken at two sites in Canterbury, New Zealand. The climate at both sites is temperate with mild winter and warm, dry summers. Mean annual rainfall is 600 mm (NIWA 2014). Soil types at the two sites are also similar but farming management practices were different.

The first site is an intensively managed commercial dairy farm, Beacon Farm, located near Hororata (lat. 43.58° S, long. 171.92° E, elevation 203 m above sea level). Prior to conversion to a dairy farm in 2008, the site was a dry-land sheep farm with low application of nitrogen fertiliser. The site is dominated by perennial ryegrass (*Lolium perenne* L.) with minor presence of white clover (*Trifolium repens* L.). The soil is a shallow (0.20-0.45 m depth), well drained, stony silt loam (typic

distrustept). Water is supplied at the site with a pivot irrigator to maintain soil volumetric water content (θ_s) above $0.25 \text{ m}^3 \text{ m}^{-3}$ (Fig2). Management also includes regular applications of nitrogen fertiliser and intensive, short duration grazing events (over 100 cows ha^{-1} for 1 to 2 days).

The second site is located at Ashley Dene Farm, Lincoln (latitude 43.40° S , longitude 172.20° E , elevation 35 m above sea level). The site is flat and was managed under dry sheep farming for more than 50 years prior to the experiment. The site presents a mixed community of grasses with numerous species including perennial ryegrass and white clover, as well as dandelion (*Taraxacum spp*), chicory (*Cichorium intybus L*), Lucerne (*Medicago sativa L*) and plantain (*Plantago lanceolata L*). The soil is a stony silt loam with shallow topsoil (0.2 m in depth), excessively drained and classified as a mix of Balmoral and Lismore according to New Zealand classification (Hewitt, 2010). Field plots were treated to simulate the first year of a land conversion to intensive dairy farming (Fig3). A factorial experimental design was adopted to investigate the effects of irrigation and addition of nitrogen fertiliser separately and in combination. Irrigation regime, fertiliser application rates and grazing management were replicated from the management regimes at Beacon Farm.



Figure 1.2: High stock numbers and the pivot irrigator at Beacon Farm



Figure 1.3: The experimental set up at Ashely Dene Farm.

1.6 Thesis outline

In Chapter 2, I present the results of a controlled-environment study of the short-term response of F_N and its components to simulated grazing events in irrigated intact grassland mesocosms extracted from Beacon Farm. Daily measurements of F_N , A , R_E and R_S were made after concurrent and delayed clipping events and addition of two different levels of nitrogen fertiliser. I used and compared two different techniques to partition R_S into its autotrophic and heterotrophic components: the root-exclusion technique and the natural abundance $\delta^{13}\text{C}$ technique, a novel isotopic method allowing measurements of R_H in the presence of roots, with no disturbance of the soil structure. The two approaches allowed testing for the effects of two levels of nitrogen addition on R_H in presence and absence of roots.

In Chapter 3, I present the result of a field study where F_N and R_S were measured continuously at Beacon farm for two extended periods of months at two different times during the growing season. Diurnal and daily changes in F_N and R_S were measured and their responses to environmental

variables modelled. Extending the findings from Chapter 2, a methodology to account for above-ground biomass variations through seasons and grazing cycles on model parameters was developed.

In Chapters 4 and 5, I present the results from two studies undertaken at the experimental field site at Ashely Dene Farm. In Chapter 4, I present the result of a study where soil heterotrophic respiration was measured using the non-disruptive natural abundance $\delta^{13}\text{C}$ technique and determined the effects of irrigation and nitrogen addition one and six months after the irrigation and addition of nitrogen treatment applications started. In order to develop further our understanding of soil organic matter dynamics, I measured a range of soil characteristics and tested the emerging hypothesis that soil structure and microbial accessibility to their substrate is predominant in regulating soil organic matter decomposition. The objective of the study in Chapter 5 was to investigate the effects of irrigation and addition of nitrogen on seasonal measurements of F_N , A , R_L and R_S in intensively grazed grassland. I used continuous measurements of environmental variable to develop predictive models for the components of carbon balance, accounting for biomass variations based on findings in the previous chapters. The models were used to produce annual estimates of the net ecosystem carbon balance and characterise the single and interactive net effect of irrigation and nitrogen addition during the first year after treatment were applied.

Chapter 6 is a synthesis of the four previous chapters. I summarise the integrated effects of irrigation, nitrogen fertilisation and intensive grazing management on grassland ecosystem carbon balance and soil organic matter decomposition. Finally, I discuss the implications of these findings for the economic and environmental sustainability of converting dryland farming to intensive dairy production and its potential as a climate mitigation option.

1.7 Thesis contribution

The findings from this thesis will contribute to scientific knowledge through publications in peer-reviewed, international journals.

The study in Chapter 2 is published in *Geoderma* as:

Moinet, G.Y.K., Cieraad, E., Rogers, G.N.D., Hunt, J.E., Millard, P., Turnbull, M.H., and Whitehead, D., 2016. Addition of nitrogen fertiliser increases net ecosystem carbon dioxide uptake and the loss of soil organic carbon in grassland growing in mesocosms. *Geoderma*, 266: 75–83.

The study in Chapter 4 is accepted for publication in *Geoderma* and will appear in 2016.

Both studies in Chapter 3 and 5 are currently under review by *Agriculture, Ecosystems & Environment*.

**CHAPTER 2 Addition of nitrogen fertiliser increases net ecosystem carbon
dioxide uptake and the loss of soil organic carbon in grassland growing in
mesocosms**

2.1 Introduction

The terrestrial biosphere absorbs approximately one third of anthropogenic carbon emissions (Schimel et al., 2001) and is crucial for mitigating the increase in atmospheric carbon dioxide (CO₂) concentration and the impacts of climate change (Pachauri et al., 2014). Grazed grasslands cover 26% of the earth's ice free land surface (Steinfeld et al., 2006) and represent 70% of agriculture land (FAOSTAT 2011). Grasslands have high inherent soil organic matter content (Miller and Donahue, 1990), which is comprised of more than 55 % of carbon (Stockmann et al., 2013), and is a key factor in soil productive capacity (Jenny, 1941; Miller and Donahue, 1990). Maintaining soil organic matter in grasslands is therefore critical, for both the Earth's carbon balance and sustainable land productivity (Conant et al., 2001).

In New Zealand, conversion of dryland grazed grasslands to dairy farming is a major land-use change (MacLeod and Moller, 2006). Grassland ecosystems represent 30% of the total land surface area and are an important component of the national carbon budget (Trotter et al., 2004). Grazed grasslands used for dairy farming typically are intensively managed, including high stock numbers, high inputs of nitrogen fertiliser and irrigation at sites with low rainfall. Such practices are known to result in changes in the rates of soil organic matter decomposition and soil carbon stocks (Paul et al., 1996; Conant et al., 2001) but there are few studies to quantify these impacts.

Using sequential measurements of soil carbon from cores across 31 sites converted to dairy farming over two to three decades, Schipper et al. (2007, 2010) observed a mean (\pm standard error) net loss in soil carbon of 730 ± 160 kg C ha⁻¹ y⁻¹. In contrast, in a short-term two-year study to measure net ecosystem CO₂ exchange using eddy covariance, Mudge et al. (2011) estimated an increase in net carbon uptake for a dairy grassland. Eleven years after conversion of a dryland site to dairy farming using irrigation, Kelliher et al. (2015) found a 28% increase in soil carbon in the upper 0.3 m of soil compared with the change in an adjacent non-irrigated site. However, the difference in carbon content at a depth of 0.8 m was not significant. These apparently contradictory findings

highlight the need for further studies to interpret the spatial and temporal complexities and environmental and management drivers of soil carbon dynamics.

The ecosystem carbon balance depends on the net ecosystem CO₂ exchange (F_N) comprising the input of carbon from photosynthesis (A) and losses from ecosystem respiration (R_E). Ecosystem respiration consists of respiration from the above-ground component of plants (R_L) and soil respiration (R_S). Soil respiration is comprised of autotrophic respiration (R_A) originating from roots and their associated mycorrhizal fungi and rhizosphere microbes, and heterotrophic respiration (R_H) from microbial decomposition of soil organic matter, such that (Amundson, 2001; Paterson et al., 2009)

$$F_N = R_E - A = R_L + R_S - A = R_L + R_A + R_H - A. \quad (2.1)$$

For long-term analysis of carbon balance, leaching and exported biomass can also be significant components (Soussana et al., 2007).

Estimates of F_N using eddy covariance are used widely to determine if an ecosystem is a sink or a source of carbon to the atmosphere (Baldocchi, 2008) but further detail is required to reveal the mechanisms driving changes in soil organic carbon (Kuzyakov, 2006). Soil respiration (R_S) is a major component and can account for 60-90% of R_E (Kuzyakov, 2006). The autotrophic component (R_A) represents the rapid turnover of a recently assimilated carbon pool that has only a small effect on long-term changes in soil organic carbon whereas R_H represents the slow turnover (up to millennia) of much larger carbon pools (Trumbore, 2000; Stockmann et al., 2013).

Determining differences in the drivers regulating changes in R_H and R_A is important, especially to predict changes in soil carbon stocks with changes in climate and management practices (Kuzyakov, 2006). However, partitioning R_S into its heterotrophic and autotrophic components is problematic. One difficulty is that the presence of roots can influence R_H , the so-called 'rhizosphere priming effect' (Kuzyakov, 2002). Many approaches for partitioning R_H from R_S , such as the root exclusion techniques are based on manipulations to remove R_A , for example, using trenches to exclude roots (Buchmann, 2000; Lee et al., 2003; Jiang et al., 2005) or shading and clipping leaves (Craine et al.,

1999). In a comprehensive meta-analytical review of studies designed to partition R_S into its components, Subke et al. (2006) documented a wide range in the ratio of $R_H:R_S$ and suggested that this could be due partially to the different techniques employed. The review also highlighted potentially overlooked interactions between soil respiration components as a consequence of disrupting the ecosystem. Dungait et al. (2012) showed that the losses of soil organic carbon is regulated by microbial accessibility to soil organic matter and this is related closely to soil physical structure (Six et al., 2002). This structure can be modified by soil physical disturbance such as sieving (Zakharova et al., 2014, 2015). This suggests that attempts to partition R_H from R_S needs to be done in intact, undisturbed systems. One approach to achieve this is the use of stable carbon isotopes (Hanson et al., 2000). These methods are based on measurable differences in the ^{13}C isotopic signatures ($\delta^{13}\text{C}$) of the CO_2 emitted from R_H and R_A ($\delta^{13}\text{C}_{R_A}$ and $\delta^{13}\text{C}_{R_H}$, respectively). Most studies to date have used C_3/C_4 plant isotopic shifts to increase the difference between $\delta^{13}\text{C}_{R_A}$ and $\delta^{13}\text{C}_{R_H}$. However, such an approach is restricted to ecosystems where C_3 or C_4 plants have invaded naturally (Millard et al., 2008) or have been introduced (Uchida et al., 2010) into C_3 or C_4 systems. In pure C_3 systems, the isotopic signature of respiration from soil organic matter turnover ($\delta^{13}\text{C}_{R_H}$) is typically 2-4‰ enriched compared with that from the roots and associated microbes ($\delta^{13}\text{C}_{R_A}$) (Bowling et al., 2008). Midwood et al. (2008) demonstrated that this difference can be estimated in an undisturbed C_3 system and used to partition R_S . This 'natural abundance $\delta^{13}\text{C}$ ' approach has been used successfully by Millard et al. (2010) and Graham et al. (2012).

Photosynthesis and R_E decrease immediately after with grazing, then increase over a number of weeks as the new leaves expand (Parsons and Penning, 1988). In artificial ryegrass swards, Kuzyakov et al. (2002) showed that 80% of the carbon respired by the rhizosphere originated from recently assimilated carbon by photosynthesis. Defoliation of plants by removing photosynthetic material reduces carbon allocation below-ground (Craine et al., 1999; Kuzyakov, 2006) and thus has a strong impact on R_A (Bremer et al., 1998; Cheng and Kuzyakov, 2001). It is well known that the addition of nitrogen fertiliser to grassland increases photosynthesis and light use efficiency (Evans, 1989; Sinclair

and Horie, 1989; Muchow and Sinclair, 1994) and leaf respiration (Reich et al., 2008). The effect of high nitrogen addition on R_H is more difficult to predict because no studies are available on undisturbed grasslands. However, priming effects as a consequence of added nitrogen have been observed mostly to be positive (Hart et al., 1986; Raun et al., 1998; Sembiring et al., 1998).

My objectives in this study were to investigate the effects of clipping and application of nitrogen fertiliser on the components of the net ecosystem CO_2 exchange for an intensively grazed grassland. I extracted intact cores with soil and plants from a grassland site and grew the grass in well-watered mesocosms in controlled conditions for six months. I measured F_N , R_E , A and R_S daily after clipping and addition of nitrogen fertiliser to determine the time constants for recovery of ecosystems growing with high and low additions of nitrogen fertiliser. At the end of these measurements, I measured the effects of addition of nitrogen on R_H using natural abundance $\delta^{13}\text{C}$. Comparing the results obtained from the isotopic technique to those from a root exclusion technique, I also investigated the magnitude and direction of rhizosphere priming, at high and low nitrogen supply.

2.2 Materials and methods

2.2.1 Preparation of the mesocosms

Material for the study was collected from Beacon Farm, a commercial dairy farm on the Canterbury plains, New Zealand (lat. 43.58° S, long. 171.92° E, elevation 203 m above sea level). The site was formally a dry-land sheep farm, with low application of nitrogen fertiliser, and conversion took place four years prior to the start of my study. The cores used in the mesocosms comprised mixed species but were dominated by perennial ryegrass (*Lolium perenne* L.), with minor presence of dandelion (*Taraxacum officinale* F. H. Wigg) and white clover (*Trifolium repens* L.). The soil is a shallow (0.20-0.45 m depth) stony silt loam (typic dystrustept) and well drained. The soil characteristics (mean \pm standard error, $n = 4$) were bulk density $1.16 \pm 0.03 \text{ g L}^{-1}$, bulk soil ^{13}C isotopic signature ($\delta^{13}\text{C}$) $27.4 \pm 0.07 \text{ ‰}$, volumetric percentage of stones $7.8 \pm 1.4\%$, and carbon and nitrogen concentrations 46.8 ± 0.02 and $3.4 \pm 0.01 \text{ g kg}^{-1}$, respectively.

In May 2013, 28 intact soil cores (200 mm diameter, 300 mm depth) were sampled randomly from a 250 m² area and placed in cylinders of PVC. The bases of the cylinders were sealed with 1 mm mesh netting. The mesocosms were placed in two growth cabinets (Model HGC 1514, Weiss Gallenkamp, UK) with conditions set to a constant 14 °C, photoperiod 15 hours and relative humidity 85%. Gaps between the soil and sides of the cylinders were filled with petroleum wax to prevent pathways for drainage of water. To prepare for the root exclusion technique, twelve mesocosms were chosen randomly for a 'bare soil' treatment, from which all plant material was eliminated. The grass was clipped at the soil surface and the mesocosms covered with black plastic sheets to prevent photosynthesis for four months. The other 16 mesocosms comprised the 'planted soil' treatment. A collar for measurements of soil respiration rates (100 mm diameter, 70 mm deep) was placed to a depth of 30 mm in the centre of each mesocosm. The grass inside the collars was removed using black plastic sheets for four months, allowing roots from the surrounding plants to colonize underneath the rings. Water was applied to the soil surface daily to retain soil water content near field capacity. The plants in the planted mesocosms were clipped to a constant height every two weeks and the biomass was collected, dried at 65 °C for three days and weighed. The leaves were analysed for carbon and nitrogen concentrations using a Dumas elemental analyser (Europa Scientific ANCA-SL, Crewe, UK).

Following each fortnightly clipping of the plants in the planted mesocosms, two nitrogen treatments were applied to both the planted and bare mesocosms. The high nitrogen treatment, N₁, was supplied using 144 mL of a nutrient solution with 41 g N L⁻¹ (ammonium nitrate). The low nitrogen treatment, N₀, was 144 ml of the same nutrient solution but with a lower concentration of 10 g N L⁻¹ (ammonium nitrate). In a preliminary experiment, for the low nitrogen treatment, I determined the lowest nitrogen supply that allowed the grass to survive in the experimental growing conditions. The application rates were equivalent to approximately 400 kg N ha⁻¹ y⁻¹ and 100 kg N ha⁻¹ y⁻¹, for N₁ and N₀ treatments, respectively. The treatments were maintained in the controlled conditions for two months prior to the start of the measurements.

Preparation of the material resulted in the establishment of 12 bare soil mesocosms, 6 for each nitrogen treatment, all free from plants as the result of a period of over 6 months without any photosynthetic activity, and 16 planted mesocosms, 8 for each nitrogen treatment. When the measurements started, nitrogen treatments had been applied seven times over a period of 3.5 months on all 36 pots, and clipping had been done concurrently on the 24 planted mesocosms.

2.2.2 *Measurements of net ecosystem carbon dioxide exchange and soil respiration*

Net ecosystem CO₂ exchange was measured on each mesocosm using a purpose-built cylindrical chamber (200 mm diameter and 210 mm height) made from polycarbonate. The bottom edge was covered with a ring of high density foam to form a seal. Measurements of CO₂ exchange in the chamber were made using a portable photosynthesis system (LI-6400XT, LI-COR Inc., Lincoln, NE, USA) designed to work as a closed system. After the chamber was placed on the top of a mesocosm, measurements of the CO₂ partial pressure were made over a period of 70 s. The chamber had an open vent to the atmosphere with a 9 mm diameter polyethylene tube (Xu et al., 2006) to avoid pressure fluctuations (Hutchinson and Livingston, 2001; Rochette and Hutchinson, 2005) and a small fan moving the air at 50 L min⁻¹ (V249L, 6V, Micronel®) was mounted inside the chamber in order to maintain well-mixed conditions. Incident irradiance (Q , 400-700 nm) was measured with a quantum sensor (Q40205, LI-COR Inc., Lincoln, NE, USA) placed at the top inside the chamber. Air temperature was measured using a thermocouple (Type E, Omega Engineering Ltd., Stamford, CT, USA) shaded from incident irradiance.

On each measurement day, F_N was measured for each mesocosm in the planted soil treatment under full irradiance (650-700 $\mu\text{mol m}^{-2} \text{s}^{-1}$). Subsequent measurements of F_N were taken at four levels of shade, achieved by draping sheets of shade cloth over the chamber, and finally a dark cloth excluding all light to give a measurement of R_E . A linear equation was used to estimate light use efficiency, α , from the light response curve described by (Luo et al., 2000) as

$$A = \alpha Q + R_E \quad (2.2)$$

where A is the rate of gross photosynthesis.

Immediately following the measurements of F_N , three replicate measurement of soil respiration rate were made using a soil respiration closed dynamic system (LI-8100, LI-COR Inc., Lincoln, NE, USA) with the chamber placed on the central collar.

2.2.3 Partitioning soil respiration

Both the natural abundance $\delta^{13}\text{C}$ and the root exclusion techniques were used to partition R_H from R_S . For the root exclusion technique, R_H was assumed to be equal to the value of R_S measured from the bare soils (Craine et al., 1999). The proportion of respiration derived from heterotrophic respiration (fR_H) was estimated by comparison of mean values of respiration fluxes between planted soils and bare soils. The natural abundance $\delta^{13}\text{C}$ technique requires the measurement of ^{13}C isotopic signatures of the CO_2 respired from the undisturbed soil (soil efflux) ($\delta^{13}\text{CR}_S$) from roots and associated microorganisms ($\delta^{13}\text{CR}_A$) and from soil organic matter decomposition ($\delta^{13}\text{CR}_H$). The rate of heterotrophic respiration and fR_H are calculated using a mass balance approach (Lin et al., 1999; Millard et al., 2010) where

$$fR_H = 1 - \frac{(\delta^{13}\text{CR}_S - \delta^{13}\text{CR}_H)}{(\delta^{13}\text{CR}_A - \delta^{13}\text{CR}_H)} \quad (2.3)$$

and

$$R_H = fR_H \times R_S. \quad (2.4)$$

Simultaneous measurements of $\delta^{13}\text{CR}_S$ from six mesocosms were made by collecting air respired from the soil surface using a partially automated open chambers system described by Midwood et al. (2008). The chambers were placed on the rings in each mesocosm and approximately 500 ml of respired air was collected into bags (Tedlar® Keika Ventures, Chapel Hill, NC, USA) that were flushed twice with CO_2 free air and evacuated prior to use.

Measurements of the isotopic signatures of the end members, $\delta^{13}\text{CR}_H$ and $\delta^{13}\text{CR}_A$, were made following the technique described by Millard et al. (2010). After the soil surface CO_2 efflux sample had been collected, samples of roots and soils were collected from each mesocosm. The rings for measuring R_S were removed and a steel tube identical in diameter of the rings was hammered into

the soil to a depth of 200 mm. The presence of large stones in some of the mesocosms prevented sampling deeper than 170-180 mm and this was taken into account in the statistical analysis of the data. The soil from the core was broken up loosely and roots were removed by hand. Samples of root-free soil and roots were placed in separate Tedlar® bags which were sealed and flushed three times with CO₂ free air, then filled with approximately 500 ml of CO₂ free air. An aliquot of gas was removed and the CO₂ partial pressure checked to make sure it fell within the range of 300-700 μmol mol⁻¹ needed to ensure optimum precision for the isotope analysis. The concentration was then adjusted if needed, by either adding CO₂ free air or extending the period of incubation. Incubations were kept to the minimum time possible (typically 5 to 7 min for the root-free soils, and 20 min for the roots) to minimise shifts in δ¹³C values caused by a switch to different carbon substrates due to root death or physical disturbance of the soil (Millard et al., 2008; Zakharova et al., 2014). All gas samples were analysed for δ¹³C values using a cavity ringdown spectrometer (G2121-I, Picarro Inc., Santa Clara, CA, USA).

2.2.4 *Experimental design*

The experimental period consisted of two phases. For the first phase I selected randomly ten planted mesocosms, five for each nitrogen treatment. To estimate the effect of clipping and addition of nitrogen on the recovery of ecosystem CO₂ exchange components, I made daily measurements of F_N , R_S and α during 19 days after concurrent clipping and nitrogen additions. To disentangle the effects of clipping and adding nitrogen, the grass was subsequently clipped without nitrogen addition and F_N , R_S and α were measured daily for 9 days. On the tenth day after clipping, nitrogen was applied, without clipping and F_N , R_S and α were measured daily for 12 days.

The second phase consisted of measuring heterotrophic soil respiration, R_H , using the natural abundance δ¹³C and the root exclusion technique. All 28 mesocosms were used. Just after the first phase was completed, the treatments applied were: concurrent clipping and nitrogen addition for the planted mesocosms, and nitrogen addition to the bare mesocosms. Measurements to determine R_H were made on day 7 after treatment application. For the root exclusion technique, measurements

were contained within 1 hour. For the natural abundance technique, measuring R_H from 16 mesocosms required 8 hours of the daylight period, during which potential variations of $\delta^{13}CR_S$ were checked using two mesocosms selected randomly for repeated sampling. In addition, four root samples and four root-free soil samples were selected randomly for longer incubation times, up to 2.5 h, in order to estimate the effect of length of incubation on $\delta^{13}CR_H$ and $\delta^{13}CR_A$.

For each mesocosm, soil water content (θ_s , Model SM300, Delta-T Devices Ltd., Cambridge, UK) and soil temperature (T_s , Model HH 603A, Omega Engineering Ltd., Stamford, CT, USA) were measured at a depth of 50 mm daily. After all the measurements were completed, soil and roots samples were collected, dried, ground to a powder in a ball mill and analysed for carbon and nitrogen concentrations using a Dumas elemental analyser (Europa Scientific ANCA-SL, Crewe, UK).

2.2.5 Statistical analyses

Changes in F_N , R_S , R_E and α after concurrent clipping and adding nitrogen fertiliser, clipping alone and adding nitrogen fertiliser alone, were tested using non-linear mixed-effect models conducted in the 'nlme' package (Pinheiro and Bates, 2014) of R version 3.2.1 (R Development Core Team, 2014). Each measurement of F_N , R_S , R_E and each calculated value of α was treated as a sample. To account for non-independence of repeated measurements, replicate number was included as a random effect in each model. F_N and α were modelled as common asymptotic exponential functions of number of days after treatment (n) (Crawley, 2007) as

$$F_N = a + b \exp(-c n) \quad (2.5)$$

where a is the steady-state value of F_N , b is the difference between a and the value of F_N at day 0 and c characterises the shape of the curve, and

$$\alpha = p (1 - \exp(-q n)) \quad (2.6)$$

where p is related to the initial value and to the steady-state value of α and q characterises the shape of the curve.

To characterise the time constants for the recovery of α and F_N , the number of days to reach 95% of the changes (n_{95}) was calculated from p and c respectively as

$$n_{95} = \ln(1/0.05) / X \quad (2.7)$$

where X represents q and c for the functions for α and F_N , respectively.

R_E was observed to decrease after grazing for a period of three days before starting to increase. To capture this initial decrease, a 3rd degree polynomial function was tested to model R_E . R_S was modelled as a linear function of n . Models with different coefficients for the high nitrogen treatment, N_1 , and the control treatment, N_0 , were compared with models fixing the same coefficients for N_1 and N_0 . A top-down stepwise regression approach was used to model fR_H and R_H . For the natural abundance technique, fR_H was modelled as a function of root and soil carbon and nitrogen concentrations (R_S) nitrogen treatment and core sampling depth. R_H was modelled similarly without the inclusion of R_S . For the root exclusion technique, R_H was modelled as a function of soil carbon and nitrogen concentrations and nitrogen treatment. Soil temperature, T_S and soil water content, θ_S , at a depth of 50 mm were also included. Model comparisons were based on Akaike's Information Criterion (AIC), the model with the lowest AIC being the most strongly supported. As a rule of thumb, models with $\Delta AIC < 2$ were also considered to be strongly supported (Burnham and Anderson, 2002). Treatment values of R_H obtained with the two techniques were compared with a Student t -test. The effects of addition of nitrogen on root and soil carbon and nitrogen concentrations were assessed using analysis of variance (ANOVA). Analyses of specific leaf area and leaf nitrogen concentration over time included replicate number as a random effect and was assessed with linear modelling. Differences in T_S and θ_S between nitrogen treatments and measurement phases were assessed using analysis of variance. Analyses of residuals were undertaken to check on model assumptions, including independence from T_S and θ_S .

All values are given as mean \pm standard errors.

2.3 Results

2.3.1 Soil temperature and soil water content

Air temperature in the controlled environment cabinets remained constant to within 1 °C of the set point, but soil temperature (T_s) increased during the day due to radiation loading from the lamps (21.6 ± 0.07 °C, range 19.4 - 25.8 °C). There was no significant difference in T_s for the mesocosms in the two nitrogen treatments ($P = 0.22$). Volumetric soil water content (θ_s) was $43.3 \pm 0.2\%$ and ranged from 33.4 to 53.4%. For the N_1 treatment, mean θ_s ($42.0 \pm 0.3\%$) was significantly lower than the value for the N_0 treatment ($44.6 \pm 0.3\%$) ($P < 0.001$). T_s and θ_s were not significantly different between the measurement phases.

2.3.2 Soil, root and leaf properties

For both the planted and bare soil treatments, there were no differences in soil carbon and nitrogen concentrations between the N_0 and N_1 treatments (Table 2.1). Root nitrogen concentration in the N_1 treatment was higher than that of the N_0 treatment (Table 2.1) but the difference was not significant ($P = 0.09$). No differences were found in root carbon concentrations ($P = 0.7$). Accordingly, no differences were found in the C:N ratios for soil and roots between the treatments (Table 2.1). A linear model best described cumulative leaf dry mass with time (Figure 2.1) with different slopes for the N_0 and N_1 treatments (0.118 ± 0.003 and 0.169 ± 0.005 g d⁻¹, respectively), and with the same initial values not significantly different from 0. This resulted in higher cumulative leaf dry mass for the N_1 treatment (27.61 ± 1.68 g) compared with the value for the N_0 treatment (19.60 ± 2.05 g) at the end of the experiment ($P = 0.02$). No significant changes were measured in specific leaf area throughout the experiment (Table 2.2) for the N_0 and N_1 treatments ($P = 0.3$ and $P = 0.9$, for nitrogen treatment and date of the clipping event, respectively). Leaf nitrogen concentration (Table 2.2) showed significant variability with sampling date and nitrogen treatment ($P < 0.001$ and $P = 0.02$, respectively). Mean nitrogen concentration was higher for leaves in the N_1 treatment compared with the value for leaves from the N_0 treatment (24.2 ± 0.4 and 21.2 ± 0.6 g kg⁻¹ respectively). The overall

leaf nitrogen concentration on the last clipping event was significantly lower (by $2.3 \pm 0.5 \text{ g kg}^{-1}$) than that for all values during the measurement period.

Table 2.1: Soil and root carbon and nitrogen concentrations and C:N ratios at the end of the experiment for the low, N_0 , and high nitrogen, N_1 , treatments. All values shown are mean \pm standard error (n = 5).

	Planted soils		Bare soils	
	N_0	N_1	N_0	N_1
root nitrogen (g kg^{-1})	7.8 ± 0.3	8.7 ± 0.4	–	–
root carbon (g kg^{-1})	238.3 ± 14	228.1 ± 22	–	–
root C:N	30.7 ± 2.3	26.3 ± 2.9	–	–
soil nitrogen (g kg^{-1})	3.2 ± 0.1	3.3 ± 0.1	3.2 ± 0.1	3.2 ± 0.1
soil carbon (g kg^{-1})	37.8 ± 0.7	38.0 ± 0.8	38.1 ± 0.8	37.6 ± 0.5
soil C:N	11.6 ± 0.1	11.7 ± 0.3	11.9 ± 0.1	11.7 ± 0.1

Table 2.2: Leaf nitrogen concentration and specific leaf area at different times throughout the measurement period when the grass was clipped. The mention 'NA' indicates non available data. All values shown are mean \pm standards error (n = 5).

Days since start of the experiment	Days since clipping	Leaf nitrogen (g kg^{-1})		Specific Leaf Area ($\text{m}^2 \text{kg}^{-1}$)	
		N_0	N_1	N_0	N_1
14	14	22.4 ± 0.9	23.7 ± 0.8	292.0 ± 55.9	228.6 ± 64.9
27	14	22.6 ± 0.7	25.2 ± 0.8	NA	NA
104	13	21.7 ± 0.8	24.9 ± 0.5	269.3 ± 7.3	251.9 ± 12.2
127	23	18.3 ± 1.2	22.7 ± 0.8	209.0 ± 10.6	251.9 ± 15.4

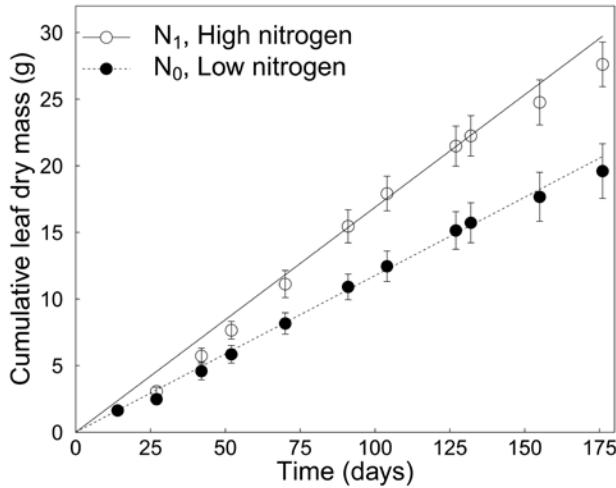


Figure 2.1: Cumulative leaf dry mass with time throughout the experiment for the low (N_0) and high (N_1) nitrogen treatments. The vertical bars show standard errors of the mean.

2.3.3 Net ecosystem carbon dioxide exchange and light use efficiency

The estimated parameters describing changes in F_N (a , b and c) and α (p and q) as functions of number of days after treatment (n) are shown in Table 2.3. The best model describing the change in F_N after concurrent clipping and nitrogen addition was an exponential decrease (Equation 2.5) to a steady-state value becoming a small net sink of carbon, near neutral ($a = -0.19 \pm 0.33 \mu\text{mol m}^{-2} \text{s}^{-1}$) for the N_1 treatment, while remaining a net source of carbon for the N_0 treatment (Figure 2.2). Changes in F_N were also greater in magnitude for the N_1 treatment than for the N_0 treatment (e.g., the estimated value of b was higher for the N_1 treatment). The shapes of the curves were not statistically different and 95% of the changes occurred within the first seven days for both the N_1 and N_0 treatments ($n_{95} = 7.1$ d). The best model describing the response of α after clipping and addition of nitrogen was an increasing exponential function (Equation 2.6) with the steady-state value for the N_1 treatment being higher than the value for the N_0 treatment. The shapes of the curves were not significantly different between nitrogen treatments and 95% of the change (n_{95}) occurred in 9.1 days. Asymptotic exponential functions best described changes of F_N and α after clipping alone and addition of nitrogen fertiliser alone. There were no significant differences in the response of N_1 and N_0 treatments for measurements made after clipping alone, neither for F_N nor for α . Significant

differences appeared after adding nitrogen alone, where the value for c for the N_0 treatment was very close to 0, suggesting there was almost no further decrease in F_N after addition of the N_0 treatment. For the N_1 treatment the system became a small net carbon sink within three days after addition of nitrogen alone ($n_{95} = 2.6$ d), reaching a similar steady-state value to that for the measurements made after concurrent clipping and nitrogen addition. The estimated steady-state value of α following addition of nitrogen only was higher for the N_1 treatment than for the N_0 treatment, but the shapes of the curves were not statistically different, with $n_{95} = 1.7$ d.

2.4 Ecosystem respiration and soil respiration

Changes in R_E with time were best described by a 3rd degree polynomial function. Values of R_E following concurrent clipping and nitrogen addition were higher for the N_1 treatment than the N_0 treatment except for the initial value, for which the difference was not statistically significant (Figure 2.3). There was a small decrease in R_E on the first two days after clipping alone, and this was not significantly different for the N_1 and N_0 treatments. R_E was nearly constant after addition of nitrogen alone, except for the N_1 treatment which slightly increased from $n = 5$ d.

Changes in R_S after concurrent clipping and nitrogen addition were linear (Figure 2.3) with the same initial value ($6.38 \pm 0.30 \mu\text{mol m}^{-2} \text{s}^{-1}$) but differences in slopes for the nitrogen treatments. This was also the case for measurements made after clipping alone and addition of nitrogen alone, with initial values of 5.45 ± 0.23 and $5.67 \pm 0.28 \mu\text{mol m}^{-2} \text{s}^{-1}$, respectively. However, absolute values of the estimated slopes were all below, or very close to, the instrument detection limits of $0.02 \mu\text{mol m}^{-2} \text{s}^{-1} \text{d}^{-1}$, with the maximum slope value of $-0.04 \pm 0.02 (\mu\text{mol m}^{-2} \text{s}^{-1}) \text{d}^{-1}$ for the N_1 treatment after only clipping.

For the measurements made after concurrent clipping and nitrogen addition, a trend was observed in the residuals as a function of T_S . A new model was thus fitted including T_S and this resulted in an improvement (lower AIC and independence of the residuals). There was a positive linear effect of T_S on R_S with a slope of $0.30 \pm 0.03 (\mu\text{mol m}^{-2} \text{s}^{-1}) \text{ } ^\circ\text{C}^{-1}$.

Table 2.3: Estimated values of the parameters of modelled net ecosystem CO₂ exchange, F_N (a , b and c), and light use efficiency, α (p and q) for the low (N_0) and high nitrogen (N_1) treatments, after concurrent addition of nitrogen and clipping, clipping alone and addition of nitrogen alone. Values of parameters centred are not significantly different between the nitrogen treatments. All values shown are mean \pm standards error.

Model	Parameter	Clipping + addition of nitrogen		Clipping alone		Addition of nitrogen alone		
		N_0	N_1	N_0	N_1	N_0	N_1	
F_N	a	($\mu\text{mol m}^{-2} \text{s}^{-1}$)	1.11 \pm 0.26	-0.19 \pm 0.33	2.05 \pm 0.25		-1.36 \pm 0.53	-0.22 \pm 0.49
	b	($\mu\text{mol m}^{-2} \text{s}^{-1}$)	4.87 \pm 0.63	7.42 \pm 0.87	3.63 \pm 0.31		2.85 \pm 0.44	
	c	($(\text{m}^2 \text{s} \mu\text{mol}^{-1}) \text{d}^{-1}$)	0.42 \pm 0.04		0.55 \pm 0.09		0.03 \pm 0.02	0.66 \pm 0.17
α	p	($\mu\text{molC} \mu\text{mol quanta}^{-1}$)	0.018 \pm 0.001	0.023 \pm 0.001	0.011 \pm 0.001		0.013 \pm 0.001	0.017 \pm 0.001
	q	($(\mu\text{mol quanta} \mu\text{molC}^{-1}) \text{d}^{-1}$)	0.33 \pm 0.05		0.24 \pm 0.04		1.75 \pm 0.3	

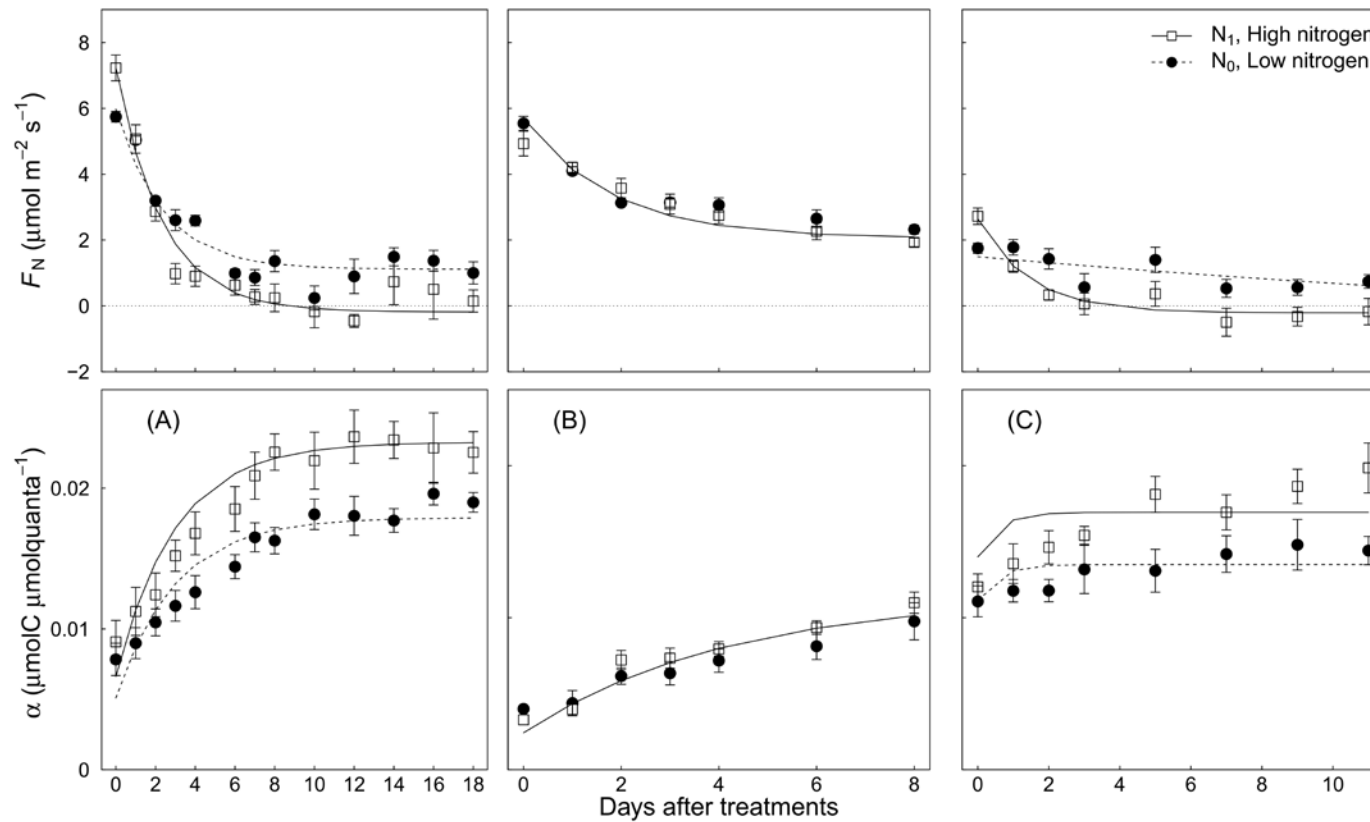


Figure 2.2: Net ecosystem CO₂ exchange (F_N) and light use efficiency (α) modelled as a function of number of days after (A) clipping and addition of nitrogen, (B) clipping only and (C) addition of nitrogen only for the low (N_0) and high (N_1) nitrogen treatments. The vertical bars show standard errors of the mean. A single solid line is used when the model does not differ significantly between the nitrogen treatments.

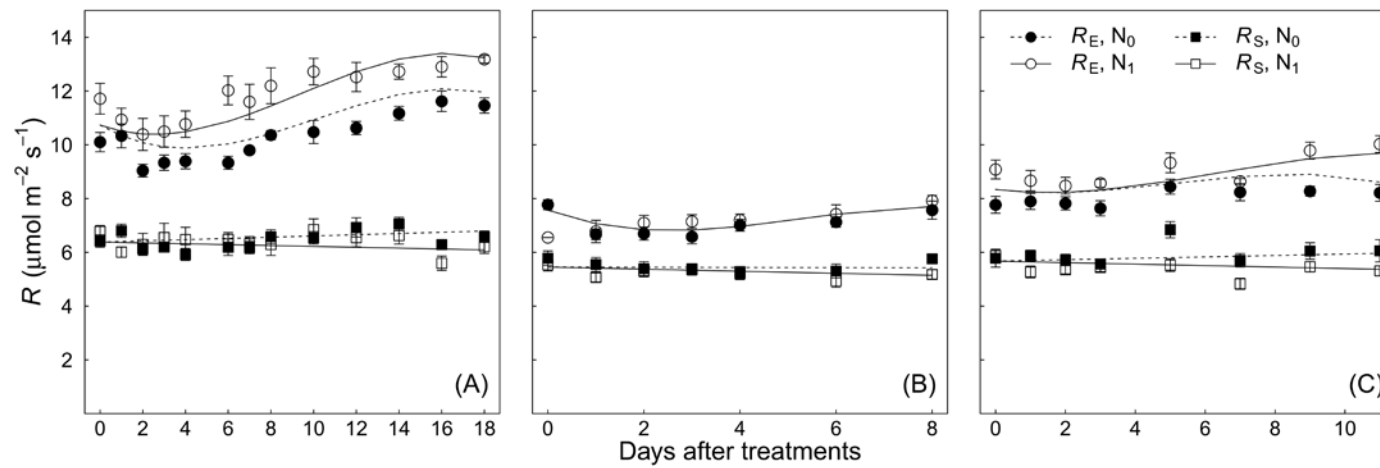


Figure 2.3: Soil respiration (R_S) and ecosystem respiration (R_E) modelled as a function of number of days after (A) concurrent clipping and addition of nitrogen, (B) clipping alone and (C) addition of nitrogen alone, for the low (N_0) and high nitrogen (N_1) treatments. The vertical bars show standard errors of the mean. A single solid line is used when the model does not differ significantly between nitrogen treatments.

2.5 Partitioning soil respiration using the natural abundance $\delta^{13}\text{C}$ technique

During the 8 hours of measurements, there were no changes in the values of $\delta^{13}\text{C}_{\text{R}_\text{S}}$ from the two test mesocosms ($P = 0.29$). $\delta^{13}\text{C}_{\text{R}_\text{A}}$ from four mesocosms did not vary over a 2.5 h incubation period ($P = 0.7$). Changes in $\delta^{13}\text{C}_{\text{R}_\text{H}}$ over the incubation time followed an exponential decay function with values for $a = -28.89 \pm 0.24\text{‰}$, $b = 0.037 \pm 0.012\text{‰}$ and $c = 4.05 \pm 0.40 \text{ d } \text{‰}^{-1}$. For one mesocosm from the 16 measured, $\delta^{13}\text{C}_{\text{R}_\text{A}}$ was close to, but slightly enriched compared with $\delta^{13}\text{C}_{\text{R}_\text{S}}$, suggesting that variability associated with measurements resulted in no difference between $\delta^{13}\text{C}_{\text{R}_\text{S}}$ and $\delta^{13}\text{C}_{\text{R}_\text{A}}$, so the value of fR_{H} for that replicate was constrained to 0.

Values of $\delta^{13}\text{C}_{\text{R}_\text{S}}$, $\delta^{13}\text{C}_{\text{R}_\text{A}}$ and $\delta^{13}\text{C}_{\text{R}_\text{H}}$ were not significantly different between nitrogen treatments. Overall, mean values of $\delta^{13}\text{C}_{\text{R}_\text{S}}$ were $3.6 \pm 0.3\text{‰}$ more depleted than the values for $\delta^{13}\text{C}_{\text{R}_\text{H}}$ and $1.8 \pm 0.4\text{‰}$ more enriched than the values for $\delta^{13}\text{C}_{\text{R}_\text{A}}$ (Table 2.4).

The best model describing fR_{H} and R_{H} included nitrogen treatment, soil core depth and T_{S} . The estimated effect of T_{S} was small ($0.04 \pm 0.02 \text{ } ^\circ\text{C}^{-1}$ and $0.31 \pm 0.16 \text{ } \mu\text{mol m}^{-2} \text{ s}^{-1} \text{ } ^\circ\text{C}^{-1}$ for fR_{H} and R_{H} , respectively). Values of fR_{H} were higher when the presence of stones prevented the core from being sampled to a depth of 200 mm. This resulted in an increase in R_{H} of $1.69 \pm 0.37 \text{ } \mu\text{mol m}^{-2} \text{ s}^{-1}$. This occurred in 3 and 4 mesocosms for the N_1 and N_0 treatments, respectively. Thus, there was no co-variation between soil core depth and nitrogen treatment. The value of fR_{H} was significantly higher for the N_1 treatment (Table 2.4). This resulted in a higher value of R_{H} for the N_1 treatment ($2.06 \pm 0.55 \text{ } \mu\text{mol m}^{-2} \text{ s}^{-1}$) compared with the value for the N_0 treatment ($1.26 \pm 0.29 \text{ } \mu\text{mol m}^{-2} \text{ s}^{-1}$) (Figure 2.4).

2.5.1 Root exclusion technique and method comparison

From the measurements using the bare soil mesocosms, R_{H} increased linearly with the soil C:N ratio and T_{S} (Figure 2.3), but there were no significant differences between the nitrogen treatments (Figure 2.4). R_{H} was $4.34 \pm 0.13 \text{ } \mu\text{mol m}^{-2} \text{ s}^{-1}$, which was significantly higher than the mean value of R_{H} measured with the natural abundance isotope technique ($P < 0.001$) (Figure 2.3). The overall mean

value for fR_H from the root exclusion technique (0.86) was also higher than the overall mean value estimated using the natural abundance $\delta^{13}\text{C}$ approach ($fR_H = 0.33$).

Table 2.4: Carbon isotopic signatures for air collected from soil respiration ($\delta^{13}\text{CR}_S$) incubation of root-free soil ($\delta^{13}\text{CR}_H$) and incubation of roots ($\delta^{13}\text{CR}_A$) and calculated values of the proportion of soil respiration resulting from heterotrophic respiration (fR_H) for the low (N_0) and high nitrogen (N_1) treatments. The asterisk indicates a significant difference in values between nitrogen treatments. All values shown are mean \pm standard error.

		N_0	N_1
$\delta^{13}\text{CR}_S$	(‰)	-29.37 ± 0.23	-29.34 ± 0.26
$\delta^{13}\text{CR}_A$	(‰)	-30.83 ± 0.48	-31.45 ± 0.49
$\delta^{13}\text{CR}_H$	(‰)	-25.41 ± 0.18	-26.27 ± 0.45
fR_H		0.26 ± 0.06 *	0.39 ± 0.10 *

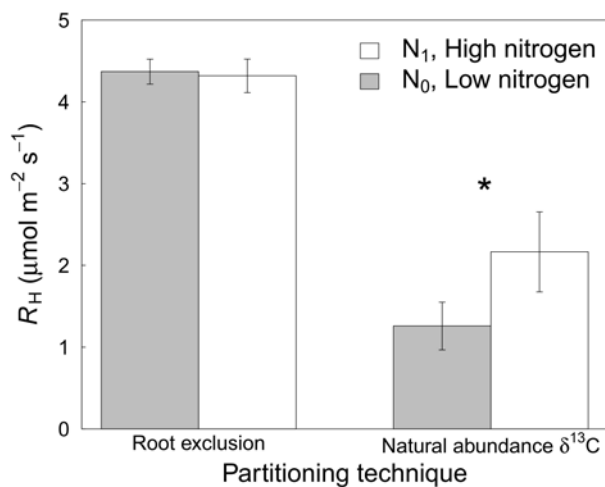


Figure 2.4: Rates of soil heterotrophic respiration (R_H) on day 7 after concurrent clipping and addition of nitrogen using two partitioning techniques, for the low (N_0) and high (N_1) nitrogen treatments. The vertical bars represent standard errors of the mean. The asterisk indicates a significant difference in values between nitrogen treatments.

2.6 Discussion

This study contributed new insights to carbon cycling in managed grasslands by integrating measurements of net ecosystem CO_2 exchange and its components with measurements to partition

R_H from R_S in undisturbed mesocosms. I showed that the increase in net ecosystem CO_2 uptake (decrease in F_N) with the addition of high concentration of nitrogen fertiliser masked a smaller, concomitant increase in soil organic matter turnover (increase in R_H). The additional carbon input to the system was at least partly allocated to above-ground biomass, as shown by the greater cumulative biomass in the N_1 treatment compared with N_0 treatment.

2.6.1 *Net ecosystem CO_2 exchange*

My findings highlight a strong decrease in F_N to a steady-state value with increasing time after clipping that was associated strongly with increasing α . The addition of high nitrogen resulted in a smaller steady-state value of F_N and higher steady-state value of α , but time constants for the responses were similar for both nitrogen treatments. This demonstrates that addition of high nitrogen resulted in an increase in α , leading to an increase in A that exceeded the increase in R_E . This resulted in a greater net carbon uptake for the high nitrogen treatment (N_1) compared with the control treatment (N_0). The additional cumulative biomass in response to added nitrogen was attributable mainly to increased canopy photosynthesis. The resulting similar specific leaf area but higher leaf nitrogen concentration in the N_1 treatment compared with values for the N_0 treatment also suggests that photosynthesis per unit leaf area was enhanced by increasing Rubisco activity associated with leaf nitrogen concentration (Friend, 1991). Consistent with other studies, the effects of adding high nitrogen increased rates of photosynthesis more than leaf respiration (Field and Mooney, 1986). The lack of a difference in soil and root nitrogen concentration between the nitrogen treatments suggests that most of the added nitrogen was utilised by the plants for above-ground biomass growth.

In my study, as the changes in R_S with time and between the treatments were very small, differences in R_E were dominated by changes in leaf respiration rates. Ourry et al. (1988) showed that regrowth of perennial ryegrass after clipping can be described by two physiological phases. During the first six days, nitrogen supply to leaves is derived from remobilisation from reserves in roots and stubble, then nitrogen is supplied by root uptake from the soil. I interpret the limited

response of A and biomass growth in the treatment where leaves were clipped without adding nitrogen to the exhaustion of nitrogen root reserves during the few days following the treatment. When nitrogen was added without clipping during the second phase of development, there was a rapid stimulation in A that was larger than the proportional increase in leaf respiration rate, resulting in enhanced biomass production. Moreover, high nitrogen supply has also been shown to reduce the initial rate of nitrogen remobilisation and uptake by roots (Millard et al., 1990). Atkinson (1986) demonstrated an increase in leaf respiration rate within 20 hours after defoliation in sheep fescue (*Festuca ovina* L.) and a similar observation was made in tobacco leaves (*Nicotiana tabacum* L.) in the few hours following defoliation (Macnicol, 1976), attributed to a wounding response. This could explain the initial higher values of R_E in the first two days after clipping in my mesocosms.

2.6.2 Components of soil respiration

The exponential increase in R_S resulting from increasing T_S is well documented (Lloyd and Taylor, 1994; Davidson et al., 2000; Brown et al., 2009) and maximum values of R_S are associated with values of θ_S near field capacity (Davidson et al., 2000). Brown et al. (2009) observed mean rates of R_S in a ryegrass-dominated grassland in New Zealand of around $3 \mu\text{mol m}^{-2} \text{s}^{-1}$ in field conditions, roughly half of the measured values from my controlled environment conditions. This suggests that, in my study, T_S and θ_S were not limiting for R_S . Furthermore, the small variations in T_S and θ_S did not affect R_S , R_A and R_H significantly.

Several studies have demonstrated a strong decrease in R_S following clipping. Bremer et al. (1998) showed a decrease of 20 to 50% in R_S in the first two days after clipping in a tallgrass prairie and Cheng and Kuzyakov (2001) observed a decrease of 50% in R_S from wheat mesocosms after a shading treatment was applied. In my study, the response of R_S was insignificant in comparison. Kuzyakov (2002) cites numerous studies that have shown negative rhizosphere priming effects where the presence of plant roots decreases decomposition rates of soil organic matter by 10 to 30%. One mechanism proposed to explain negative rhizosphere priming effects is competition for nutrients between living roots and soil microorganisms (Jingguo and Bakken, 1997; Bottner et al.,

1999). The review by Wang and Fang (2009) highlights that the short-term effects of clipping on R_S are attributable to the physiological response of plants. It is likely that clipping reduced carbon allocation below ground (Craine et al., 1999; Kuzyakov, 2006) resulting in reduced root and rhizosphere activity. A decrease in R_A in my mesocosms would have led to a proportional increase in R_H , with a neutral net effect of clipping on R_S .

Using the isotope natural abundance technique, my data suggest that high nitrogen supply resulted in increased fR_H and R_H . This result is supported by several studies showing increases in soil organic matter decomposition rates with the addition of nitrogen (Hart et al., 1986; Raun et al., 1998; Sembiring et al., 1998). A competition mechanism involved in the rhizosphere priming would also explain this result. Millard et al. (1990) found that addition of high nitrogen reduced ryegrass root biomass. Other studies in grasslands observed a decrease in R_S due to reduced carbon allocation below-ground as a result of nitrogen addition (Jong et al., 1974; Ammann et al., 2007). Although I were not able to measure root biomass directly, a reduction in biomass in response to high nitrogen supply seems like a reasonable assumption. By reducing root activity in the planted soils, addition of nitrogen would have enhanced competitiveness of the soil microorganisms, therefore increasing R_H .

The higher estimates of R_H using the root exclusion technique compared with the isotope approach in my study could be attributable partly to the presence of remnant decaying roots. Nakane et al., (1996) and Craine et al., (1999) showed the presence of decaying roots could be responsible for increases in R_S by up to 20% in a forest ecosystem (Nakane et al., 1996). However, this would not account for the larger difference in R_H of 50% observed between the two techniques in my study. My findings support the existence of a negative rhizosphere priming effect as a coexisting mechanism to explain this large difference.

These observations indicate that the root exclusion technique is not appropriate to determine R_H . In a similar study to ours, Chen et al. (1996) showed that ryegrass roots alone (separated from the rhizosphere) accounted for between 49 and 58% of R_S , which is closer to the result I obtained from

the natural abundance $\delta^{13}\text{C}$ technique (68% for root and the rhizosphere). This supports the validity of my use of the natural abundance $\delta^{13}\text{C}$ technique.

2.7 Conclusions

The decrease in F_N associated with addition of high nitrogen in my study was concurrent with an increase in R_H . My data strongly support the existence of a negative rhizosphere priming effect on soil organic matter decomposition. Based on these observations, I conclude that (i) measuring F_N and its components R_E and A alone can be misleading when trying to predict long-term changes in soil organic carbon stocks, and (ii) when making measurements to partition the components of soil respiration in response to treatments, it is important to use non disturbed systems. This can be achieved using the natural abundance $\delta^{13}\text{C}$ technique.

**CHAPTER 3 Phytomass index improves estimates of net ecosystem carbon
dioxide exchange in intensively grazed grassland**

3.1 Introduction

Grazed grasslands cover over a quarter of earth's ice free land surface (Steinfeld et al., 2006), representing 70% of agriculture land (FAOSTAT 2011), and contain about 12% of global soil organic carbon (Schlesinger, 1977). Research has shown that land management practices influence the balance between uptake and losses of carbon, with major consequences for atmospheric CO₂ concentration and soil carbon stocks (Conant et al., 2001; Lal, 2004, 2009; Soussana et al., 2010). Whether an ecosystem is gaining or losing carbon depends on the net ecosystem CO₂ exchange (F_N), comprising the uptake of carbon from photosynthesis (A) and losses from ecosystem respiration (R_E). Ecosystem respiration consists of respiration from the above-ground component of plants (R_L) and soil respiration (R_S). Understanding the drivers regulating these fluxes is critical for elucidating the responses of terrestrial ecosystems to environmental variables and predicting carbon balance and future carbon stocks under different land management practices.

Grazing intensity is a contributing factor to explain large differences in changes of the carbon content at different sites ($\pm 150 \text{ gC m}^{-2} \text{ y}^{-1}$ over decades) (McSherry and Ritchie, 2013). On a shorter time-scale, F_N can be affected with different intensities depending on the timing and intensity of above-ground biomass removal by grazing (Lohila et al., 2004; Nieveen et al., 2005; Soussana et al., 2007; Campbell et al., 2015). In addition to directly exporting carbon from the ecosystem, grazing reduces leaf area and thus A and R_L , and temporarily suspends grass production (Parsons et al., 1983; Soussana et al., 2007). The response of soil respiration is less clear. Short-term changes in R_S following defoliation are likely to be associated with physiological responses (Wang and Fang, 2009) that result in decreases in R_S due to reduced allocation of carbon below-ground (Craine et al., 1999). However, some studies have observed no changes in R_S after above-ground biomass removal in managed grasslands (Rogiers et al., 2004; Jia et al., 2012; Chapter 2).

To account for the effect of plant development and biomass removal from grazing on F_N , an empirical 'phytomass index' can be calculated based on the difference between night time and day time F_N (Lohila et al., 2004; Campbell et al., 2015). Because calculation of the phytomass index (P_i) is

based on measured values of F_N , this takes into account changes in plant activity and is anticipated to be a better predictor of primary production than leaf area index or measurements of above-ground plant dry mass harvested intermittently (Lohila et al., 2004). The approach using phytomass index has been used successfully to account for above-ground biomass fluctuations in gap-filling eddy covariance data from intensively grazed grassland (Lohila et al., 2004; Campbell et al., 2015). In this study, I extend the P_i approach to improve estimates of F_N and its components (A , R_E and R_S and R_L) by combining calculated values of P_i with measurements of the components of ecosystem carbon balance. In addition, I set out to model P_i from environmental variables and evaluate the potential of the model to improve predictions of F_N in grazed grassland when continuous measurements are not available. The objectives of the study were to (i) investigate the suitability of the phytomass index methodology to account for biomass removal and regrowth following grazing in estimating F_N and its components (A , R_E , and R_S and R_L) in an intensively managed dairy grassland, (ii) develop a model for the phytomass index from environmental variables (P_i') and evaluate its success in explaining changes in biomass compared with the use of calculated P_i and (iii) assess the suitability of the approach using the phytomass index (with calculated P_i and modelled P_i') in the development of a model to estimate F_N accounting for the effect of above-ground biomass variations due to grazing. My approach was to make continuous measurements of the components of grassland carbon balance for two periods in early and late summer with contrasting environmental conditions and combine these with measurements of biomass production across grazing cycles.

3.2 Materials and methods

3.2.1 Site description

The study was undertaken during the 2013-14 growing season at Beacon Farm, an intensively managed commercial dairy farm on the Canterbury Plains, New Zealand (lat. 43.58° S, long. 171.92° E, elevation 203 m above sea level). Prior to conversion to a dairy farm in 2008, the site was a dry-land sheep farm with low application of nitrogen fertiliser. The site is dominated by perennial

ryegrass (*Lolium perenne* L.) with minor presence of white clover (*Trifolium repens* L.). The soil is a shallow (0.20-0.45 m depth), well drained, stony silt loam (typic dystrustept) with mean \pm standard error ($n = 4$), bulk density $1.16 \pm 0.03 \text{ g L}^{-1}$, volumetric percentage of stones $7.8 \pm 1.4\%$, and carbon and nitrogen concentrations 46.8 ± 0.02 and $3.4 \pm 0.01 \text{ g kg}^{-1}$, respectively. Water was supplied at the site with a pivot irrigator to maintain soil volumetric water content (θ_s) above $0.25 \text{ m}^3 \text{ m}^{-3}$. Measurements to provide hourly values of rainfall, air temperature (T_a) and photosynthetically active irradiance (Q , 400-700 nm) were continuously made at the site. Soil temperature (T_s , Type E Thermocouple, Omega Engineering Ltd., Stamford, CT, USA) and soil volumetric water content (θ_s , model SM300, Delta-T Devices, Burwell, Cambridge, UK) were made every hour at three locations at depths of 20 and 100 mm. Above-ground biomass was measured at the site just prior to each grazing event. Further description of the site is given by Laubach et al. (2015) and Hunt et al. (2016).

3.2.2 Measurements of carbon dioxide exchange

I used seven circular closed dynamic chambers (diameter 200 mm, model LI-COR 8100-104, Lincoln, NB, USA) and an infra-red CO_2 gas analyser (LI-COR 8100-101, NB, USA) to measure rates of CO_2 exchange from the grassland. The tops of the chambers remained open and were closed automatically during for measurements of CO_2 exchange using an automated multiplexer system (model LI-COR 8150) with an hourly cycle for each chamber with 2.5 min delay between each measurement. Three chambers with opaque tops and four with transparent tops were used to measure soil respiration (R_s) and net ecosystem CO_2 exchange (F_N), respectively. Rates of CO_2 exchange were calculated from the linear change in measurements of CO_2 concentration in the chamber (2 s readings) during a closure time of 60 s, disregarding an initial 15 s and the last 30 s of measurement to avoid non-linearity in the rate of change in CO_2 concentration. Measurements were discarded when the coefficient of determination for the linear change in CO_2 concentration was smaller than 0.9, except for measurements from the transparent chambers when measurements of F_N were close to zero.

3.2.3 Experimental design

Chamber measurements (F_N and R_S) were made continuously during two successive periods: in spring and early summer (89 days, late September to late December) and again in late summer and early autumn (62 days, February to April).

In order to exclude the dairy cows, the system was installed in the middle of the site in a fenced 50 m² plot. The chambers were placed on PVC rings (100 mm depth) inserted in the soil at a depth of 50 mm one month prior to the start of the measurements. The three chambers for measurements of R_S were placed in gaps between plants and any remaining plants inside the rings were clipped to the soil surface regularly. The grass in the four clear chambers and in the enclosed area was clipped and removed to coincide with the cows being allowed to graze the paddock. This occurred four times during the first measurement period and two times during the second period. In order to simulate the effects of increased rate of grass growth following the urine deposition in the paddock outside the enclosure, urea equivalent to 400 kg N ha⁻¹ y⁻¹ was applied in and around the rings subsequent to clipping. In intact mesocosms extracted from the same site, Chapter 2 showed that adding nitrogen fertiliser concurrently with clipping did not affect the timing for the recovery of F_N and the effect on R_S was negligible.

To model above-ground biomass, I used measurements of above-ground dry-mass collected at the site prior to each grazing events and measurements of soil temperature, soil water content and incident irradiance that are well known to regulate crop growth (Monteith and Moss, 1977). Between each grazing event, I calculated cumulative growing degree days (G_{DC}) and cumulative irradiance (Q_C) following Monteith (1981) and water stress integral (S_θ) following Myers (1988). Growing degree days were calculated as the sum of daily median soil temperature at 100 mm depth minus the threshold below which growth was considered to cease (Monteith, 1981), chosen to be 6 °C (Ritchie and Nesmith, 1991; Gramig and Stoltenberg, 2007). Water stress integral was calculated as the sum of the daily differences between the seasonal maximum θ_s and daily mean θ_s (Myers, 1988; Watt et al., 2003).

3.2.4 Phytomass index

To account for changes in the biomass of the pasture on rates of CO₂ exchange between grazing events, a phytomass index was calculated following Lohila et al. (2004) (referred to as calculated P_i). For each day, the difference between mean value of F_N at night ($Q < 1 \mu\text{mol m}^{-2} \text{s}^{-1}$) and the value at saturating irradiance ($Q > 700 \mu\text{mol m}^{-2} \text{s}^{-1}$) was calculated and normalised to the maximum value measured at the peak of the growing season when rates of F_N were highest. Using an independent approach, data from the increase in biomass between grazing events and environmental variables were used to model the phytomass index (modelled P_i'). This approach combined modelled above-ground biomass (estimated from G_{DC} , Q_C and S_θ) and the environmental variables T_S measured at 20 and 100 mm depth, θ_s and Q . As these variables were strongly correlated, the inclusion of T_S and Q in the model was tested separately. A backwards stepwise regression approach was used to establish which of these variables had a significant effect on the phytomass index. The performance of the model for the phytomass index was tested by cross validation using the hold-out method (Ross, 2009). The data were split into two parts comprising data from alternate days. Half of the data were used to develop the model (training set) and the other half to test the model (testing set).

3.2.4.1 Models for CO₂ fluxes and statistical analyses

The components of the net ecosystem CO₂ exchange are described by:

$$F_N = R_E - A = R_L + R_S - A \quad (3.1)$$

where F_N is the net ecosystem CO₂ exchange (a negative value indicates a net uptake of CO₂), A is the uptake of carbon from photosynthesis and R_E is ecosystem respiration, comprising respiration from the leaves, R_L and soil respiration, R_S . Initially, each component was modelled separately. The response of gross photosynthesis (A) to irradiance (Q) was modelled with the widely used rectangular hyperbole (Luo et al., 2000) where

$$A = \frac{\alpha Q A_{max}}{\alpha Q + A_{max}} \quad (3.2)$$

α is the light use efficiency and A_{max} is the rate of gross photosynthesis under saturating irradiance.

The responses of R_S and R_E to soil temperature (T_s , °K) and soil water content (θ_s) both measured at a depth of 100 mm were modelled using an Arrhenius-type curve (Lloyd and Taylor, 1994) modified to include the effect of θ_s using a Gompertz function (Janssens et al., 2003; Bahn et al., 2008) where

$$R = R_{10} e^{E_0 \frac{1}{56.02} - \frac{1}{T_s - 227.13}} e^{-e^{(f - g\theta_s)}} \quad (3.3)$$

R refers to either R_S or R_E , R_{10} is the respiration rate at a basal temperature of 10 °C, E_0 is related to the activation energy of enzymatic reactions and f and g are parameters defining the shape of the sigmoidal response of R to θ_s .

Leaf respiration responds strongly to air temperature (T_a) (Tjoelker et al., 2001) and this was modelled using a similar Arrhenius-type curve where

$$R_L = R_{10} e^{E_0 \frac{1}{56.02} - \frac{1}{T_a - 227.13}} \quad (3.4)$$

Both night time and day time measurements from the chambers with opaque tops were used for measurements of R_S , and night time measurements from the chambers with transparent tops were used for R_E . Values of R_L were calculated for each hour at night time from the difference between mean measurements of R_E and R_S .

The calculated (P_i) and modelled (P_i') estimates of phytomass index were then included as multipliers in the models of components of F_N (Equations 3.2 to 3.4) to account for the effects of changes in biomass following grazing events.

For each hour during the day and for each chamber with a transparent top, gross photosynthesis (A) was calculated from the difference between measured F_N and modelled R_E , with daily R_E calculated from the mean measured R_S from the three chambers and modelled R_L from Equation 3.4 including calculated P_i .

Cross-validations using the hold-out method were done to test the predictive performance of each model described by Equations 3.2 to 3.4 and to compare the performance of the models including calculated P_i and modelled P_i' . The data were split into two parts comprising data for alternate hours to test the models for A , R_E , R_S and R_L .

Parameters from the fitted models for R_S , R_L and A were then combined and used to model hourly values of F_N , without the incorporation of the phytomass index (F_N) and with the incorporation of modelled $P_i'(F_N')$ and calculated $P_i(F_N'')$, such that

$$F_N = R_{10L} e^{E_{0L} \frac{1}{56.02} - \frac{1}{T_a - 227.13}} + R_{10S} e^{E_{0S} \frac{1}{56.02} - \frac{1}{T_s - 227.13}} e^{-e^{(f-g\theta_s)}} - \left(\frac{\alpha Q A_{max}}{\alpha Q + A_{max}} \right) \quad (3.5)$$

$$F_N' = P_i' R_{10L} e^{E_{0L} \frac{1}{56.02} - \frac{1}{T_a - 227.13}} + R_{10S} e^{E_{0S} \frac{1}{56.02} - \frac{1}{T_s - 227.13}} e^{-e^{(f-g\theta_s)}} - P_i' \left(\frac{\alpha Q A_{max}}{\alpha Q + A_{max}} \right) \quad (3.6)$$

$$F_N'' = P_i R_{10L} e^{E_{0L} \frac{1}{56.02} - \frac{1}{T_a - 227.13}} + R_{10S} e^{E_{0S} \frac{1}{56.02} - \frac{1}{T_s - 227.13}} e^{-e^{(f-g\theta_s)}} - P_i \left(\frac{\alpha Q A_{max}}{\alpha Q + A_{max}} \right) \quad (3.7)$$

Cumulative F_N was calculated in order to compare estimates of ecosystem CO_2 exchange over both measurement periods for measured and modelled values of F_N . Negative values indicate that the system is a net source of CO_2 .

All analyses were performed using R version 3.2.1 (R Development Core Team, 2014) using the non-linear mixed-effect models from the 'nlme' package (Pinheiro and Bates, 2014). Each measurement of F_N , R_S , R_E and each calculated value of A and R_L was treated as a sample. To account for non-independence of repeated measurements, replicate (chamber) number was included as a random effect in each model (except for R_L for which a single value was calculated for each hour) and a first-order autoregressive function was used. For the model cross-validations, root mean square errors (RMSE) and adjusted coefficients of determination (R^2) are reported. Uncertainties around estimates for cumulative F_N were evaluated as the 95% intervals of sets of 1 000 values of cumulative F_N (one set for each model and each period of measurements) generated using Monte Carlo simulations. The sets of parameters for F_N (A_{max} , α , R_{10L} , E_{0L} , R_{10S} , E_{0S} , f and g) were generated randomly from the variance-covariance tables from each fitted model (Equations 3.5, 3.6 and 3.7) using the 'MASS' package (Venables and Ripley, 2002).

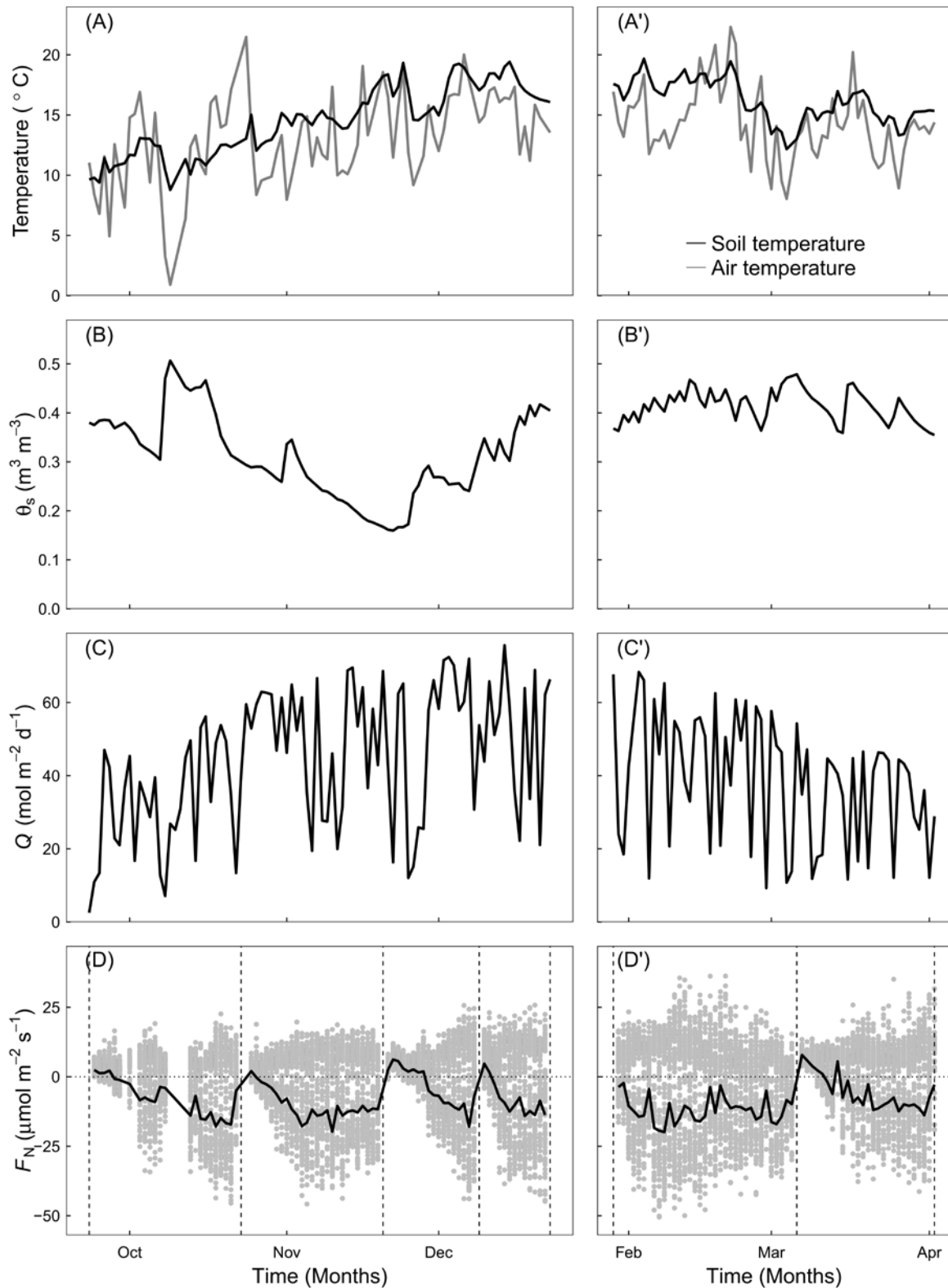


Figure 3.1: Variations in environmental variables at the Beacon Farm site for the two measurement periods (spring and early summer, and late summer to early autumn): (A and A') daily mean of soil temperature (T_s) at 100 mm depth (black line) and air temperature (T_a , grey line); (B and B') daily mean soil volumetric water content at 100 cm depth (θ_s); (C and C') daily total irradiance (Q) and (D and D') hourly values of F_N for each of the four clear chambers (grey points) and daily mean (black line). The vertical dashed lines show the timings of simulated grazing events.

3.3 Results

3.3.1 Growing conditions and seasonal variations

A storm in spring damaged the irrigation system over a period of two months when no irrigation was applied, resulting in soil volumetric water content (θ_s) falling to $0.16 \text{ m}^3 \text{ m}^{-3}$ (lower than the target of $0.25 \text{ m}^3 \text{ m}^{-3}$) in the middle of the first measurement period, in late spring (Figure 3.1A). This resulted in lower daily mean \pm standard error θ_s for the first measurement period, from October to late December of $0.32 \pm 0.01 \text{ m}^3 \text{ m}^{-3}$ compared with the value for the second measurement period from February to April of $0.41 \pm 0.01 \text{ m}^3 \text{ m}^{-3}$. With daily mean \pm standard error T_a of $12.2 \pm 0.4 \text{ }^\circ\text{C}$ and T_s of $13.4 \pm 0.4 \text{ }^\circ\text{C}$, the first measurement period was, overall, slightly cooler than the second measurement period ($T_a = 14.3 \pm 0.4 \text{ }^\circ\text{C}$ and $T_s = 16.2 \pm 0.2 \text{ }^\circ\text{C}$) (Figure 3.1B). Irradiance (Q) was very similar for both periods with maximum daily values being 75.6 and 68.3 $\text{mol m}^{-2} \text{ d}^{-1}$ and means of 42.6 ± 1.8 and $38.7 \pm 2.2 \text{ mol m}^{-2} \text{ d}^{-1}$ for the first and the second measurement period, respectively (Figure 3.1C).

All components of the ecosystem CO_2 exchange followed the pattern of temperature and soil volumetric water content, showing higher mean values for the second period (Table 3.1). Interestingly, the ratio of R_E to A remained similar (with 0.44 and 0.42 for the first and second period, respectively), showing that overall, photosynthesis and ecosystem respiration increased proportionally.

3.3.2 Effect of simulated grazing on F_N and phytomass index

There was a clear saw tooth pattern in net ecosystem CO_2 exchange (F_N) associated with each grazing event (Figure 3.1D). Immediately after grazing events, day time F_N was positive, indicating that ecosystem respiration exceeded photosynthesis, and the system continued to be a source of CO_2 during the subsequent few days. After this initial phase, daytime values of F_N became negative and showed values lower than $-30 \text{ } \mu\text{mol m}^{-2} \text{ s}^{-1}$ after each grazing event. Ecosystem respiration (night time F_N) decreased by over 25% on average just after grazing events and increased after grazing to

values frequently exceeding $20 \mu\text{mol m}^{-2} \text{s}^{-1}$ (Figure 3.1D). The contribution of R_S to R_E varied strongly from 22 to 98% but no clear pattern was observed following grazing events (data not shown). The mean contribution was similar for both periods with values of 64 ± 3 and $65 \pm 3\%$ for the first and second periods, respectively.

Table 3.1: Seasonal variations in the components of net ecosystem CO_2 exchange. Mean values of soil respiration (R_S), night time ecosystem respiration (R_E), and leaf respiration (R_L) calculated as the difference between hourly means of R_E and R_S are represented for the two measurement periods (spring and summer, 89 days, and late summer to early autumn, 62 days). Values are mean \pm standard errors.

	Spring and early summer	Late summer and early autumn
R_E ($\mu\text{mol m}^{-2} \text{s}^{-1}$)	8.50 ± 0.08	9.89 ± 0.11
R_S ($\mu\text{mol m}^{-2} \text{s}^{-1}$)	4.64 ± 0.03	5.75 ± 0.05
R_L ($\mu\text{mol m}^{-2} \text{s}^{-1}$)	4.21 ± 0.10	5.18 ± 0.16
A ($\mu\text{mol m}^{-2} \text{s}^{-1}$)	19.27 ± 0.23	23.40 ± 0.30

Above-ground biomass production between each grazing event was well described by the linear model including the three-way interaction of G_{DC} , Q_C and S_θ ($R^2 = 0.91$, $P < 0.0001$). Calculated phytomass index (P_i) followed a similar pattern, with values increasing rapidly from zero to high values (0.7-1.0) following grazing. In three instances, calculated P_i was even slightly negative on the first day after grazing, showing that F_N under saturating irradiance was positive and numerically greater than the night time value. When a scheduled grazing event was delayed by the farmer and grass was allowed to grow for a longer period of time, calculated P_i decreased to intermediate values (Figure 3.2A).

The model with the best fit to predict the phytomass index selected from the backwards stepwise regression incorporated the three-way interaction of G_{DC} , Q_C and S_θ with an additive effect of T_S measured at 20 mm depth and θ_S . Modelled phytomass index (P_i') followed a similar saw-tooth pattern as that displayed by F_N and calculated P_i (Figure 3.2A). Overall, this model performed well

(RMSE = 0.12, $R^2 = 0.61$), but values of modelled $P_i' > 0.7$ were underestimated by the model (Figure 3.2B).

Table 3.2: Summary results from the cross validations realised for models of ecosystem respiration (R_E), soil respiration (R_S), and leaf respiration (R_L) using the hold-out method. Root mean square errors (RMSE) and adjusted coefficient of determination (R^2) are given for values calculated on half the data set (testing set) using Equations 3.3 (R_E and R_S) and 3.4 (R_L), with no phytomass index, including calculated P_i and including modelled P_i' .

	model	$f(T_s, \theta_s)$	$f(T_s, \theta_s, P_i)$	$f(T_s, \theta_s, P_i')$
R_E	RMSE	4.14	4.20	4.31
	R^2	0.23	0.21	0.17
R_S	RMSE	2.05	2.99	2.55
	R^2	0.24	-0.61	-0.18
R_L	RMSE	2.90	2.45	2.63
	R^2	0.03	0.30	0.20

3.3.3 Model performances

Ecosystem respiration and its components R_S and R_L all increased with increasing temperature (T_s for R_E and R_S , or T_a for R_L) (Figure 3.3). Both R_E and R_S were affected significantly by soil volumetric water content (θ_s) ($P < 10^{-4}$). However, the predictive performance of models fitted using Equations 3.3 or 3.4 was rather low for R_S and R_E and extremely low for R_L (Table 3.2). There was considerable variation in the three components of respiration at the given temperatures (Figure 3.3), with R_S ranging from 0.5 to 16.3 $\mu\text{mol m}^{-2} \text{s}^{-1}$ and R_E from 0.7 to 36.2 $\mu\text{mol m}^{-2} \text{s}^{-1}$. For R_L , this was explained partially by the variation in the phytomass index, with R_L remaining low with increasing T_a at low values of P_i (Figure 3.3A). Accordingly, the model for R_L was clearly improved by including calculated P_i or modelled P_i' (Table 3.2). For R_E , variations in the phytomass index were also partially responsible for the high variability, with most low values of R_E at high temperatures corresponding with low values of calculated P_i (< 0.5) (Figure 3.3C). However, including calculated P_i or modelled P_i'

into the model for R_E did not increase its predictive performance (Table 3.2). Introducing P_i into the model for R_S (Figure 3.3B) considerably decreased its predictive performance, with R^2 becoming negative (Table 3.2).

In a few instances, gross photosynthesis (A) appeared to be negative. In most cases, these negative values of A were associated with low values of P_i (Figure 3.4) but some were associated with intermediate values of calculated P_i and relatively low values of irradiance ($Q < 500 \mu\text{mol m}^{-2} \text{s}^{-1}$) (Figure 3.4A). The response of A to Q was not well described by the model in Equation 3.2 (RMSE = 11.7, $R^2 = 0.36$) with marked variability in A at the same values for Q because of the variation in P_i (Figure 3.4A and B). Therefore, including modelled P_i' improved the model considerably (RMSE = 8.9, $R^2 = 0.63$, Figure 3.4C). Replacing modelled P_i' with calculated P_i further improved the model (RMSE = 7.2, $R^2 = 0.75$). In contrast to the P_i model, the P_i' model underestimated measured values of A greater than $50 \mu\text{mol m}^{-2} \text{s}^{-1}$ (Figure 3.4D).

The model for F_N from Equation 3.5, not including the phytomass index, predicted measured values of F_N well overall (RMSE = 8.5, $R^2 = 0.64$, Figure 3.5A). However, low values of P_i were associated with a strong underestimation of F_N , especially when values of F_N were strongly negative; and conversely, high values of P_i were associated with a strong overestimation of F_N (Figure 3.5A). The model in Equation 3.7, including P_i , showed the best predictive performance (RMSE = 6.1, $R^2 = 0.82$, Figure 3.5C). The model using Equation 3.6 (including modelled P_i') showed intermediate performance (RMSE = 7.0, $R^2 = 0.75$, Figure 3.5B), as it slightly overestimated strongly negative values of F_N (high daytime uptake of CO_2 by the system).

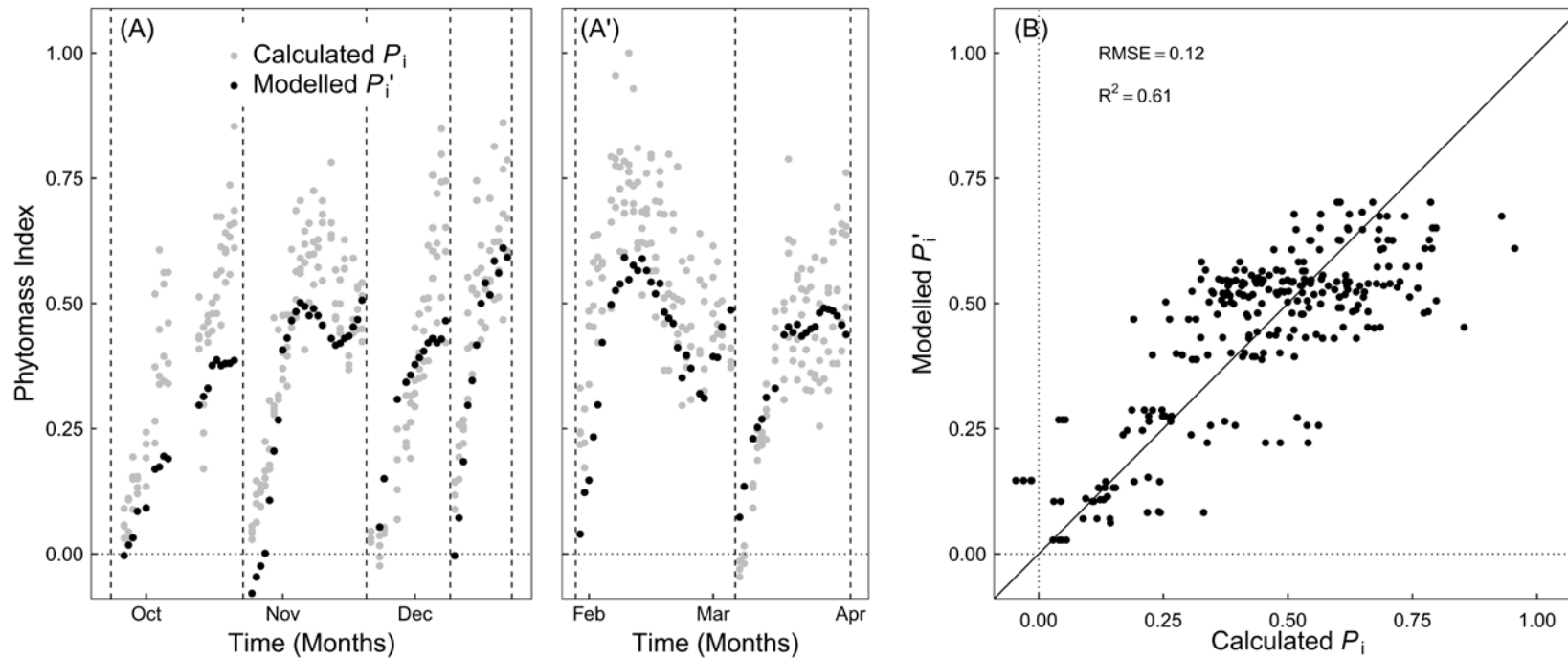


Figure 3.2: Calculated (P_i , grey symbols) and modelled (P_i' , black symbols) phytomass index for the site at Beacon Farm for the first measurement period (A, spring and early summer) and the second period (A', late summer to early autumn) and; (B) cross-validation for the model for the phytomass index. Parameters were derived from the model fitted on half the data set (training set) and the model cross-validation shown in (B) was performed on the other half (testing set) consisting of alternate days. The vertical dashed lines show the timings of simulated grazing events.

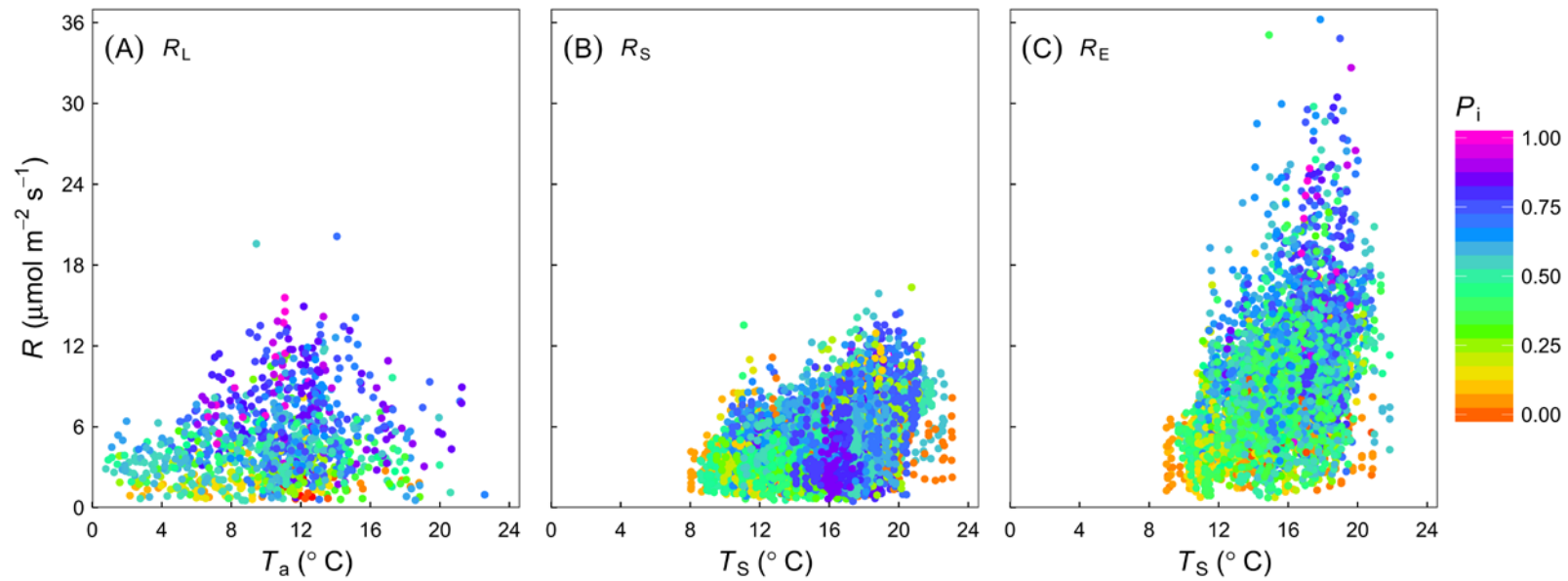


Figure 3.3: Response of: (A) leaf respiration (R_L) to air temperature (T_a), (B) soil respiration (R_S) to soil temperature (T_S), and (C) ecosystem respiration (R_E) to T_S . The symbols are hourly values of: (A) calculated R_L from the difference between hourly means of R_E and R_S , (B) the three dark chambers at night and day for R_S and (C) the four clear chambers at night for R_E . All data points are coloured according to the calculated phytomass index (P_i).

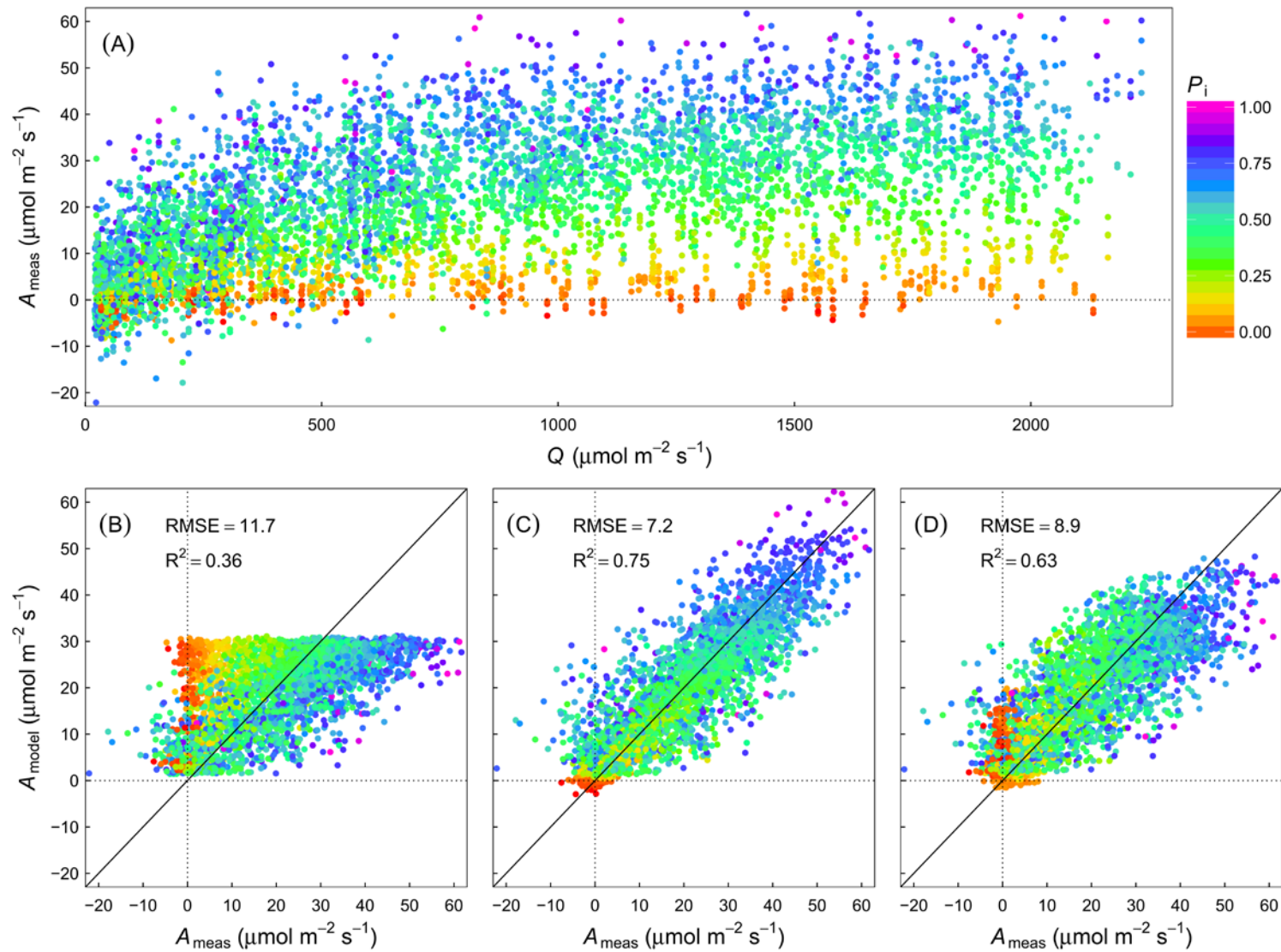


Figure 3.4: (A) Light response of measured day time gross photosynthesis (A_{meas}) to photosynthetically active radiation (Q), and hold-out cross validation of models fit with (B) standard light response model (Equation 3.2); (C) light response model including the calculated phytomass index (Equation 3.2 including P_i) and; (D) light response model including the modelled phytomass index (Equation 3.2 including P'_i). Model parameters were derived from models fitted on half the data set (training set) and the model cross-validations shown in (B), (C) and (D) were performed on the other half (testing set) consisting of alternate hours. The data are classified in relation to P_i as shown by the colours.

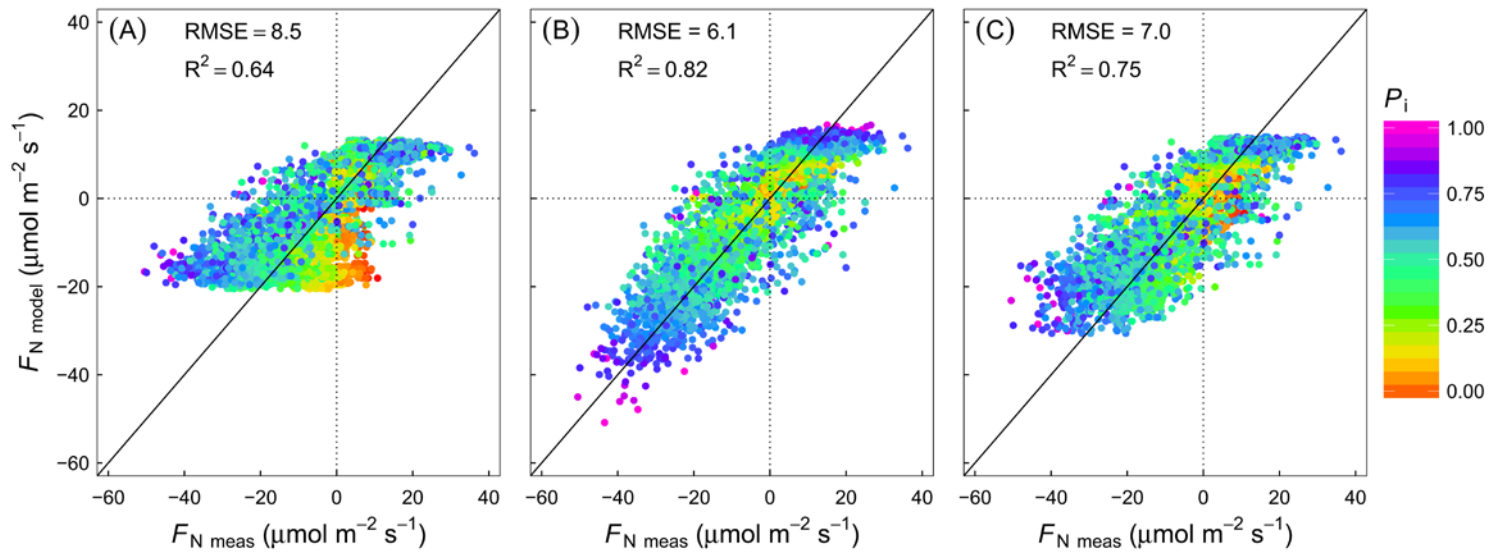


Figure 3.5: Cross-validations of models using the hold-out method for net ecosystem CO₂ exchange (F_N) fitted with the combination of models for soil respiration, leaf respiration and net photosynthesis: (A) without the phytomass index (Equation 3.5), (B) incorporating the calculated phytomass index (P_i , Equation 3.6) and (C) incorporating the modelled phytomass index (P'_i , Equation 3.7). The parameters were derived from models fitted on half the data set (training set) and the model cross-validations shown were performed on the other half (testing set) consisting of alternate hours. The data for F_N are classified in relation to P_i as shown by the colours.

3.3.4 Cumulative net ecosystem CO₂ exchange and net ecosystem carbon balance

Over both measurement periods, cumulative F_N decreased, indicating the ecosystem was a net sink for CO₂. This decrease was separated by short periods when the ecosystem was a source of CO₂ to the atmosphere immediately after grazing events (Figure 3.6). With 167.9 ± 20.2 gC m⁻² absorbed over 89 days, the mean rate of uptake was 1.88 ± 0.23 gC m⁻² d⁻¹ for the first period, in spring and early summer. The ecosystem showed slightly slower mean rates of uptake during the second period in late summer and early autumn of 1.47 ± 0.69 gC m⁻² d⁻¹.

Cumulative F_N estimated from the models that included calculated P_i (Equation 3.7) and modelled P_i' (Equation 3.6) fitted the data well and described well the dynamics of CO₂ exchange (Figure 3.6). Estimated cumulative values with their uncertainties at the end of each period appeared to be within one standard error of the mean of the measured values from the four chambers and were not significantly different (Table 3.3). In contrast, the model from Equation 3.5, not including the phytomass index, was not able to describe the alternating periods of increasing and decreasing CO₂ exchange observed from the measured values of cumulative F_N . Cumulative F_N presented a relatively steady decrease (compared with the measured values) for the first measurement period and an increase resulting in a positive value (indicating a CO₂ source) at the end of the second period (Figure 3.6). This resulted in significantly different estimates of cumulative F_N from those estimated from measured F_N for the second period, but not for the first period.

Table 3.3: Cumulated net ecosystem CO₂ exchange (F_N) during the two measurement periods (spring and summer, and late summer to early autumn). Cumulative F_N values are calculated from hourly measured and modelled values of F_N . Estimates from the model not including the phytomass index (Equation 3.5), the model including modelled phytomass index (Equation 3.6) and the model including calculated phytomass index (Equation 3.7) are shown. Values shown are mean (\pm standard error, n=4) from the four clear top chambers for the measured values. For the modelled estimates, the upper and lower limits of 95% intervals from the Monte Carlo simulations (1 000 runs) are included.

		Spring and early summer (89 days)			Late summer and early autumn (62 days)		
Measured (\pm standard error)	(gC m ⁻²)	-167.9 \pm 20.2			-91.5 \pm 42.5		
Modelled		estimate	2.5%	97.5%	estimate	2.5%	97.5%
Equation 3.5 (no P_i)	(gC m ⁻²)	-102.8	-176.4	-67.4	30.8	-23.6	60.5
Equation 3.6 (including P_i')	(gC m ⁻²)	-86.0	-150.9	-93.3	-34.7	-93.3	-38.0
Equation 3.7 (including P_i)	(gC m ⁻²)	-126.1	-196.7	-89.3	-55.0	-113.6	-23.2

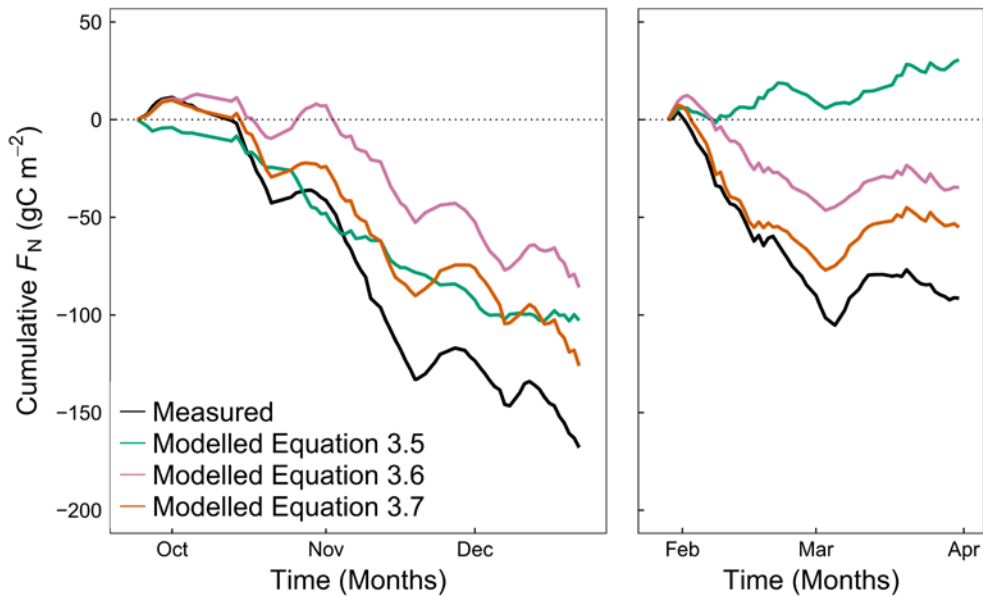


Figure 3.6: Cumulative net ecosystem CO₂ exchange (F_N) for the two measurement periods in spring and early summer (left panel), and late summer to early autumn (right panel) at the Beacon Farm site. Black lines represent measured values of F_N (mean of the four clear chambers). The green, pink and orange lines represent modelled values of F_N without the phytomass index (Equation 3.5), incorporating the calculated phytomass index (P_i , Equation 3.6), and incorporating the modelled phytomass index (P'_i , Equation 3.7), respectively.

3.4 Discussion

The use of the phytomass index has been demonstrated to improve estimations of F_N in rotationally grazed grasslands (Lohila et al., 2004) and has proven to be useful for gap-filling eddy covariance data when comparing carbon balance for sites with different grazing timings and intensities (Campbell et al., 2015). In my study, the use of chambers with transparent and opaque tops enabled us to test the application of the phytomass index to improve estimates of F_N as well as its components A , R_E , R_L and R_S . My findings show that the effects of grazing on F_N are attributable mainly to changes in the above-ground components, A and R_L associated with changes in leaf area. Furthermore, I was able to establish a model to predict the phytomass index from environmental variables. On this basis, I demonstrate that the use of the phytomass index could be extended in

accounting for the effect of grazing in models developed to estimate and predict carbon balance for grazed grasslands with changing environmental conditions and management practices.

3.4.1 *Phytomass index and components of net ecosystem CO₂ exchange*

Lohila et al. (2004) showed that P_i calculated from measurements of F_N followed the seasonal course of canopy leaf area closely. In my study, calculated P_i followed the cycles of above-ground biomass imposed by the timing of grazing events and subsequent recovery. Not surprisingly, my model for the phytomass index included the three-way interaction of G_{DC} , Q_C and S_θ used to model above-ground biomass harvested during grazing events. Because P_i is calculated from measurements of F_N at night and day time, the phytomass index also takes into account plant activity (Lohila et al., 2004) and this was accounted for by the significant response of the phytomass index to T_S and θ_S in my model.

The models including the phytomass index (both calculated and modelled) explained changes in A and R_L following grazing events much better than the same models not including the phytomass index. My findings are consistent with those from many earlier studies that demonstrate decreases and recovery in canopy photosynthesis and leaf respiration rates in grasslands associated with reductions in above-ground biomass with grazing and subsequent increases in leaf area (Detling et al., 1979; Parsons and Penning, 1988). However, predictive performances of the models for R_L and R_E remained relatively poor even when calculated P_i or modelled P_i' was included. Leaf respiration was calculated from R_E and R_S measured from different sites (chambers) and R_S represented over two third of R_E . I attribute the poor performances of the models for R_E and R_L to the high variability observed in R_S . In addition, although R_L depends on total leaf area, initial increases after grazing have been observed due to a wounding response of the leaves (Macnicol, 1976; Chapter 2). Such a mechanism would have weakened the linear increase of R_L with the phytomass index and thus weakened my models of R_L .

There is evidence that changes in the supply of photosynthetic assimilates below-ground are important for regulating R_S (Högberg and Read, 2006; Trumbore, 2006). Removal of foliage by

clipping has been reported to result in short term changes in R_s concurrently with decreased photosynthesis in grasslands (Bremer et al., 1998; Bahn et al., 2006). The poor explanatory ability of my models does suggest that R_s is responding to variables other than T_s and θ_s and the responses could be different for different time scales from hours to years (Bahn et al., 2008; Kuzyakov and Gavrichkova, 2010). There is an opportunity to explore correlations between photosynthesis and R_s on different timescales and multi-temporal scales using more recent research techniques such as wavelet coherence analyses (Vargas et al., 2010, 2011). Instead, the use of the phytomass index is a coarse estimation of above-ground ecosystem activity based on daily changes in driving variables. Therefore, it is not a suitable tool to account for time lags in relationships occurring within a day, or for the correlations between soil temperature and irradiance, recognised to be a source of error in accounting for the effects of A on R_s (Kuzyakov and Gavrichkova, 2010). In my study, including phytomass index did not improve the response of R_s to soil temperature and soil water content. This shows that grazing events affected F_N mainly through above-ground processes with no significant short-term effects on R_s at a daily (but not necessarily hourly) timescale, consistent with findings from earlier studies (Rogiers et al., 2004; Nieveen et al., 2005; Chapter 2).

3.4.2 *Grazing effects on the net ecosystem CO₂ exchange*

At this intensively managed dairy grassland, net ecosystem CO₂ exchange (F_N) measured using the chambers was affected strongly by grazing events. I observed a 'saw-tooth' pattern similar to that in previous studies investigating the effect of grazing animals on F_N using eddy covariance (Soussana et al., 2007; Wohlfahrt et al., 2008; Campbell et al., 2015; Hunt et al., 2016). The system appeared to be a sink for CO₂, with a small difference in the rate of CO₂ uptake between the two measurement periods.

The model including modelled P_1' performed well in estimating F_N although the predictive performance for the model including calculated P_1 was better. Estimations of cumulative net CO₂ uptake from both these models were not significantly different and appeared equally good in accounting for the effect of grazing on the cumulative net CO₂ exchange. The model that did not

include the phytomass index described the components of F_N poorly, and also resulted in erroneous estimation of cumulative F_N at the end of the second period of measurement. Although this was not the case for the first period, my results suggest that not accounting for variations in the above-ground biomass through grazing cycles produces unreliable and potentially significantly biased estimates of the net ecosystem CO_2 balance.

3.5 Conclusions

Removal and regrowth of the above-ground components of the vegetation following grazing events resulted in significant cycles on the ecosystem CO_2 balance at this intensively managed grassland site. The effects were dominated by changes induced on canopy photosynthesis and respiration. I showed that these effects could be accounted for by introducing estimates of a phytomass index to account for variability in F_N , A and R_L through grazing cycles. I demonstrated this by calculating changes in the phytomass index from direct measurements of ecosystem CO_2 exchange and I was also able to model the phytomass index using environmental variables. I show that not accounting for the effect of grazing could severely mislead conclusions on the net ecosystem CO_2 exchange of grazed grassland, and therefore on net ecosystem carbon balance. I contend that modelling a phytomass index can be used as an approach for improving models of grazed grassland ecosystem carbon balance and allowing improved prediction of the effects of changing climate and farm management practices.

**CHAPTER 4 Soil heterotrophic respiration is insensitive to changes in soil
water content but related to microbial access to organic matter**

4.1 Introduction

Soil organic matter has long been known to be critically important to maintain ecosystem services, including sustainable production of food and fibre, water retention and biodiversity (Jenny, 1941; Miller and Donahue, 1990; Powlson et al., 2011). Findings from the past few decades have supported the concept that the chemical structure of soil organic matter regulates its microbial degradation and that the existence of compounds in the soil, referred to as ‘humic substances’, are inherently recalcitrant to microbial degradation (Schmidt et al., 2011; Lehmann and Kleber, 2015). However, recent research is challenging this contention, with findings showing that the chemical structure of organic matter is unrelated to its residence time (Marschner et al., 2008; Kleber and Johnson, 2010; Schmidt et al., 2011). The emerging interpretation is that microbial access to substrate is regulating soil organic matter cycling, with chemical recalcitrance restricted to a marginal role (Schmidt et al., 2011; Dungait et al., 2012; Lehmann and Kleber, 2015). The idea of limited substrate availability to microbes within the soil matrix casts doubt on major assumptions used in models that address the response of soil carbon exchange to climate change, especially the description of the response of soil organic matter decay to temperature (Davidson and Janssens, 2006) and water status (Moyano, 2013). New experimental approaches to characterise the relative importance of chemical recalcitrance and physical protection of soil organic matter in regulating the stability and decay of soil organic matter are required (Schmidt et al., 2011; Dungait et al., 2012; Lehmann and Kleber, 2015).

In terrestrial ecosystems, the rate of soil respiration (R_S) is the largest component (60-90%) of CO_2 losses from the soil to the atmosphere (Longdoz et al., 2000) and is the result of two processes: root and rhizosphere respiration (autotrophic respiration, R_A), and microbial decomposition of soil organic matter (heterotrophic respiration, R_H). Because R_A has little effect on long-term changes in soil organic matter (Kuzyakov, 2006), understanding the variables regulating R_H , independent from those regulating R_S and R_A , is critically important to forecast future changes in soil organic matter stocks and, subsequently, changes in the atmospheric CO_2 concentration. Empirical evidence for

concluding the dominance of chemical recalcitrance in regulating soil organic matter turnover is derived mainly from studies involving laboratory incubations on samples removed from the soil (Kirschbaum, 1995; Davidson and Janssens, 2006; Manzoni et al., 2012). Alternatively, observations have been made from field studies using techniques that disturb the soil environment and remove the autotrophic component to measure R_H , for example by trenching, shading or burning the vegetation (Kuzyakov, 2006). These techniques potentially overlook the direct effects of the roots and the rhizosphere on R_H (Subke et al., 2006; Paterson et al., 2009). Soil structure is linked intimately to the processes that stabilise organic matter and protect it from microbial degradation. These mechanisms include the formation of aggregates that isolate the substrate and its binding to silt and clay particles (Six et al., 2000; 2002). These stabilisation mechanisms create conditions in which the substrate concentration located near to decomposers is reduced within the soil matrix (Davidson and Janssens, 2006; Dungait et al., 2011). The formation of aggregates and their stability result from complex interactions within the soil matrix, involving the whole soil biota, including roots (Bronick and Lal, 2005). Zakharova et al. (2014) showed that physical disturbance of soil resulted in the release of previously protected labile sources of carbon that became accessible for microbial degradation. Modifying the aggregation structure of the soil through physical extraction, including sieving and/or root removal, creates an artificial environment in which microbial access to chemically labile organic matter is temporarily unlimited (Zakharova et al., 2014). Thus, results from studies that modify soil structure, or supply the soil with substrate for microbial degradation, must be interpreted with caution, because they are likely to underestimate the importance of organic matter protection in regulating soil organic matter decomposition.

Application of stable carbon isotope techniques have provided the opportunity to investigate the variables regulating R_H in field conditions while avoiding disturbance of soil structure (Kuzyakov, 2006; Subke et al., 2006; Paterson et al., 2009). These methods are based on measurable differences in the ^{13}C isotopic signatures ($\delta^{13}\text{C}$) of the CO_2 respired from R_H and R_A ($\delta^{13}\text{C}_{R_A}$ and $\delta^{13}\text{C}_{R_H}$, respectively). Most studies to date have used C_3/C_4 plant isotopic shifts to amplify the difference

between $\delta^{13}C_{RA}$ and $\delta^{13}C_{RH}$. In C_3 ecosystems $\delta^{13}C_{RH}$ is typically 2-4‰ enriched compared with the values of $\delta^{13}C_{RA}$ (Bowling et al., 2008). This difference has been shown to be measurable (Midwood et al., 2008) and extends the application of the natural abundance of ^{13}C to C_3 systems more generally (Millard et al., 2010; Graham et al., 2012; Snell et al., 2014; Chapter 2).

Considerable effort has been undertaken to relate fractions of soil organic matter that can be separated chemically or physically to theoretical pools of carbon of biological relevance, with different turnover times (Wander, 2004; von Lützow et al., 2007). Isolating fractions representing a passive carbon pool has proven to be particularly difficult, but labile fractions have been identified with more success (von Lützow et al., 2007). This has been achieved using water soluble organic matter fractions, including dissolved and hot water extractable organic matter (Ghani et al., 2003; Gregorich et al., 2003). These methods assume that easily degradable substrate will be more water soluble than other fractions of soil organic matter (McLauchlan and Hobbie, 2004). Thus, the 'lability' of the carbon isolated through this method is defined by its chemical structure. To relate fractions more closely to bioavailability, particulate organic matter can also be isolated by physical fractionation on the basis of particle size. Different particle sizes represent different aggregate levels providing different degree of physical protection to organic matter (Six et al., 2002). Small particle sizes (53–2000 μm) are defined as the organic matter not bound to mineral particles (Gregorich et al., 2006), which define higher level of organic matter protection (Six et al., 2002). Coarse (250–2000 μm , macro-organic matter) and fine (53–250 μm , particulate organic matter) fractions can be distinguished (Willson et al., 2001; Wander, 2004). Six et al. (2001) defined the coarse fraction as unprotected and the fine fraction as the first level of physical protection. Here, the lability of the carbon is defined by its degree of physical protection, with decreasing particle size providing higher degree of protection (e.g. reduced lability) by isolation from microbial biomass and reduced oxygen diffusion. These labile fractions (e.g. macro-organic matter and particulate organic matter) often show correlation with total soil organic carbon content (McLauchlan and Hobbie, 2004) and the proportions of each fraction have been used as early indicators to forecast changes in soil organic

matter levels under different land management practices and environmental conditions (Ghani et al., 2003; Gregorich et al., 2006). Specific surface area (S_A) of the soil can also be measured as an indicator of physical protection to organic matter (Parfitt et al., 2001; Kahle et al., 2002) and was related to the mean residence time of added labile carbon in soils of different mineralogy (Saggar et al., 1999). Parfitt et al. (2001) provided a rapid easy method to measure S_A in similar soils in New Zealand, based on the water content of air-dried soil samples. As specific surface area largely resides in the clay fraction (Parfitt et al., 2001), this may provide a higher degree of protection compared to the fine and coarse particle size fractions defined above and thus provides an easy indicator to estimate the degree of protection. In this study, an approach is proposed to relate estimates of R_H and R_A in an undisturbed pure C_3 grassland to both environmental fluctuations and indicators of physical soil protection of soil organic matter. I partition the components of R_S and estimate values of R_H , R_A and the fraction of R_S attributable to R_H , fR_H , using the natural abundance ^{13}C technique in a factorial field experiment with treatments that manipulated water and nitrogen availability, with relevance to the widespread pastoral agriculture intensification in New Zealand, where irrigation and addition of nitrogen fertiliser are applied. I relate estimates of R_H and R_A to chemically (hot water extractable carbon) and physically (macro and particulate organic matter) defined labile pools of carbon as well as soil specific surface area, an indicator of organic matter protection capacity. My objectives were to (i) observe the effects of the irrigation and nitrogen addition treatments on respiration rates and labile fractions of soil organic matter and (ii) test the hypothesis that R_H , as opposed to R_A , is under the control of both environmental fluctuations and the availability of soil organic matter.

4.2 Materials and methods

4.2.1 Site description

The measurements were made at a field site located at Ashley Dene Farm, Lincoln, Canterbury, New Zealand (latitude 43.40° S, longitude 172.20° E, elevation 35 m above sea level). The site was

flat and had been managed under extensive sheep farming for more than 50 years prior to the experiment, with no irrigation and no input of nitrogen fertiliser. The soil was a deep stony silt loam, excessively drained and described as a mixture of Balmoral and Lismore according to New Zealand classification (Hewitt, 2010).

4.2.2 *Experimental design*

The experimental design consisted of six circular plots with a radius of 2 m (area 12.5 m²) distributed in a 50 by 30 m area. Three plots were selected randomly for irrigation (treatment I₁), and the three remaining plots were left unirrigated (treatment I₀). Within each plot, half was selected randomly for the addition of mineral nitrogen fertiliser (treatment N₁), and the other half was left with no fertiliser added (treatment N₀). The experimental layout was a full factorial design with the nitrogen treatment nested in the irrigation treatment, and with three replicates of each of the four combinations, for a total of twelve semi-circular plots: non-irrigated / non-fertilised (control, I₀N₀), non-irrigated / fertilised (I₀N₁), irrigated / non-fertilised (I₁N₀) and irrigated / fertilised (I₁N₁). The treatments were first applied early spring (October 2014).

The circular plots were split in a north-south direction for the nitrogen treatments to avoid differences in incident irradiance. Sprinklers were placed at a height of 2 m above the centre of each of the irrigated plots, allowing irrigation of the whole surface area with 15 mm of water every three days. When wind speed was high, irrigation was delayed to avoid uneven distribution of water within each plot and loss of water to the surrounding areas. To simulate rotational grazing by animals, the grass was clipped every three weeks and nitrogen fertiliser, in the form of 17 g of NH₄NO₃ diluted in 10 L of water, was applied evenly over the whole plot using a watering can, equivalent to 10 kgN ha⁻¹ for each application (roughly equivalent to 200 kgN ha⁻¹ y⁻¹). The non-fertilised plots were treated by adding 10 L of water only. Environmental variables were recorded at half-hourly intervals on each day of measurements while partitioning measurements were being made. These included air temperature (T_a), relative humidity (humidity and temperature transmitter, model Humitter 50U/50Y(X), Vasaila, Helsinki, Finland) and wind speed (anemometer, model

A101M, Vector Instruments, Clwyd, UK). Measurements of soil temperature at a depth of 50 and 100 mm (T_s , thermocouples, Type E, Omega Engineering Ltd., Stamford, CT, USA) and volumetric soil water content 80 mm (θ_s , soil moisture sensor model ML3, Delta-T Devices Ltd., Cambridge, UK) were made at a random location in each of the twelve plots. Rainfall was recorded starting a month prior to each campaign (rain gauge, model TE525, Campbell Scientific Inc., Logan UT, USA).

Two campaigns of measurements were undertaken. The first was in spring (November, spring campaign), one month after the start of the treatments, and the second in late summer (March, summer campaign) of the same growing season, six months after the start of the treatments. For each campaign, two weeks prior to the measurements, two PVC collars (100 mm diameter, 70 mm deep) were placed at random locations in each of the twelve plots to a depth of 25 mm for measurements of R_s and $\delta^{13}CR_s$. Measurements were made at least six days after clipping and 36 hours after rain or irrigation events.

4.2.3 Natural abundance carbon isotope technique

The natural abundance carbon isotopic techniques requires the measurement of ^{13}C isotopic signatures of the CO_2 respired from the undisturbed soil ($\delta^{13}CR_s$) as well as the isotopic signatures of respiration from soil organic matter turnover ($\delta^{13}CR_H$) and that from roots and associated microbes ($\delta^{13}CR_A$). $\delta^{13}CO_2$ values derived from root and soil organic matter represent the two end-members for a simple linear mixing model to determine the proportion of R_H (fR_H) and R_A (fR_A) contributing to total R_s . R_H and R_A can then be calculated by multiplying R_s by fR_H and fR_A , respectively, such that

$$fR_H = 1 - \frac{(\delta^{13}CR_s - \delta^{13}CR_H)}{(\delta^{13}CR_A - \delta^{13}CR_H)} \quad (4.1)$$

and

$$fR_A = 1 - fR_H. \quad (4.2)$$

4.2.4 Measurements of $\delta^{13}CR_s$

Simultaneous measurements of $\delta^{13}CR_s$ from six locations were made by collecting air respired from the soil surface using a partially automated open chambers system as described by Midwood et

al. (2008). The chambers were placed on the collars set in the soil and pressed on high density foam to form a seal. After the CO₂ concentration in the chamber was steady on a target of 450 μmol mol⁻¹, approximately 500 ml of respired air was collected into Tedlar® bags that were flushed twice with CO₂ free air and evacuated prior to use. To achieve the target concentration of 450 μmol mol⁻¹, the CO₂ free air entering the chamber and the surface efflux leaving the chamber were controlled using mass flow controllers, with a lower precision limit of 200 ml min⁻¹ (model FMA5510, Omega Engineering Ltd., Stamford, CT, USA). At low respiration rates, less than 2 μmol m² s⁻¹, the flow of CO₂ free air entering the chamber required to reach the target concentration is less than 200 ml min⁻¹. At this flow rate, the mass flow controllers become unreliable and were likely to provide excess flow resulting in the CO₂ concentration in the chamber being less than 450 μmol mol⁻¹. To exclude any artefacts resulting from this change in concentration, measurements where soil respiration rates (R_s) was less than 2 μmol m² s⁻¹ were discarded, resulting in the loss of nine replicates overall (one, three and four for the I₁N₁, I₀N₁ and I₀N₀ treatments, respectively, during the spring campaign, and one from the I₀N₁ treatment during the summer campaign). Furthermore, with the open chamber system, the rate of soil respiration is calculated from the measured CO₂ concentration in the chamber and the flows in and out of the chambers, provided by the mass flow controllers. Since these flows are unreliable when R_s was less than 2 μmol m² s⁻¹, estimation of R_s also becomes unreliable. To overcome this problem, within a few minutes after the collection of air, each chamber was removed from the collars and R_s was measured using a closed dynamic system (model LI-8100, LI-COR Inc., Lincoln, NE, USA).

4.2.4.1 Heterotrophic end member incubations and extrapolation technique

The instability in ¹³C respired from roots after excision is species-specific (Midwood et al., 2006) but δ¹³CR_A has been shown to remain stable up to 2.5 h in ryegrass mesocosms (Chapter 2). However, shifts in δ¹³CR_H have been shown to change exponentially with time after a soil core is extracted (Millard et al., 2010; Snell et al., 2014; Zakharova et al., 2015, 2014). Thus there is a need to operate as rapidly as possible so that the measured value δ¹³CR_H is as close as possible to the

value prior to disturbance (time zero), but also to wait long enough for the CO₂ concentration in the bag to be within the range 250-750 μmol mol⁻¹ needed to ensure optimum precision for the isotope analysis. This practical limitation often prevents the measurement of δ¹³CR_H to be made consistently at a given time after time zero. To overcome this, Snell et al. (2014) suggested that back extrapolation of values of δ¹³CR_H to the time zero using regression analysis would be a consistent and practical way to estimate δ¹³CR_H. However, the exact timing of the start of the exponential decrease in δ¹³CR_H prior to 5 min after excavation of the soil core is unknown. To improve the estimation of δ¹³CR_H, I tested and used an approach using regression to extrapolate measurements backwards to the values at the minimum practical time of 4 min after disturbance (Appendix A).

4.2.5 Measurements of δ¹³CR_H and δ¹³CR_A

Measurements of the isotopic signatures of the end members for root-free soil (δ¹³CR_H) and roots (δ¹³CR_A) were made following the technique described by Millard et al. (2010) and Snell et al. (2014). After R_S had been measured, samples of roots and soils were collected. The collars were removed and soil cores were extracted using a 100 mm diameter steel tube hammered into the soil to a depth of 200 mm. The soil from the core was broken up loosely and roots and stones were removed by hand and discarded. The root-free soil and the roots were placed into different air tight bags (Tedlar® Keika Ventures, Chapel Hill, NC, USA). The bags were sealed then flushed quickly three times and filled with approximately 500 ml of CO₂ free air. After an incubation period, typically 5 to 7 min for the root-free soils and 2.5 h for the roots, an aliquot of gas was removed and the CO₂ concentration checked to make sure it fell within the range 250-750 μmol mol⁻¹. The air in the bags was then sampled for measurements of δ¹³CO₂.

All gas samples were analysed for δ¹³C values using a tunable diode laser (TDL) (TGA100A; Campbell Scientific Inc., Logan UT, USA) with an instrument precision of 0.2‰.

4.2.6 Soil analyses

After measurement, the root-free soils were mixed thoroughly and a subsample from each soil core (approximately 50 g) was placed in a plastic bag and stored at -4°C . The soil samples were analysed subsequently for hot water extractable carbon (C_{HW}), dissolved organic carbon (C_{D}), specific surface area (S_{A}), macro-organic matter (C_{MOM}) and particulate organic matter (C_{POM}). Prior to analysis, the soil samples were weighed, air dried at 30°C for 24 hours and sieved through a 2 mm sieve. Total soil carbon (C_{tot}) and nitrogen (N_{tot}) concentrations were also analysed, using a CN analyser (model TruMAc, Leco Corporation, USA), from subsamples (approximately 1 g) that were pre-ground with a mortar and pestle.

4.2.6.1 Chemical extractions for carbon fractions

The methods for chemical extraction were adapted from the protocol described by Ghani et al. (2003). Subsamples (3 g) were weighed into centrifuge vials, 30 ml of deionised water added, and the vials were capped and shaken for 30 minutes. The vials were then centrifuged for 20 minutes at $2\ 942\ \text{g}$ and the supernatant filtered to $0.45\ \mu\text{m}$ through filter paper (Advantec 5C filter paper) into vials for analysis of C_{D} . The vials with the soil and the remaining water were weighed. An additional 30 ml of deionised water was added and the vials were capped and shaken to re-suspend the soil. The vials were placed in a hot water bath at 80°C for 16 hours and then centrifuged for 20 minutes. The supernatant was filtered through $0.45\ \mu\text{m}$ using filter paper into vials for analysis of C_{HW} . Hot water extractable carbon and dissolved organic carbon were measured on a carbon analyser (model 5000A analyser, Shimadzu, Tokyo, Japan).

4.2.6.2 Specific surface area and gravimetric water content

The specific soil surface area was calculated from the water content of air-dried soil (w_{ad}), using the linear regression reported by Parfitt et al. (2001) where

$$S_{\text{A}} = 2 w_{\text{ad}} \quad (4.3)$$

and w_{ad} was calculated from the difference in mass between the air-dried soil (30° C for 24 hours) and oven-dried soil (105° C to a constant mass). Gravimetric water content (W_s) was calculated as the ratio of the mass of water lost by oven drying and the mass of oven dried soil (Gardner, 1986).

4.2.6.3 Physical fractionation of macro and particulate organic matter

Particulate organic matter was separated into size fractions using the protocol described by Willson et al. (2001). Subsamples of 20 g were weighed into glass beakers and 60 ml of deionised water added. An ultrasonic probe (model Sonoplus HD 2200, mean power output 63.6 W; Bandelin Electronic, Berlin, Germany) was used to disperse particles in a 60 s treatment. The suspension was washed through two successive metal sieves with pore diameters of 250 and 53 μm . Both size fractions (250-2000 μm , macro-organic matter and 53-250 μm , particulate organic matter) were analysed for carbon and nitrogen concentration with a CN analyser (model TruMAc, Leco Corporation, USA).

4.2.7 Statistical analyses

All statistical analyses were conducted using R version 3.2.1 (R Development Core Team, 2014). To characterise changes in environmental variables between the two measurement campaigns, half hourly measurements recorded during the partitioning process were averaged for both campaigns and compared using the Students *t*-test.

Changes in soil properties (C_D , C_{HW} , S_A , C_{MOM} , C_{POM} , C_{tot} and N_{tot}), environmental variables (T_s , W_s) and components of respiration (R_s , R_A , R_H , and fR_H , $\delta^{13}CR_s$, $\delta^{13}CR_A$ and $\delta^{13}CR_H$) with irrigation and nitrogen treatments were tested with linear mixed-effect models using the 'nlme' package (Pinheiro and Bates, 2014). For each of these variables, the effects of irrigation and nitrogen addition factors and their interaction were assessed separately for each campaign. The nested structure of the experimental design was included as random effect as plot/nitrogen treatment/replicate, where 'plot' is a factor discerning the six circular treatment plots. To distinguish between the effect of changing environmental variables between the two campaigns and the effect of irrigation and

nitrogen treatments, Student *t*-tests were conducted to test for differences in the control treatment (I_0N_0) between the two campaigns.

Respiration rates were modelled separately for R_S , R_A and R_H . All models included the nested structure of the design as random effect using irrigation/plot/nitrogen/replicate factors. An Arrhenius type function describing the response of respiration to T_S (Lloyd and Taylor, 1994, Equation 4.4) and a non-linear function describing the response of respiration to W_S (Bahn et al., 2008, Equation 4.5) were fitted separately, combined, and then compared to linear functions of T_S , W_S and their interaction using the Akaike's Information Criterion corrected for small sample size (AIC_C).

$$R = R_{10}^{E_0 \left(\frac{1}{56.02} - \frac{1}{T_S - 227.13} \right)} \quad (4.4)$$

$$R = e^{-e^{(a-bW_S)}} \quad (4.5)$$

I used W_S in the models to describe the responses of respiration to soil water content because measurements were integrating the whole depth of the soil cores for each replicate. The inclusion of T_S in the models was tested and compared for measurements made at 50 and 100 mm deep.

To test for the effects of soil properties on respiration rates, a multiple regression analysis was conducted. Based on the models, linear relationships between respiration rates and T_S and W_S were used. A candidate set of models was established to identify which of the soil properties and/or T_S and W_S and their combinations best explained the variability in R_S , R_H and R_A . The models were ranked using the AIC_C to determine the Kullback-Leibler (KL) best model (Burnham and Anderson, 2002). The AIC_C identifies the model(s) most strongly supported by the data and is based on bias-corrected, maximized log-likelihood (LogLik) of the fitted model with a penalty for the number of parameters used. The model with the smallest AIC_C ($AIC_{C_{min}}$) is the most strongly supported. The ΔAIC_C value is calculated for each model i as $\Delta_i = AIC_{C_i} - AIC_{C_{min}}$. Following convention, models with $\Delta_i < 2$ are substantially supported by the data; whereas models with $\Delta_i > 2$ indicate considerably less or no support (Anderson, 2007). A measure of the strength of support for either model is described by the model probability (Akaike weights, A_{wi}). This is the probability that model i is the KL best

model, given the data and candidate set of models (Anderson, 2007). The sum of A_{wi} of the models in a candidate set equates to 1.

4.3 Results

4.3.1 *Climate and control plots during the two campaigns*

During the measurements for the spring campaign the air was significantly cooler and less humid and wind speed was higher compared with the conditions for the summer campaign (Table 1). Rainfall was lower during the spring campaign, with 26 mm in the month before the first day of measurement compared with 52 mm prior to the start of the summer campaign. Volumetric soil water content (θ_s) for the soils in the control plots (I_0N_0) was significantly lower in the spring campaign than that for the summer campaign and soil temperature was significantly higher (Table 4.1). Ranges in air temperatures were very similar for both campaigns, with minima of 8 and 10 °C for the spring and summer campaigns, respectively, and the same maximum temperature of 24 °C. However, soil temperatures measured at 50 mm deep ranged from 14 to over 30 °C during the spring campaign, whereas temperatures were contained within the range 13 to 22 °C during the summer campaign.

Soil characteristics measured in the control plots (I_0N_0) did not show significant differences between the two campaigns. Similarly, there were no differences between the two campaigns in the isotopic signatures of respired CO_2 by the soil and the two end members ($\delta^{13}CR_s$, $\delta^{13}CR_H$, $\delta^{13}CR_A$), the rates of soil, autotrophic or heterotrophic respiration (R_s , R_H , R_A) and the proportion of heterotrophic respiration contributing to total soil respiration (fR_H).

4.3.2 *Differences between the treatments*

4.3.2.1 Isotopic signatures and partitioning

There were no significant differences for $\delta^{13}CR_H$, $\delta^{13}CR_A$, $\delta^{13}CR_s$ or fR_H between the nitrogen treatments and the interactions between the nitrogen and irrigation treatments for these variables

were not significant (Table 4.2). In contrast, the value of $\delta^{13}CR_A$ was enriched for the I_0 treatment compared with that for the I_1 treatment, but the difference was not significant (spring campaign) or marginally significant (summer campaign). $\delta^{13}CR_S$ followed the same trend, but the difference was significant for the summer campaign (Table 4.2). During the summer campaign only, $\delta^{13}CR_H$ for the I_0 treatment was depleted significantly compared with that for the I_1 treatment. For the I_0 treatment, fR_H was larger compared with the value for the I_1 treatment and this difference was smaller for the spring campaign compared to the summer campaign when it was marginally significant (Table 4.2).

Table 4.1: Environmental variables during the campaigns in spring, one month after treatments started and in summer, six months after the treatments started. Soil temperature and soil volumetric water content were measured in the control, non-irrigated and non-fertilised plots. Only soil temperature measured at a depth of 50 mm is represented. The P-values are from Student *t*-tests comparing means between the two campaigns. Values for each campaign are means of half-hourly values recorded on each day when measurements for partitioning were made. All values shown are mean \pm standard error.

	Spring campaign	Summer campaign	P-value
Air temperature (°C)	16.9 \pm 0.1	18.0 \pm 0.1	< 0.001
Air saturation deficit (kPa)	0.83 \pm 0.1	0.72 \pm 0.1	< 0.001
Wind speed (m s ⁻¹)	2.9 \pm 0.1	2.0 \pm 0.1	< 0.001
Rainfall (mm)	26	52	
Volumetric soil water content (%)	0.14 \pm 0.01	0.23 \pm 0.01	< 0.001
Soil temperature (°C)	19.2 \pm 0.2	17.6 \pm 0.1	< 0.001

Overall, the isotopic signature from CO₂ respired from soil ($\delta^{13}CR_S$) was (mean \pm standard error) 3.2 \pm 0.5 and 2.3 \pm 0.6‰ more enriched compared to values of $\delta^{13}CR_A$ for the spring and summer campaigns, respectively. $\delta^{13}CR_S$ was 3.5 \pm 0.5 and 3.0 \pm 0.4‰ depleted compared to the back-extrapolated to 4 min value of $\delta^{13}CR_H$, for the spring and summer campaigns, respectively. For one replicate the back-extrapolated value of $\delta^{13}CR_H$ was depleted compared to $\delta^{13}CR_S$. This difference of

0.2‰ was close to the detection limit of the instrument and the value of fR_H for that replicate was constrained to be 1.

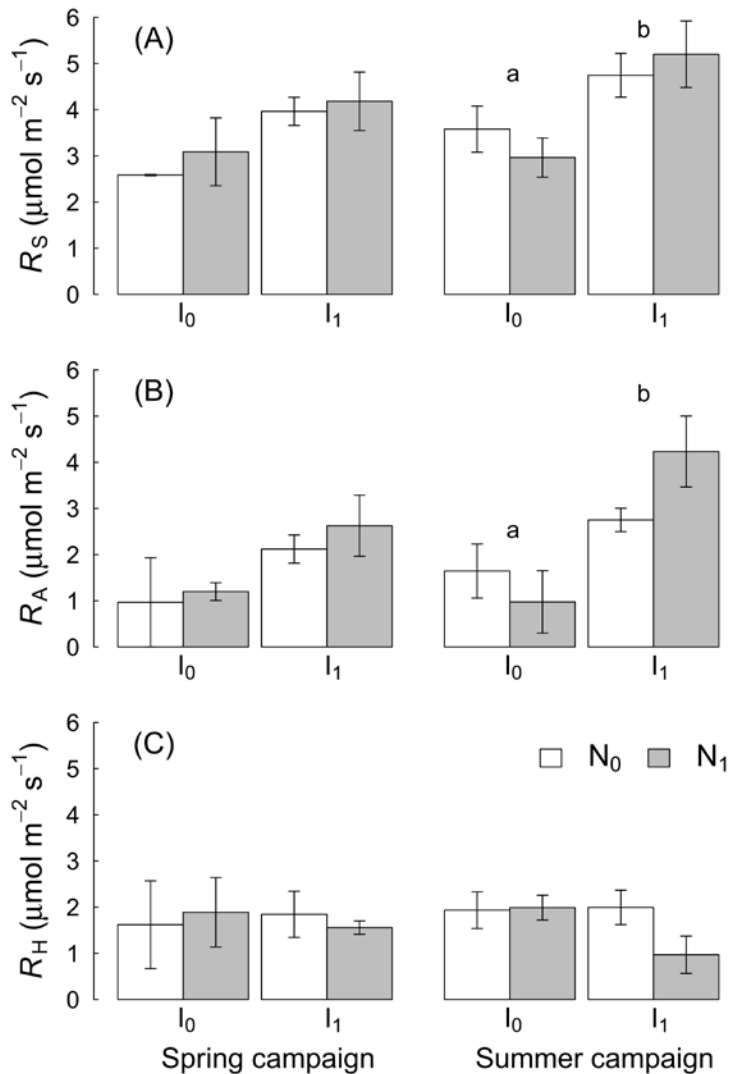


Figure 4.1: Rates of (A) soil respiration, R_S , (B) autotrophic respiration, R_A , and (C) heterotrophic respiration, R_H , for the control, I_0N_0 , non-irrigated fertilised, I_0N_1 , irrigated non-fertilised, I_1N_0 , and irrigated fertilised, I_1N_1 treatment for the spring campaign, one month after treatments started and the summer campaign, six months after the treatments started. The letters represent significant differences between irrigation treatments. The vertical bars indicate standard errors of the mean.

4.3.2.2 Respiration rates

Soil respiration (R_S) was lower for the treatment I_0 compared with that for the I_1 treatment, for both campaigns and the difference was statistically significant in the summer campaign (Table 4.2).

Autotrophic respiration (R_A) followed the same pattern as that for R_S , with the difference being

statistically significant only for the summer campaign. There were no significant differences in R_H for either campaign (Table 4.2).

There were no significant differences in R_S , R_A and R_H between the nitrogen treatments and interactions between the irrigation and nitrogen treatments was not significant (Figure 1). Although not significant, there were notable differences in R_A and R_H between the I_1N_0 and I_1N_1 treatments during the summer campaign (Figure 4.1). R_A increased from $2.8 \pm 0.3 \mu\text{mol m}^{-2} \text{s}^{-1}$ for the N_0 treatment to $4.2 \pm 0.8 \mu\text{mol m}^{-2} \text{s}^{-1}$ for the N_1 treatment, and R_H decreased from $2.0 \pm 0.4 \mu\text{mol m}^{-2} \text{s}^{-1}$ for the N_0 treatment to $1.0 \pm 0.4 \mu\text{mol m}^{-2} \text{s}^{-1}$ for the N_1 treatment.

R_S and R_A were strongly correlated, while R_S and R_H were not (Figure 4.2). The linear model describing R_S as a function of R_A gave an intercept of $2.4 \pm 0.2 \mu\text{mol m}^{-2} \text{s}^{-1}$ and a slope of 0.71 ± 0.08 , both significantly different from zero ($P < 0.0001$). The linear model describing R_S as a function of R_H gave an intercept of $3.4 \pm 0.8 \mu\text{mol m}^{-2} \text{s}^{-1}$, significantly different from zero ($P < 0.001$). The estimated slope of 0.27 ± 0.21 was not significantly different from zero ($P = 0.2$, Figure 4.2).

4.3.2.3 Soil characteristics

During the spring campaign, there were no significant differences between nitrogen treatments in soil characteristics (Table 4.2). Irrigation treatments differed only in T_S and W_S . For the I_0 treatment, W_S was significantly lower and T_S higher than those for the I_1 treatment. During the summer campaign, W_S was also significantly lower for the I_0 treatment but there were no differences in soil temperature. Only levels of C_D and C_{MOM} varied between treatments. The value of C_D was lower for the I_0 treatment compared to that for the I_1 treatment and was higher for the N_0 treatment compared to the value for the N_1 treatment. During the summer campaign, the interaction between the irrigation and nitrogen treatments for the macro-organic matter carbon (C_{MOM}) was significant. Values of C_{MOM} for the I_1N_0 and I_1N_1 treatments were not significantly different, but the values were lower than those of the control plots (I_0N_0). Values of C_{MOM} for the I_0N_1 treatment were intermediate between those for the other treatments. During the spring campaign, the value of C_{MOM} was higher

for the I_0 treatment compared with that for the I_1 treatment, but this difference was only marginally significant (Table 4.2).

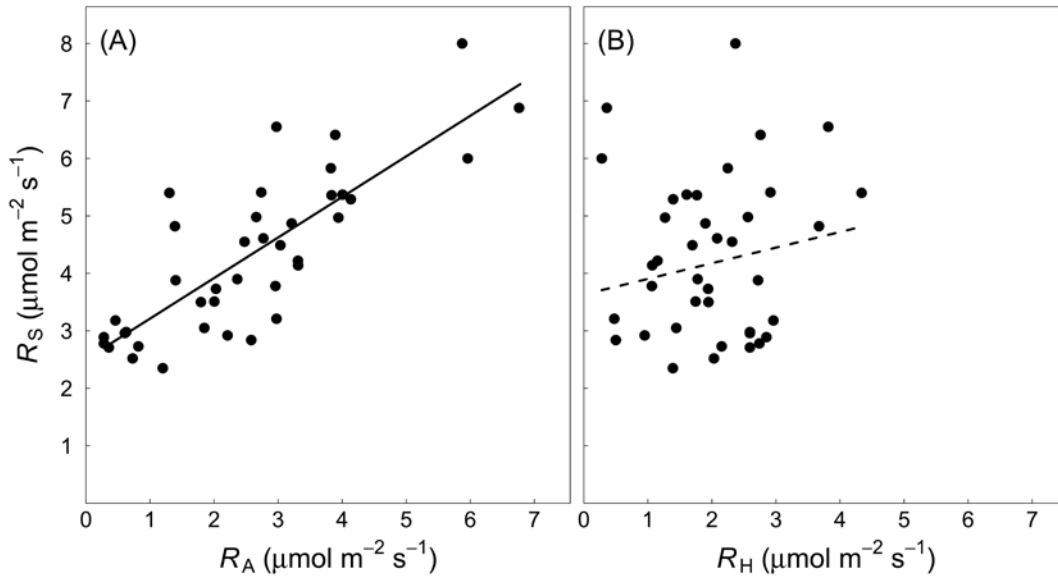


Figure 4.2: Relationship between rates of soil respiration (R_S) and (A) autotrophic respiration (R_A) and (B) heterotrophic respiration (R_H) combined for both measurement campaigns. The solid line represent a significant relationship ($P < 0.0001$) and the dashed line a non-significant relationship ($P = 0.2$).

Table 4.2: Environmental variables for the spring campaign, one month after treatments started and the summer campaign, six months after treatments started. The variables shown are soil temperature measured at a depth of 50 mm (T_s), soil gravimetric water content (W_s), total carbon concentration (C_{tot}), total nitrogen concentration (N_{tot}), specific surface area (S_A), hot water extractable carbon (C_{HW}) dissolved organic carbon (C_D), macro-organic matter carbon (C_{MOM}), particulate organic matter carbon (C_{POM}). Also shown are isotopic signatures of CO_2 respired by the root-free soil ($\delta^{13}CR_H$), autotrophic component ($\delta^{13}CR_A$), and the soil ($\delta^{13}CR_S$), the proportion of heterotrophic respiration from soil respiration (fR_H), soil respiration (R_S), autotrophic respiration (R_A) and heterotrophic respiration (R_H). Values are means \pm standard error for n replicate measurements in each treatment: control (I_0N_0), non-irrigated fertilised (I_0N_1), irrigated non-fertilised (I_1N_0) and irrigated fertilised (I_1N_1). The P-values are the results of linear models testing for the effects of irrigation and nitrogen addition treatments and their interactions. When significant ($P < 0.05$) or marginally significant ($P < 0.1$), the significant term (Signif.) is represented by I for irrigation treatment, N for nitrogen treatment and I*N for the interaction. When the interaction is significant, letters represent homogeneous Tukey groups.

	Non-irrigated, I_0		Irrigated, I_1		Signif.	P-value
	Non-fertilised, N_0	Fertilised, N_1	Non-fertilised, N_0	Fertilised, N_1		
n	2	3	6	5		
$\delta^{13}CR_H$		-21.8 \pm 0.2				> 0.1
$\delta^{13}CR_A$	-28.0 \pm 0.4		-28.8 \pm 0.1		I	0.1
$\delta^{13}CR_S$		-25.3 \pm 0.4				> 0.1
fR_H		0.48 \pm 0.06				> 0.1
R_S	2.9 \pm 0.4		4.1 \pm 0.3		I	0.1
R_A	1.1 \pm 0.3		2.3 \pm 0.3		I	0.1
R_H		1.7 \pm 0.2				0.9
Spring campaign						
W_s (g kg ⁻¹)	115.7 \pm 7.7		163.7 \pm 7.8		I	0.039
T_s (°C)	22.4 \pm 1.0		17.0 \pm 0.5		I	0.037
C_{tot} (mg C g ⁻¹ soil)		31.9 \pm 0.6				> 0.1
N_{tot} (mg N g ⁻¹ soil)		2.77 \pm 0.05				> 0.1
S_A (m ² g ⁻¹ soil)		39.2 \pm 0.9				> 0.1

	C_{HW} ($\mu\text{g C g}^{-1}$ soil C)			34.2 ± 0.6			> 0.1
	C_D (mg C g^{-1} soil C)			5.7 ± 0.2			> 0.1
	C_{MOM} (mg C g^{-1} soil C)	71.0 ± 4.5			53.1 ± 3.3	I	0.08
	C_{POM} (mg C g^{-1} soil C)			152.8 ± 12.1			> 0.1
	n	6	5	6	6		
	$\delta^{13}CR_H$	-23.0 ± 0.2			-21.9 ± 0.3	I	0.046
	$\delta^{13}CR_A$	-27.1 ± 0.4			-28.3 ± 0.3	I	0.08
	$\delta^{13}CR_S$	-24.3 ± 0.4			-26.4 ± 0.4	I	0.04
	fR_H	0.65 ± 0.09			0.30 ± 0.06	I	0.054
	R_S	3.3 ± 0.3			5.0 ± 0.4	I	0.036
	R_A	1.3 ± 0.4			3.5 ± 0.4	I	0.04
	R_H		1.7 ± 0.2				0.4
Summer campaign	W_S (g kg^{-1})	155.3 ± 3.2			220.4 ± 4.5	I	0.001
	T_S ($^{\circ}\text{C}$)			16.3 ± 0.2			> 0.1
	C_{tot} (mg C g^{-1} soil)			31.3 ± 0.4			> 0.1
	N_{tot} (mg N g^{-1} soil)			2.78 ± 0.03			> 0.1
	S_A ($\text{m}^2 \text{g}^{-1}$ soil)			39.7 ± 0.3			> 0.1
	C_{HW} ($\mu\text{g C g}^{-1}$ soil C)			35.9 ± 0.5			> 0.1
	C_D (mg C g^{-1} soil C)	5.3 ± 0.2	4.4 ± 0.1	6.4 ± 0.2	5.6 ± 0.3	I + N	< 0.01
	C_{MOM} (mg C g^{-1} soil C)	63.9 ± 6.5^a	51.8 ± 4.3^{ab}	32.9 ± 3.7^b	43.0 ± 3.4^b	I * N	0.042
	C_{POM} (mg C g^{-1} soil C)			120.7 ± 5.5			> 0.1

4.3.3 Environmental and soil property drivers of respiration rates

For each component R_S , R_A and R_H , the top eight best KL models are presented in Table 4.3. Soil and autotrophic respiration rates were explained mainly by environmental variables, W_S and T_S , and dissolved organic carbon explained a smaller part of their variability. For both R_S and R_A , T_S measured at a depth of 50 mm was a better predictor than T_S measured at 100 mm ($\Delta\text{AICc} > 6$). The best-supported models from the candidate set comprised the same combination of variables for R_S and R_A , including W_S , T_S measured at 50 mm deep and their interaction and C_D . The models yielded the relationships:

$$R_S = 7.1 - 0.08 W_S - 0.6 T_S + 0.4 C_D + 0.007 (W_S T_S)$$

$$R_A = 9.4 - 0.1 W_S - 1.0 T_S + 0.7 C_D + 0.009 (W_S T_S).$$

For R_S , the second best model, including only the interaction between W_S and T_S , was also strongly supported ($\Delta\text{AICc} = 0.7$, Table 3). For R_A , this model was the most strongly supported ($\Delta\text{AICc} > 3.6$). For both R_S and R_A , the best single-variate model included W_S . These models gave slopes of 0.022 and 0.023 ($\mu\text{mol CO}_2 \text{ m}^{-2} \text{ s}^{-1}$) ($\text{g H}_2\text{O kg}^{-1}$)⁻¹ for R_S and R_A , respectively, suggesting respiration rates changes of over 60% with the range of water content measured (Figure 4.3).

Heterotrophic respiration rates (R_H) were best explained by a combination of C_{POM} and S_A , with no contribution of T_S and W_S . Among the top eight models, none included W_S or T_S and six of the models, including the best one, included particulate organic matter carbon (C_{POM}). The best model also included specific surface area, and yielded the relationship:

$$R_H = -4.7 + 0.01 C_{\text{POM}} + 0.1 S_A.$$

The single-variate model including C_{POM} (rank 2) and the model including the interaction between C_{POM} and S_A (rank 3) were also supported strongly ($\Delta\text{AICc} < 1.4$). The first model to include an environmental variable was the single-variate model including T_S measured at 50 mm deep. This model was at the rank 9 and received no support ($\Delta\text{AICc} > 4.9$). Similarly, the single variate model including W_S was unable to explain variability in R_H (Figure 4.3).

Variable	Rank	Formula	AICc	Δ AICc	A_w	cum. A_w	LogLik
R_S	1	$R_S \sim W_S T_S + C_D$	123.4	0	0.32	0.32	-47.45
	2	$R_S \sim W_S T_S$	124.1	0.7	0.22	0.54	-49.71
	3	$R_S \sim W_S T_S + C_D + C_{tot}$	125.5	2.1	0.11	0.65	-46.46
	4	$R_S \sim W_S T_S + C_D + S_A$	126.9	3.6	0.05	0.71	-47.18
	5	$R_S \sim W_S T_S + C_{HW} S_A$	127.1	3.8	0.05	0.76	-45.07
	6	$R_S \sim W_S T_S + C_{POM}$	127.4	4.0	0.04	0.80	-49.44
	7	$R_S \sim W_S T_S + C_{tot}$	127.6	4.3	0.04	0.84	-49.59
	8	$R_S \sim W_S T_S + C_{HW}$	127.7	4.4	0.04	0.87	-49.62
R_A	1	$R_A \sim W_S T_S + C_D$	130.9	0	0.59	0.59	-51.23
	2	$R_A \sim W_S T_S + C_D + C_{tot}$	134.5	3.6	0.10	0.69	-50.98
	3	$R_A \sim W_S T_S + C_D + S_A$	134.8	3.9	0.09	0.77	-51.11
	4	$R_A \sim W_S T_S$	134.9	4.0	0.08	0.85	-55.10
	5	$R_A \sim W_S T_S + S_A$	137.1	6.2	0.03	0.88	-54.33
	6	$R_A \sim W_S T_S + C_{POM}$	137.4	6.5	0.02	0.90	-54.49
	7	$R_A \sim W_S T_S + C_{tot}$	138.2	7.3	0.02	0.92	-54.87
	8	$R_A \sim W_S T_S + C_D + S_A + C_{tot}$	138.2	7.3	0.02	0.93	-50.61
R_H	1	$R_H \sim C_{POM} + S_A$	112.0	0	0.23	0.23	-45.40
	2	$R_H \sim C_{POM}$	113.1	1.1	0.13	0.36	-47.61
	3	$R_H \sim C_{POM} S_A$	113.2	1.3	0.12	0.49	-44.28
	4	$R_H \sim C_{POM} + S_A + C_{tot}$	114.3	2.3	0.07	0.56	-44.81
	5	$R_H \sim 1$	114.4	2.5	0.07	0.63	-49.81
	6	$R_H \sim S_A$	114.9	2.9	0.05	0.58	-48.51
	7	$R_H \sim C_{POM} + C_{MOM}$	115.0	3.1	0.05	0.73	-46.94
	8	$R_H \sim C_{POM} + C_{tot}$	116.3	4.3	0.03	0.76	-47.58

Table 4.3: Summary of selected best models fitted with environmental variables and soil properties to explain variations in soil respiration (R_S) autotrophic respiration, (R_A) and heterotrophic respiration (R_H). AICc is the Akaike's information criterion corrected for small sample size; Δ AICc = AICc – AICc_{min}, where AICc_{min} is the smallest AICc, representing the best model; A_w , Akaike's weight; cum. A_w , sum of A_w ; LogLik, Log likelihood ratio.

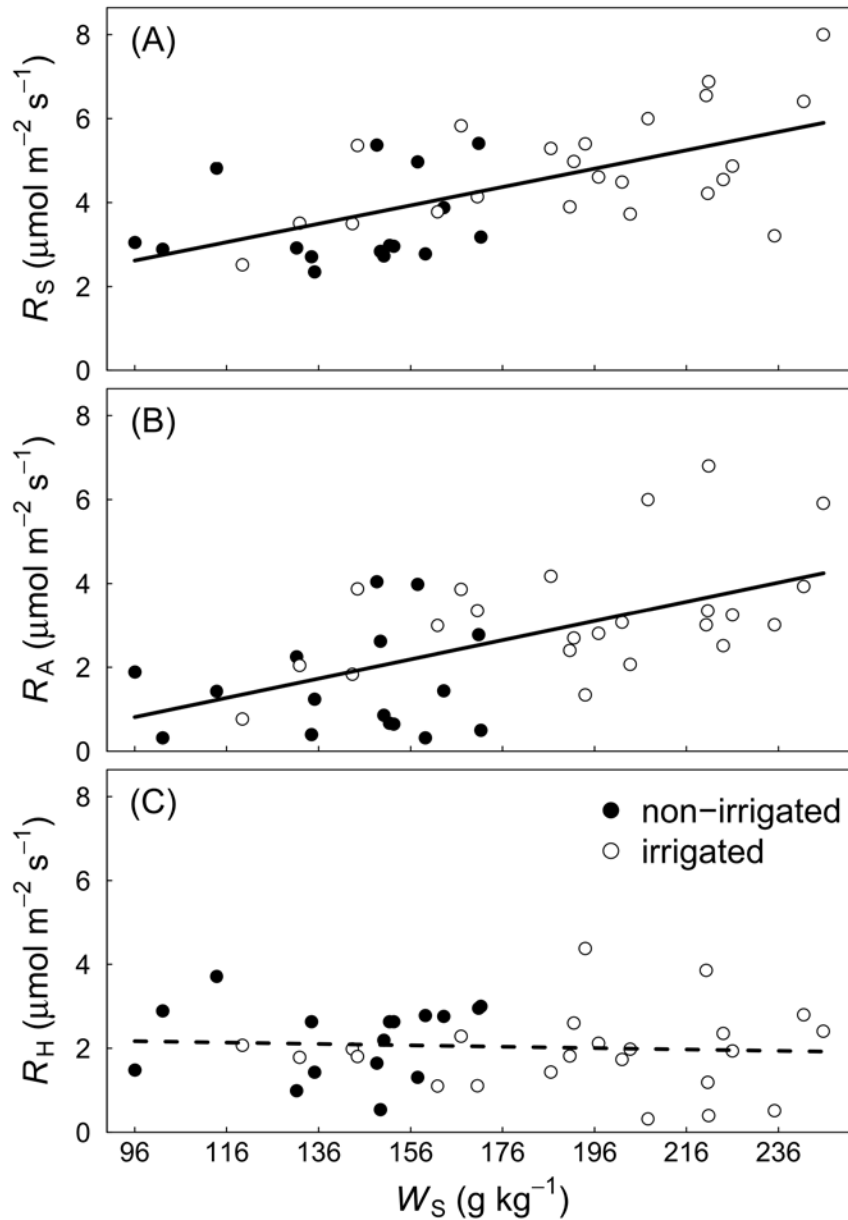


Figure 4.3: Rates of (A) soil respiration (R_s), (B) autotrophic respiration (R_A), and (C) heterotrophic respiration (R_H) in response to soil gravimetric water content (W_s). The lines are linear relationships fitted to the data with a solid line representing a significant relationship ($P < 0.0001$) and the dashed line a non-significant relationship ($P = 0.7$). Open and closed symbols represent replicates measurements for the irrigated and non-irrigated plots, respectively.

4.4 Discussion

My work has revealed differences in the responses of soil autotrophic and heterotrophic respiration rates to irrigation and nitrogen addition in field conditions. My use of the natural abundance ^{13}C technique incorporating an improvement for estimating the soil end-member has increased my understanding of the factors regulating soil organic matter dynamics. An increase in

soil respiration (R_s) appeared as a consequence of the irrigation treatment because of a positive linear relationship between the autotrophic component (R_A) and soil gravimetric water content (W_s). Decomposition of soil organic matter (R_H) was insensitive to changes in W_s and T_s , but was correlated to indicators of physical organic matter protection, measured as specific surface area (S_A) and availability, measured as particulate organic matter carbon (C_{POM}).

4.4.1 *Contribution of R_H to R_s*

Subke et al. (2006) reviewed studies partitioning R_s and found that estimates of fR_H vary strongly depending on the technique used and the ecosystem studied. The studies in temperate grasslands analysed by these authors all reported values of fR_H close to 0.6 or more but none of them used isotopic methods. Using the natural abundance $\delta^{13}C$ technique in well-watered temperate grasslands, Chapter 2 reported values of fR_H of 0.33 using undisturbed soils growing in mesocosms, and Graham et al. (2012) reported values averaging 0.29 in a field experiment. In a savannah with a mix of C_3 and C_4 plants, Millard et al. (2008) found values of fR_H close to 0.5 when irrigation was applied. My estimates of fR_H of 0.43 and 0.30 after one and six month of irrigation, respectively, are close to the results from these studies using the natural abundance of stable carbon isotopes.

4.4.2 *Response to nitrogen addition*

In grasslands, increases in photosynthesis and light use efficiency in response to addition of nitrogen fertiliser are well documented (Evans, 1989; Sinclair and Horie, 1989; Muchow and Sinclair, 1994). Above-ground productivity may not increase if water supply is limiting, but nitrogen supply may become a major limiting factor for growth when water deficits are relieved (Huxman et al., 2004; Y. Bai et al., 2010; Li et al., 2011). Although not significant, there was an increasing trend in R_A as a result of addition of nitrogen in well-watered condition in the summer campaign, and this was probably attributable to increased photosynthesis promoting increased root activity. In field conditions, ryegrass has been shown to take up amounts up to 35 kg N ha⁻¹ when sown as an intercrop (Thomsen and Hansen, 2014), and this practice is used commonly to reduce the rates of

nitrate leaching (Valkama et al., 2015). Consistent with this, in Chapter 2 I measured no increase in total soil and root nitrogen concentration but significant increases in leaf nitrogen concentration in ryegrass growing in mesocosms and supplied with $400 \text{ kg N ha}^{-1} \text{ y}^{-1}$ in well-watered conditions. Thus, not surprisingly at my site dominated by perennial ryegrass, total soil nitrogen concentration and soil characteristics remained unchanged as a result of addition of mineral nitrogen fertiliser at a rate of $200 \text{ kg N ha}^{-1} \text{ y}^{-1}$.

4.4.3 *Response to irrigation*

I found a strong positive correlation between R_S and R_A , with large increases in R_S and R_A with irrigation, and these were statistically significant for the summer campaign, 6 months after the treatments were imposed. R_S and R_A were strongly correlated with soil temperature and water content. In contrast, R_H varied very little between the treatments in both campaigns and no correlation was found between R_S and R_H . Accordingly, R_H was not affected by variations in soil water content and soil temperature that resulted from the irrigation up to six months after treatment were imposed. These findings suggest that variations in R_S are almost entirely attributable to changes in the activity of the roots and their associated rhizosphere microbes, with the decomposition of organic matter being insensitive to fluctuations in T_S measured at 50 and 100 mm deep and W_S .

4.4.4 *Drivers of heterotrophic respiration, R_H*

In a meta-analysis of the effects of soil water content on R_H from soil incubations, Manzoni et al. (2012) observed an effect of incubation time on respiration rates and attributed this to decreasing substrate concentration. Assuming a first order kinetic decay of substrate concentration with soil incubation time, Moyano et al. (2013) modelled the effect of different substrate availability on the response of R_H to soil water content and found that the maximum respiration rates expected for ideal water contents (field capacity) decreased markedly when substrate concentration decreased. Decreasing substrate concentrations were reported in a different meta-analysis using incubated soils and were found to modify the temperature response of organic matter decay (Giardina and Ryan,

2000). According to models of enzyme catalysed processes, in conditions of limited substrate concentration, decomposition rates are expected to follow Michaelis-Menten kinetics and the apparent temperature sensitivity of R_H may decrease or disappear (Davidson and Janssens, 2006). Evidence from laboratory incubations show that beyond thresholds of soil water content, R_H is inhibited because of physiological adjustments and microbial death when soil water content is too low and because of anaerobic conditions when soil water content is too high (Moyano et al., 2013). The range of soil water content observed at my site was thus unlikely to include extreme values limiting microbial activity independently from substrate availability. The range of soil temperature I measured was also limited and did not include temperatures below 13 °C. Yet variations in these environmental variables were large enough to significantly impact R_A , especially soil water content, which induced changes larger than 60%. Because the technique I used is likely to capture *in situ* organic matter availability and protection in the soil matrix, low substrate availability can explain the stability of R_H in my experiment. My results support findings from the few others studies using isotopic techniques that R_H is independent of changes in soil temperature (Giardina and Ryan, 2000; Graham et al., 2012).

The interaction between specific surface area, an indicator of soil protection capacity, and particulate organic matter, a physically unprotected labile fraction, provided the best description of differences in R_H in my study. This provides a strong indication that rates of organic matter decomposition are regulated by accessibility of decomposers to substrates. As no changes were observed between treatments at my site, the correlation between R_H and S_A and C_{POM} was attributable to spatial heterogeneity. Few studies have attempted to use labile fractions as early indicators of changes in soil organic matter content under different land management practices. Ghani et al. (2003) observed a decrease in the hot extractable water carbon fraction after five years of nitrogen fertiliser addition in grazed grasslands in New Zealand. Cambardella and Elliott (1992) showed a decrease in the particulate organic matter levels after 20 years of different tillage practices compared with those in a no tillage treatment. With my measurements at 1 and 6 months after the

treatments started, it is not surprising that I did not demonstrate changes in hot water extractable and particulate organic matter fractions of carbon. Furthermore, from these observations it appears conceivable that soil physical protection of organic matter may change under sustained irrigation and nitrogen addition for longer period of time, with possible consequences for soil organic matter decomposition. However, the magnitude and direction of these changes cannot be inferred and long-term studies are also needed.

4.4.5 Drivers of autotrophic respiration, R_A

Differences in above-ground net productivity in temperate grasslands are regulated mainly by soil water content (Flanagan et al., 2002; Hunt et al., 2004; Zhang et al., 2014). In a long term study, Flanagan and Adkinson (2011) found that interactions between temperature and soil water content improved predictions of net productivity significantly. Further, there is growing evidence that root and rhizosphere respiration is driven by short-term changes in photosynthesis (Högberg and Read, 2006). In controlled conditions, ryegrass labelled carbon was respired from roots 0.93 to 1.47 hours after shoots were exposed to $^{13}\text{CO}_2$ enriched air, depending on temperature (Barthel et al., 2014). The strong correlation between R_A and the interaction of soil water content and temperature in my study is consistent with these findings.

Dissolved organic carbon increased in response to irrigation and this was correlated with R_A . Soil water content largely determines the amount of organic matter that is recovered in the dissolved fraction (Zsolnay, 2003). In a ^{14}C labelling study, ryegrass was shown to allocate more than 1% of the carbon to the dissolved organic carbon pool within the few hours after labelling (Domanski et al., 2001). This suggests that the increased C_D in my irrigated plots may have been derived from the release of fresh plant material. Reviewing the effects of land management practices on C_D across different ecosystems, Chantigny (2003) found contrasting results from inorganic nitrogen addition. In grasslands, the limited data available suggest a positive relationship between dissolved organic

carbon losses through leaching and mineral nitrogen fertiliser addition (McTiernan et al., 2001). This is consistent with the small decrease in C_D in my plots with added nitrogen in the second campaign.

Changes in macro-organic matter carbon (C_{MOM}) might also be explained by changes in root turnover and activity. Macro-organic matter has been shown to be composed partially of plant residues (Magid and Kjærgaard, 2001; Willson et al., 2001). Higher root mortality in the conditions of low soil water content in my non-irrigated plots would have resulted in an increase in dead root material retained on a 250 μm sieve and this could explain higher macro-organic matter content. This is supported by the low rates of R_A in the non-irrigated plots and with findings in the literature. For example, Zhou et al. (2012) reported a significant reduction in root death rate in a tallgrass prairie in response to irrigation. Similar results were found by Bai et al. (2010) as a consequence of increased precipitation in a temperate, low-productivity grassland. Accordingly, it has been observed that water deficits can increase fine roots mortality and reduce root biomass in forest ecosystems (Green et al., 2005; Meier and Leuschner, 2008).

4.5 Conclusions

I found a strong effect of irrigation on R_S and R_A in a grassland up to six months after the treatments were imposed, associated with positive correlations between R_S , R_A and soil water content. In contrast, I showed that soil organic matter decomposition was insensitive to the same changes in soil temperature and soil water content. My work provides support for the few earlier studies (Giardina and Ryan, 2000; Millard et al., 2010; Graham et al., 2014; Chapter 2) where heterotrophic respiration has been measured using non-disruptive techniques including the use of carbon isotopes, challenging the idea that soil temperature and water content are strong drivers of changes in R_H . Further, I have shown that there is a correlation between rates of heterotrophic respiration and soil physical properties associated with physical protection of organic matter, namely physically unprotected organic matter and soil specific surface area.

Most models describing rates of soil organic matter turnover define compartments of organic matter in kinetically defined pools with different turnover times (Smith et al., 1997; von Lützow et al., 2007; Schmidt et al., 2011; Dungait et al., 2012). Recognising microbial access to organic matter as a predominant factor in regulating soil organic matter decomposition casts doubt on the biological relevance of these pools and their usefulness in models to predict changes in soil organic matter in response to climate change and land use change. My study provides empirical evidence for the existence of a correlation between microbial access to organic matter and soil organic matter cycling. Further studies are required to confirm the significance of this relationship on the long-term regulation of soil mineral composition and the effects of physical protection of soil organic matter on R_H (Schmidt et al., 2011).

**CHAPTER 5 Effects of irrigation and addition of nitrogen fertiliser on net
ecosystem carbon balance in a New Zealand grazed grassland**

5.1 Introduction

Managing agricultural lands to sequester soil carbon is consistent with the urgent need to meet the requirement for food production for an increasing world population and mitigate the rate of climate change by partly offsetting anthropogenic CO₂ emissions (Lal, 2004, 2009). Globally, grazed grasslands account for 70% of agricultural lands (FAOSTAT 2012) and they represent an important component of the global carbon cycle. Irrigation and addition of nitrogen fertiliser provide options to increase productivity and potentially enhance soil carbon stocks (Conant et al., 2001; Lal, 2009). Increased pasture productivity may lead to increased soil organic carbon storage if gross primary production (A) exceeds the losses through ecosystem respiration (R_E) and biomass export by grazing animals (F_{export}). However, the balance between carbon inputs and losses (net ecosystem carbon balance, N_B) is dependent on management decisions determining the timing and intensity of grazing, water and nitrogen inputs (Ammann et al., 2007; Soussana et al., 2010).

In New Zealand, conversion of dryland extensively grazed grasslands to dairy farming is a major land-use change typically involving intensification that includes large inputs of nitrogen fertiliser and irrigation in regions with relatively low rainfall (MacLeod and Moller, 2006). Grasslands represent 40% of the New Zealand land surface area (MacLeod and Moller, 2006) and store 50% of the national carbon inventory (Tate et al., 2005). With increased productivity, this management also supports intensive rotational grazing, with higher stock numbers per unit area grazing for shorter periods repeatedly through the year. A key step to determine both the economic and environmental sustainability of New Zealand dairy production is to understand soil carbon dynamics in relation to pasture management incorporating intensification.

Available data quantifying the impact of dairy farming management on soil carbon dynamics in New Zealand is scarce. Using repeated soil core sampling through time, Schipper et al. (2007, 2010) showed losses of soil carbon under long-term pastoral management, particularly under intensively managed dairy pasture, but the findings were later shown to be confounded by soil type (Schipper et al., 2014). Short-term approaches to estimate net ecosystem carbon balance using the eddy

covariance show different results at different sites, with studies showing grassland as a net sink (Rutledge et al., 2015) or a source (Campbell et al., 2015) of carbon to the atmosphere even under similar non-irrigated but intensively managed dairy systems. Only one study in New Zealand has described the dynamics of carbon balance in an intensively managed dairy system incorporating irrigation and addition of nitrogen fertiliser (Hunt et al., 2016). The findings showed an increase in net ecosystem carbon uptake in the fifth year after conversion in comparison with an adjacent, non-converted, extensively sheep-grazed pasture with no irrigation and low fertiliser input. However, this contrasts with observations from other soil core sampling studies, showing decreases in soil carbon content after 60 years of irrigation (Condrón et al., 2010; Schipper et al., 2013), or no effect at a depth of 0.8 m, 11 years after conversion to dairy farm management with irrigation and intensive grazing (Kelliher et al., 2015).

Improved understanding of the mechanisms regulating the components of net ecosystem carbon balance and changes in soil carbon storage is essential to explain differences between observations at different sites under different conditions and to forecast the effects of different management practices. While eddy covariance studies can be used to quantify net ecosystem CO₂ exchange at paddock scales, they do not allow partitioning of ecosystem respiration into its above and below-ground components, or separating the effects of key management practices such as irrigation and addition of nitrogen fertiliser. Furthermore, while large changes may occur rapidly after land use change (Soussana et al., 2010), no studies in New Zealand so far reports changes in ecosystem carbon balance immediately after conversion to intensively managed dairy farming.

In this study, we measured the net ecosystem carbon balance and its components at a field site within the first year of conversion from a dryland, grazed grassland to an intensive, rotationally grazed system incorporating irrigation and the addition of nitrogen fertiliser. Net ecosystem CO₂ exchange (F_N), gross canopy photosynthesis (A), ecosystem respiration (R_E), above-ground plant respiration (R_L), soil respiration (R_S) and biomass export through grazing (F_{export}) were measured seasonally on adjacent plots at the same site comprising control treatments (no irrigation, no

application of nitrogen fertiliser) with treatments incorporating irrigation and addition of fertiliser for a year. To characterise the effects of irrigation and addition of nitrogen fertiliser in intensively rotationally grazed pastures, I simulated intensive grazing for all treatments with regular clipping of the grass, each followed with addition of nitrogen. My objectives were to (i) characterise the single and interactive effects of irrigation and nitrogen fertiliser on seasonal measurements of carbon balance components in an intensively grazed grassland ecosystem, and (ii) estimate and model annual net ecosystem carbon balance and its components from physiological response of A , R_L and R_S to irradiance (Q), soil volumetric water content (θ_s), soil temperature (T_s) and air temperature (T_a) for each treatment.

5.2 Materials and methods

5.2.1 Site description

The measurements were made at a field site located at Ashley Dene Farm, Lincoln, Canterbury (latitude 43.40° S, longitude 172.20° E, elevation 35 m above sea level). The site was flat and had been managed under dry sheep farming for more than 50 years prior to the experiment. The soil is a stony silt loam with shallow topsoil (0.2 m depth), excessively drained and classified as a mix of Balmoral and Lismore according to New Zealand classification (Hewitt, 2010). The climate at Ashley Dene is temperate, with mild winters and warm, dry summers. Mean annual rainfall is 600 mm (NIWA 2014).

5.2.2 Experimental design

The experimental design consisted of six circular plots with a radius of 2 m (12.5 m² area). Three plots were selected randomly for the irrigation (treatment I_1), and the three remaining plots were left non-irrigated (treatment I_0). Within each plot, one half was selected randomly for the addition of mineral nitrogen fertiliser (treatment N_1), and the other half was left with no fertiliser added (treatment N_0). The circular plots were split in a north-south direction for the nitrogen treatments to

avoid differences in incident irradiance. The experimental layout was a full factorial nested design with the nitrogen treatments nested within the irrigation treatments, resulting in four combinations. With three replicates of each of the four combinations, there were a total of twelve semi-circular plots: non-irrigated / non-fertilised (control, I_0N_0), non-irrigated / fertilised (I_0N_1), irrigated / non-fertilised (I_1N_0) and irrigated / fertilised (I_1N_1). In each of the twelve plots, two 200 mm diameter and two 100 mm diameter PVC collars were inserted into the soil to a depth of 30 mm. The 200 mm diameter collars included plant leaves and were used for measurements of net ecosystem CO_2 exchange (F_N) and ecosystem respiration (R_E). The 100 mm diameter collars excluded the plant leaves by being placed in the soil between grass patches, were kept free of above-ground vegetation throughout the whole experiment and were used for measurements of soil respiration (R_S). The design resulted in 24 replicates (collars), six for each treatment for measurements of F_N , R_E and R_S .

The treatments were first applied in early spring (October 2014). Sprinklers were placed at a height of 2 m above the centre of each of the irrigated plots, allowing irrigation of the whole surface area with 15 mm of water every three days. When wind speed was high, irrigation was delayed to avoid losses of water to surrounding areas and uneven distribution of water within each plot. There was no irrigation during winter, from May to September. To simulate rotational grazing, the grass was clipped regularly (approximately every three weeks in spring and summer and every four to six weeks in autumn and winter) and nitrogen fertiliser, in the form of 17 g of NH_4NO_3 diluted in 10 L of water, was applied evenly over the whole plot using a watering can, equivalent to 10 kgN ha^{-1} for each application. The non-fertilised plots were treated by adding 10 L of water only. Hereafter, simulated grazing events are referred to as grazing events.

Environmental variables were recorded on site at half-hourly intervals throughout the whole experiment, from October 2014 to September 2015. These included air temperature (T_a) and relative humidity (humidity and temperature transmitter, model Humitter 50U/50Y(X), Vasaila, Helsinki, Finland), wind speed (anemometer, model A101M, Vector Instruments, Clwyd, UK), photosynthetically active irradiance (Q , Q40205, LI-COR Inc., Lincoln, NE, USA) and rainfall (rain

gauge, model TE525, Campbell Scientific Inc., Logan UT, USA). At a random location in each of the twelve plots, soil temperature (T_s , thermocouples, Type E, Omega Engineering Ltd., Stamford, CT, USA) was measured at depths of 50 and 100 mm and volumetric soil water content (θ_s , soil moisture sensor model ML3, Delta-T Devices Ltd., Cambridge, UK) was measured at a depth of 80 mm.

5.2.3 Measurements of CO_2 exchange and biomass

F_N , R_S and R_E were measured on thirteen occasions throughout the measurement period, just prior to each grazing event. Measurements began on 2 October 2014 (day 0), just prior to the starts of the treatments. F_N was measured using the purpose-built cylindrical cleared top chamber (200 mm diameter and 210 mm height) described by Chapter 2 and attached to a portable photosynthesis system (LI-6400XT, LI-COR Inc., Lincoln, NE, USA) designed to work as a closed system. The chamber was vented to the atmosphere to avoid pressure fluctuations and a small fan moving the air at 50 L min^{-1} (V249L, 6V, Micronel®) was mounted inside the chamber to maintain well-mixed conditions. Incident irradiance (Q40205, LI-COR Inc., Lincoln, NE, USA) and air temperature (thermocouple Type E, Omega Engineering Ltd., Stamford, CT, USA) were recorded inside the chamber. After each measurement of F_N , the chamber was covered with a dark cloth and a new measurement was made to obtain R_E . For each measurement, the chamber was placed on the 200 mm diameter collar and CO_2 concentration in the chamber was recorded for 70 s. Gross canopy photosynthesis (A) was obtained for each replicate on each measurement day by subtracting F_N from R_E . Simultaneous with measurements of F_N and R_E , R_S was measured using a soil respiration closed dynamic system (LI-8100, LI-COR Inc., Lincoln, NE, USA) placed on the 100 mm diameter collar in the same plot. Measurements of F_N , R_E and R_S were made between 1000 and 1600 NZST.

In order to obtain F_{export} , the grass clipped from each collar during grazing events was oven dried to constant mass at 70°C and weighed. For five of the measurement days, including day 0, the dried biomass was ground to a powder in a ball mill for carbon and nitrogen concentration analysis using a Dumas elemental analyser (Europa Scientific ANCA-SL, Crewe, UK). The amount of dry mass

collected in each collar was multiplied by the leaf nitrogen and carbon concentrations to obtain canopy nitrogen content and F_{export} , respectively.

5.2.4 Responses of CO_2 exchange to environmental variables

In order to derive estimates of N_B and F_N and their components for the whole measurement period (hereafter referred to as annual estimates), I developed models using physiological response curves of the components of carbon exchange to natural variations of T_a , T_s , θ_s and Q . For the purposes of modelling, I subtracted values of R_s from values of R_E measured simultaneously to obtain values of leaf respiration (R_L) in each of the twelve plots, such that R_L and R_s could be modelled separately. Leaf respiration responds strongly to air temperature (T_a) (Tjoelker et al., 2001) and this was modelled using an Arrhenius-type function where

$$R_L = R_{10} e^{E_0 \frac{1}{56.02} - \frac{1}{T_a - 227.13}} \quad (5.1)$$

R_{10} is the respiration rate at a basal temperature of 10 °C and E_0 is related to the activation energy of enzymatic reactions.

The responses of R_s to soil temperature (T_s) and soil volumetric water content (θ_s) were modelled using an Arrhenius-type curve (Lloyd and Taylor, 1994) modified to include the effect of θ_s using a Gompertz function (Janssens et al., 2003) where

$$R_s = R_{10} e^{E_0 \frac{1}{56.02} - \frac{1}{T_s - 227.13}} e^{-e^{-(g-f\theta_s)}} \quad (5.2)$$

R_{10} is the respiration rate at a basal temperature of 10 °C, E_0 is related to the activation energy of enzymatic reactions and g and f are parameters defining the shape of the sigmoidal response of R_s to θ_s .

The response of gross photosynthesis (A) to irradiance (Q) was modelled with the widely used rectangular hyperbole (Luo et al., 2000), where

$$A = \frac{\alpha Q A_{\text{max}}}{\alpha Q + A_{\text{max}}} \quad (5.3)$$

α is the light use efficiency and A_{max} is the rate of gross photosynthesis under saturating irradiance.

5.2.5 Phytomass index

In rotationally grazed grasslands, F_N and its above-ground components can be severely affected by the removal of above-ground biomass due to grazing (Lohila et al., 2004; Nieveen et al., 2005; Soussana et al., 2007; Campbell et al., 2015). An empirical phytomass index (P_i) can be calculated from continuous CO_2 flux measurements as the difference between average values of F_N during the day time and night time (normalised on seasonal maximums), and this methodology has been used successfully to account for above-ground biomass variation throughout grazing cycles and seasonally in grazed grasslands (Chapter 3). I adopted this methodology, modelling the phytomass index from environmental variables. I then produced new parameters in the models for R_L , R_S and A by multiplying Equations 5.1, 5.2 and 5.3 by P_i .

In a chamber study with continuous measurements of F_N , in Chapter 3 I modelled the phytomass index from parameters related to above-ground plant activity. In addition, Lohila et al. (2004) observed that P_i closely followed variations in canopy leaf area throughout the year. Thus, in the absence of a continuous record of F_N , I estimated values of P_i from measurements of above-ground biomass normalised on the annual maximum value. Measurement of dry-mass collected during each clipping event was assigned to the value of P_i on the last day of each grazing cycle. I then modelled P_i as a function of cumulative growing degree day between each grazing event (G_{DC}), used widely to describe rates of plant growth (Ritchie and Nesmith, 1991; Gramig and Stoltenberg, 2007). Here I adapted my previous methodology (Chapter 2) in which I observed that pasture growth increased to a steady state in an asymptotic exponential fashion with time after grazing in irrigated grassland growing in mesocosms. I estimated values of P_i for each day between each grazing event as an asymptotic exponential function of G_{DC} , starting from 0 on the day of the grazing events, and reaching a steady-state value, considered equal to the value of P_i calculated from biomass measurements (P_{imax}) for each grazing events. The function adapted from Chapter 2 was:

$$P_i = \frac{P_{imax}}{1 - e^{-z G_{DCmax}}} \times (1 - e^{-z G_{DC}}). \quad (5.4)$$

G_{DCmax} is the value of G_{DC} on grazing days, corresponding to values for P_{imax} , and z is the parameter defining the shape of the curve that can be calculated from the value of G_{DC} for which 95% of P_{imax} is reached (G_{DC95}). Following Chapter 2, mean G_{DC} at nine days after grazing was close to 100 °C and this value was used as G_{DC95} throughout the whole year for all treatments, so that $z = 0.03 \text{ °C}^{-1}$.

5.2.6 Statistical analyses

The effects of irrigation and nitrogen addition on seasonal measurements of F_N , R_E and R_S were assessed using linear mixed effect models conducted using the 'nlme' package (Pinheiro and Bates, 2014) of R (version 3.2.1, R Development Core Team, 2014). The proportion of R_E contributed by R_S , the canopy nitrogen content and the above-ground biomass accumulated in each 200 mm diameter collar over the whole year were analysed in the same way. The proportion of R_E contributing to R_S was calculated from the simultaneous measurement of R_E and R_S . Each measurement of F_N , R_E , R_S , each calculated proportion, each value of canopy nitrogen content and each value of cumulated biomass was treated as a replicate. Irrigation, nitrogen addition, measurement date (except for the cumulated biomass) and their interactions were included as fixed effects. The nested structure of the experimental design was included as random effect as plot/nitrogen treatment/replicate, where 'plot' is a factor discerning the six circular treatment plots.

The effect of irrigation and addition of nitrogen fertiliser on the responses of R_L , R_S and A to environmental variables were evaluated using non-linear mixed effect model conducted in the 'nlme' package of R to fit values of R_L , R_S and A using Equations 5.1, 5.2 and 5.3, respectively. Irrigation and nitrogen treatments were investigated as fixed effect on the model parameters (R_{10} , E_0 , A_{max} and α). To avoid the inclusion of the correlated variables irrigation treatment and θ_s , only nitrogen was tested as a fixed effect in the model for R_S . For each model, the nested structure of the experimental design was included as random effects (irrigation treatment/plot/nitrogen treatment/replicate). A first-order autoregressive function was used to account for temporal autocorrelation in repeated measurements of the same collar (Crawley 2007). The final fixed effect

structure was selected by comparing the models including nitrogen and irrigation treatments as fixed effect and the models not including them. Model comparison was based on the Akaike's Information Criterion (AIC), the model with the lowest AIC being the most strongly supported. As a rule of thumb, when two models presented a $\Delta AIC < 2$, the simpler model was selected (Burnham and Anderson, 2002). In order to assess the effect of above-ground biomass on model parameters, the exact same process was repeated using the Equations 5.1, 5.2 and 5.3 with the phytomass index (P_i) as a multiplier.

The models for R_L , R_S and A not including P_i and those including P_i were combined to obtain F_N and then compared based on their predictive performance, which was evaluated by cross-validation using the hold-out method (Ross, 2009). The data were split into two equal parts by randomly selecting either of the two collar replicates in each of the twelve hemi-circular plots. Half of the data were used to develop the models described above (training set), and the other half to test the model (testing set). Root mean square errors (RMSE) and adjusted coefficients of determination (R^2) were used to compare model performances.

Parameters from the best models for A , R_L and F_N including P_i and from the best model of R_S were used to produce values for every half-hourly record of environmental variables between each grazing event. Cumulative F_N and annual estimates for R_L , R_S , A , F_N and N_B were calculated as sums of half-hourly values. Uncertainties around annual estimates were calculated using Monte Carlo simulations, where a thousand sets of parameters were generated randomly for each of R_L , R_S and A from the variance-covariance tables for each fitted model using the 'MASS' package (Venables and Ripley, 2002). The 95% confidence interval around the estimates for each component of the ecosystem carbon balance represents the uncertainty.

5.3 Results

5.3.1 Growing conditions

Total rainfall from October 2014 to September 2015 was 451 mm with a summer (December-February) dry period with less than 60 mm rainfall. Soil volumetric water content (θ_s) followed a different seasonal pattern for the treatments I_0 and I_1 (Fig. 1B). Irrigation resulted in significant increases in mean θ_s ($F = 103.2$, $P = 0.0005$) compared with the non-irrigated treatments of $0.12 \pm 0.01 \text{ m}^3 \text{ m}^{-3}$. However, even for the irrigated plots, θ_s decreased to values near $0.2 \text{ m}^3 \text{ m}^{-3}$ in mid-summer, due to regular events with high wind speeds that caused interruptions in the irrigation schedule. Addition of nitrogen fertiliser resulted in a significant ($F = 9.9$, $P = 0.03$) but small decrease in θ_s , with the daily mean being $0.03 \pm 0.01 \text{ m}^3 \text{ m}^{-3}$ higher for the treatment N_0 than that for the N_1 treatment.

Annual daily mean (\pm standard error) irradiance was $24.4 \pm 0.9 \text{ mol m}^{-2} \text{ d}^{-1}$ with a summer maximum of $66.2 \text{ mol m}^{-2} \text{ d}^{-1}$ (Fig. 1C). Mean (\pm standard error) air temperature over the measurement period was $12.1 \pm 0.2 \text{ }^\circ\text{C}$, with a mean daily maximum of $23.4 \text{ }^\circ\text{C}$ reached in December and a minimum of $-0.3 \text{ }^\circ\text{C}$ in July (Fig. 1A). Soil temperature measured at 100 mm depth followed the same seasonal pattern and ranged from 2.6 to $25.9 \text{ }^\circ\text{C}$. In mid-summer, mean daily T_s in the irrigated plots was slightly lower than that in the non-irrigated plots, so that the mean annual T_s for the treatment I_1 was significantly lower ($F = 36.2$, $P = 0.004$) by $0.6 \pm 0.1 \text{ }^\circ\text{C}$ compared with that for the I_0 treatment.

5.3.2 Seasonal measurements of the components of ecosystem CO_2 exchange

On day 0, before the treatments were applied, there were no differences in F_N , R_E or R_S between the treatments ($P > 0.1$). F_N showed marked seasonal variations that differed between the treatments (Fig. 2A). Differences between irrigation treatments appeared in summer, when positive values of F_N (net CO_2 source) were observed for the non-irrigated plots (I_0) at the driest time in January, when θ_s was below $0.2 \text{ m}^3 \text{ m}^{-3}$, while F_N remained negative (net CO_2 sink) in the irrigated

plots (I_1). In winter, all treatments were net sinks for CO_2 . Reflecting these seasonal variations, the interaction between measurement date and irrigation treatment was significant ($F = 8.6, P < 0.0001$). The I_0N_0 and I_0N_1 treatments showed very similar values of F_N overall (mean \pm standard error -2.3 ± 0.4 and $-2.8 \pm 0.5 \mu\text{mol m}^{-2} \text{s}^{-1}$, respectively) and the I_1N_0 and I_1N_1 treatments were stronger sinks of CO_2 ($F_N = -4.6 \pm 0.5$ and $-6.5 \pm 0.5 \mu\text{mol m}^{-2} \text{s}^{-1}$, respectively). The interaction between nitrogen and irrigation treatments was not significant ($F = 1.2, P = 0.3$).

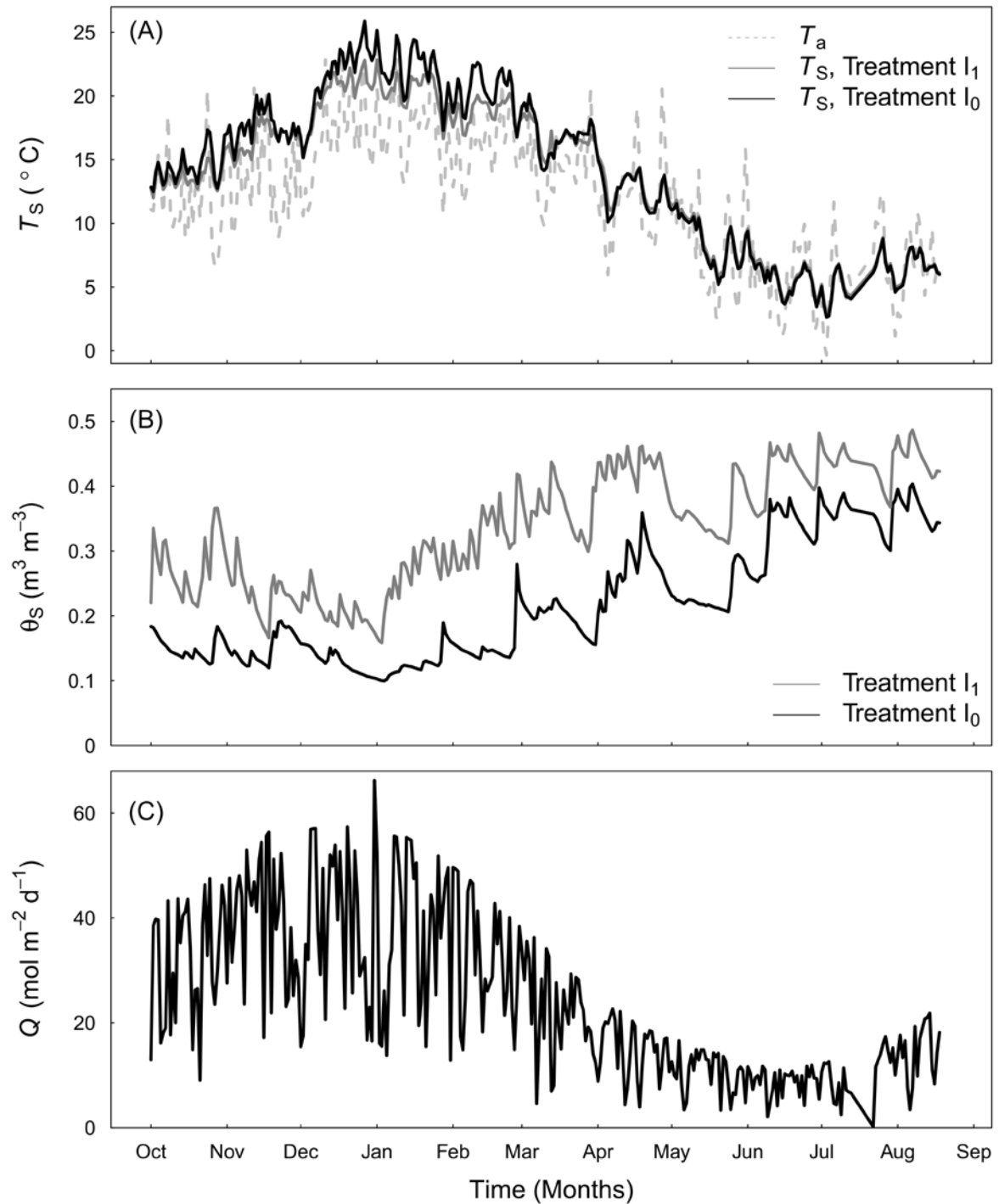


Figure 5.1: Changes in daily mean environmental variables for the measurement period from October 2014 to September 2015. (A) Air temperature (T_a , dashed grey line), and soil temperature (T_s) for the irrigated plots (treatment I_1 , continuous grey line) and the non-irrigated treatment (I_0 , continuous black line). (B) Soil volumetric water content (θ_s) for the treatments I_1 (grey line) and I_0 (black line). (C) Photosynthetically active irradiance (Q).

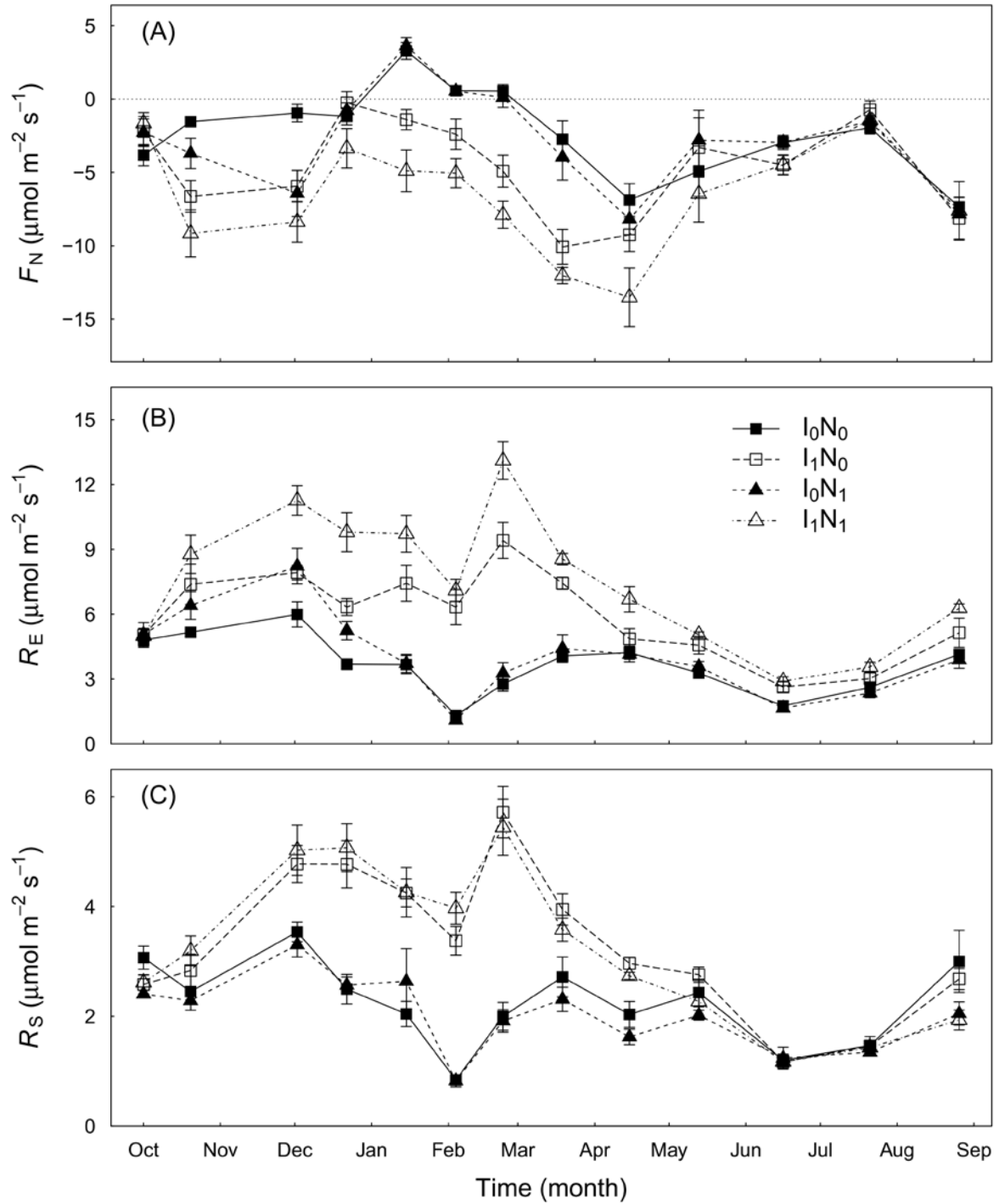


Figure 5.2: Variations in seasonal measurements of (A) net ecosystem CO_2 exchange (F_N), (B) ecosystem respiration (R_E) and (C) soil respiration (R_S) for the four treatments: non-irrigated with no nitrogen addition (I_0N_0 , filled squares), irrigated with no nitrogen addition (I_1N_0 , open squares), non-irrigated with nitrogen addition (I_0N_1 , filled triangles) and irrigated with nitrogen addition (I_1N_1 , open triangles). The vertical bars represent standard error of the mean ($n = 6$).

Table 5.1: Parameters for the models of soil respiration (R_s), leaf respiration (R_l) and gross canopy photosynthesis (A), including and not including the phytomass index (P_i). When significant ($P < 0.05$), different parameters are shown for the four treatments: non-irrigated with no nitrogen addition (I_0N_0), irrigated with no nitrogen addition (I_1N_0), non-irrigated with nitrogen addition (I_0N_1) and irrigated with nitrogen addition (I_1N_1). R_{10} is the respiration rate at a basal temperature of 10 °C, E_0 is the activation energy of the enzymatic reaction, g and f are the parameters describing the response of respiration to soil volumetric water content, α is the light use efficiency and A_{\max} is the rate of gross photosynthesis under saturating irradiance.

		Not including P_i				Including P_i
		I_0N_0	I_1N_0	I_0N_1	I_1N_1	
R_s	R_{10} ($\mu\text{mol m}^{-2} \text{s}^{-1}$)		2.4 ± 0.1			–
	E_0 (KJ mol^{-1})		202.8 ± 60.4			–
	g		2.2 ± 0.6			–
	f		22.6 ± 5.4			–
R_l	R_{10} ($\mu\text{mol m}^{-2} \text{s}^{-1}$)	0.7 ± 0.3	2.0 ± 0.3	1.3 ± 0.3	3.1 ± 0.4	5.0 ± 0.5
	E_0 (KJ mol^{-1})		111.6 ± 48.7			157.8 ± 48.2
A	α (μmol $\mu\text{molquanta}^{-1}$)		0.12 ± 0.05			0.26 ± 0.08
	A_{\max} ($\mu\text{mol m}^{-2} \text{s}^{-1}$)	5.5 ± 1.4	12.9 ± 1.6	7.0 ± 1.1	18.4 ± 1.9	33.1 ± 1.9

Measurements of ecosystem respiration (R_E) also followed seasonal patterns (Fig. 2B). Both irrigation and nitrogen treatments had significant effects on R_E overall (mean \pm standard error of 3.7 ± 0.2 , 4.1 ± 0.2 , 6.0 ± 0.37 and $7.6 \pm 0.4 \mu\text{mol m}^{-2} \text{s}^{-1}$ for the I_0N_0 , I_0N_1 , I_1N_0 and I_1N_1 treatments, respectively). While the effect of nitrogen appeared stronger in the irrigated plots (Fig. 2B), the interaction between nitrogen and irrigation treatments was not significant ($F = 3.5$, $P = 0.13$). The interaction between measurement date and irrigation treatment was significant ($F = 26.4$, $P < 0.0001$), with higher respiration rates throughout the spring and summer for the I_1 treatment compared with that for the I_0 treatment. Addition of nitrogen fertiliser in the irrigated plots resulted in increased respiration rates in spring and summer and the interaction between measurement date and nitrogen treatment was also significant ($F = 4.4$, $P < 0.0001$).

Soil respiration (R_S) followed the same response as R_E to seasons and irrigation treatments, but no differences were observed between nitrogen treatments ($F = 1.0$, $P = 0.3$). The value of R_S of $3.3 \pm 0.2 \mu\text{mol m}^{-2} \text{s}^{-1}$ was identical for the I_1N_0 and I_1N_1 treatments and the I_0N_0 and I_0N_1 treatments also showed similar rates, with 2.2 ± 0.1 and $2.0 \pm 0.1 \mu\text{mol m}^{-2} \text{s}^{-1}$, respectively. For the I_0 treatment, values of R_S were lowest through spring and summer, and the interaction between measurement date and irrigation treatment was significant ($F = 28.6$, $P < 0.0001$). Across all treatments, R_S comprised $55 \pm 3 \%$ of R_E and this proportion was reduced by $10 \pm 3 \%$ by adding irrigation ($F = 9.9$, $P = 0.03$) and increased by $10 \pm 3 \%$ by addition of nitrogen fertiliser ($F = 10.6$, $P = 0.02$).

5.3.3 Cumulative biomass and canopy nitrogen content

Addition of nitrogen fertiliser increased mean \pm standard error canopy nitrogen content by $23.2 \pm 8.2 \text{ g}$ on average ($F = 7.8$, $P = 0.03$), but irrigation did not ($F = 2.1$, $P = 0.1$). Measurement date also had a significant effect ($F = 11.7$, $P < 0.0001$), with the nitrogen content decreasing after day 0, especially in spring and summer when non-fertilised plots showed lower nitrogen contents (with 36.2 ± 3.8 , 19.3 ± 2.0 and $23.7 \pm 4.3 \text{ g}$ for spring, early summer and late summer, respectively) compared to the mean at day 0 of $69.0 \pm 11.3 \text{ g}$ (Fig. 3B).

The rate of grass growth for the treatment I_1N_1 was high throughout the year, decreasing only in winter and it fell to very low values in the non-irrigated plots (I_0N_0 and I_0N_1) in summer from December to March (Fig. 3A), resulting in differences in cumulative dry mass. For the I_1N_0 treatment cumulative dry mass continued to increase slowly in summer reaching a significantly higher value than that than for the I_0N_1 treatment only at the end of summer (Fig. 3A). In autumn and winter, growth rates decreased, and more so for the I_1N_0 treatment than for the I_0N_1 treatment so that cumulative biomass over the whole year for these two treatments was similar (19.5 ± 2.8 and 25.0 ± 3.3 g for I_0N_1 and I_1N_0 , respectively). Both nitrogen addition and irrigation had a significant effect on cumulative biomass over the whole year ($F = 8.6$, $P = 0.03$ and $F = 22.6$, $P = 0.009$ for nitrogen addition and irrigation treatments, respectively), with lowest in the I_0N_0 treatment (14.2 ± 1.8 g) and biomass highest in the I_1N_1 treatment (38.1 ± 5.6 g).

5.3.4 Models of net ecosystem CO_2 exchange and its components

Parameters for the best model of R_S (RMSE = 1.05, $R^2 = 0.50$) were not different for the two nitrogen treatments (Table 1). The model including P_i was unable to predict values of R_S (RMSE = 1.90, $R^2 = -0.65$). The best model for R_L included different values of R_{10} for the four combinations of irrigation and nitrogen treatments, but the same value for E_0 . Irrigation and addition of nitrogen fertiliser increased R_{10} , with a synergistic effect so that the I_1N_1 treatment showed the highest value (Table 1). When P_i was included in the model, differences in R_{10} were no longer significant (Table 1) and the predictive performance of this model was worse (RMSE = 1.61, $R^2 = 0.40$) than the performance of the best model not including P_i (RMSE = 1.49, $R^2 = 0.49$). When P_i was not included in the model of A , the parameter describing the maximum rate of photosynthesis (A_{max}) differed between treatments, but not that describing light use efficiency (α) (Table 1). When P_i was included in the model, differences in A_{max} were no longer significant (Table 1) and the model performed much better (RMSE = 3.85, $R^2 = 0.65$) than the best model not including P_i (RMSE = 5.10,

$R^2 = 0.35$). As a result, the model for F_N including P_i performed well (RMSE = 2.88, $R^2 = 0.63$) and much better than the model not including P_i (RMSE = 3.55, $R^2 = 0.13$) (Fig. 4).

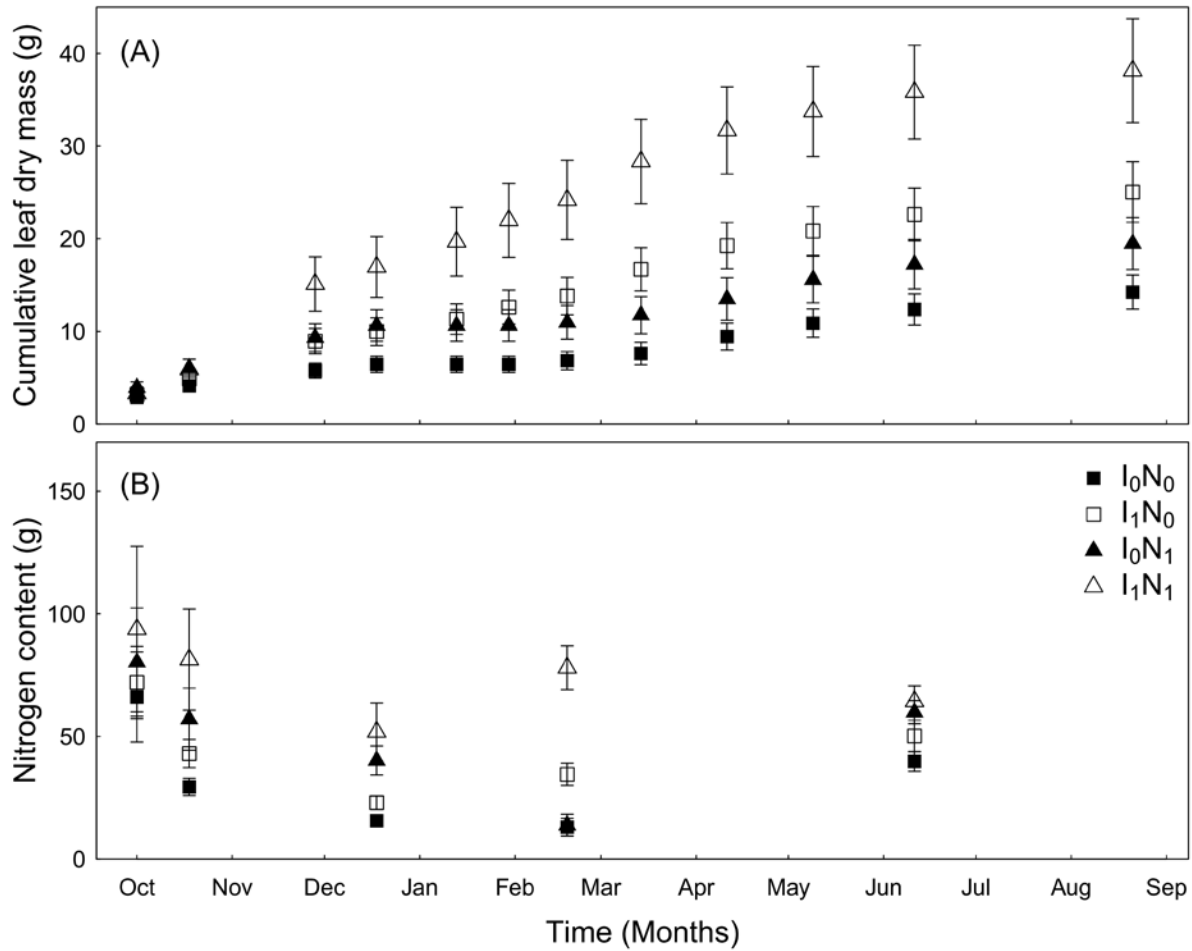


Figure 5.3: Cumulative (A) leaf dry mass and (B) canopy nitrogen content for the four treatments: non-irrigated with no nitrogen addition (I_0N_0 , filled squares), irrigated with no nitrogen addition (I_1N_0 , open squares), non-irrigated with nitrogen addition (I_0N_1 , filled triangles) and irrigated with nitrogen addition (I_1N_1 , open triangles). The vertical bars represent standard error of the mean ($n = 6$).

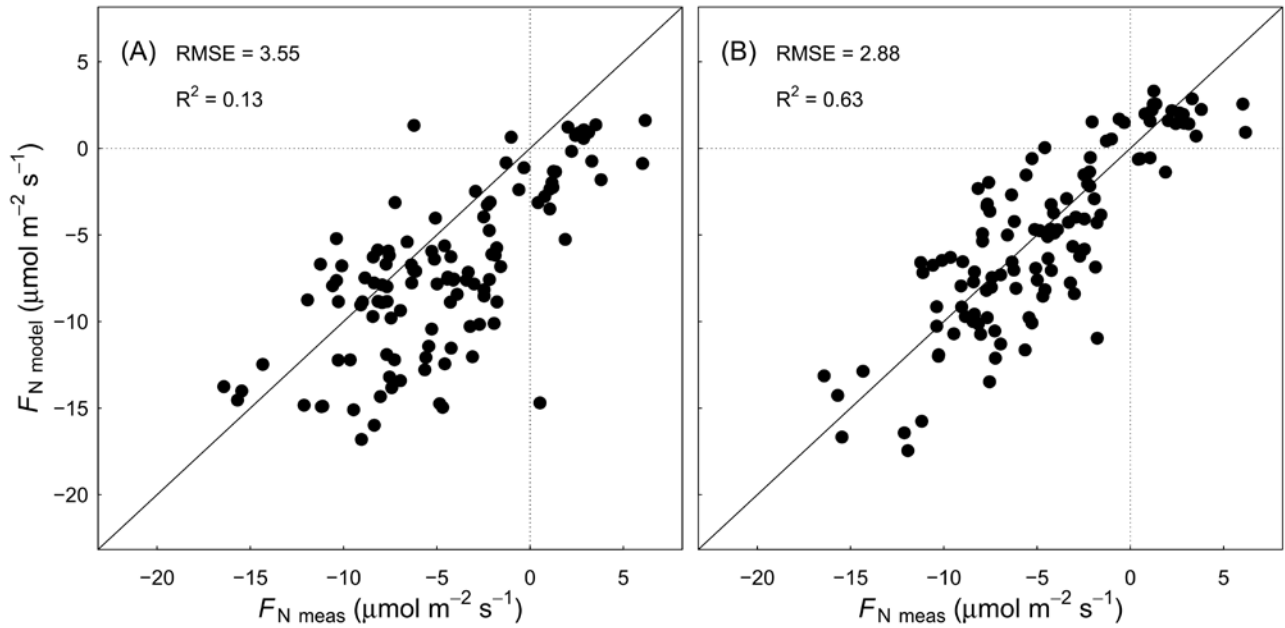


Figure 5.4: Cross-validations, using the hold-out method, of models for net ecosystem CO₂ exchange (F_N) (A) not including the phytomass index, and (B) and including the phytomass index. Model parameters were derived from models fitted using half the data set (training set) and the model cross-validations shown were performed on the other half (testing set). R^2 is the coefficient of determination, RMSE is the root mean square error, and $F_{N\text{ meas}}$ and $F_{N\text{ model}}$ are measured and modelled F_N , respectively.

5.3.5 Cumulative F_N and annual estimates of the components of carbon balance

After a very short increase following the first grazing event, cumulative F_N decreased in spring, indicating a sink of CO₂ for all treatments (Fig. 5). F_N decreased with the irrigation and nitrogen treatments with a synergistic effect leading to the strongest sink for the I_1N_1 treatment in early summer. Only the I_1N_1 treatment was a cumulative net CO₂ sink at the end of the measurement period ($F_N = -223\text{ gC m}^{-2}$) (Fig. 5). For the three other treatments, F_N showed the systems were net CO₂ sources in early summer with increasing strength until the end of winter (Fig. 5). The I_0N_0 treatment was the strongest source of CO₂ ($F_N = 383\text{ gC m}^{-2}$), and the I_0N_1 and I_1N_0 treatments showed similar intermediate values. In mid-summer, when θ_s increased in the irrigated plots, cumulative F_N for the I_1N_0 treatment decreased slightly and then remained constant until early winter. This resulted in the I_1N_0 treatment being a slightly weaker source of CO₂ ($F_N = 128\text{ gC m}^{-2}$) compared with that for the I_0N_1 treatment ($F_N = 216\text{ gC m}^{-2}$). Levels of uncertainty estimated from

the Monte Carlo simulations were very large, with the 95% intervals for annual estimates of F_N all overlapping.

Annual proportional estimates for the above-ground components of ecosystem CO_2 exchange were different for each treatment. For the irrigation and nitrogen treatments, A increased proportionally more than R_E , with the ratio of R_E to A being 1.5, 1.2, 1.1 and 0.9 for the I_0N_0 , I_0N_1 , I_1N_0 and I_1N_1 treatments, respectively. For the I_0 treatment, both A and R_L were significantly lower than the values for the I_1 treatment (Fig. 6). There was a positive synergistic effect of irrigation and nitrogen on both A and R_L , with the annual totals for the I_1N_0 treatment being significantly lower than those for the I_1N_1 treatment (non-overlapping 95% confidence intervals, Fig. 6). There was also a significant positive effect of irrigation and nitrogen, with a synergistic effect of the combination of irrigation and nitrogen (I_1N_1) on the carbon exported as grazed above-ground biomass (F_{export}). Annual total R_S was increased by irrigation with the difference for the values for I_1N_0 (the highest) and I_0N_1 (the lowest) different (by 223 gC m^{-2}), but the 95% intervals were overlapping (Fig. 6).

When adding F_{export} to R_S and R_L , total ecosystem carbon losses exceeded A , so all four treatments were a net source of carbon (negative N_B) (Figs. 6 and 7). Both the I_1N_0 and I_0N_1 treatments showed similar intermediate values of N_B (-459 and -396 gC m^{-2} for I_0N_0 and I_0N_1 , respectively) and were weaker carbon sources than the I_0N_0 treatment ($N_B = -539 \text{ gC m}^{-2}$). The I_1N_1 treatment appeared to be the weakest source of carbon, showing the least negative value ($N_B = -284 \text{ gC m}^{-2}$). None of the differences in N_B were significant, with 95% intervals overlapping (Fig. 7).

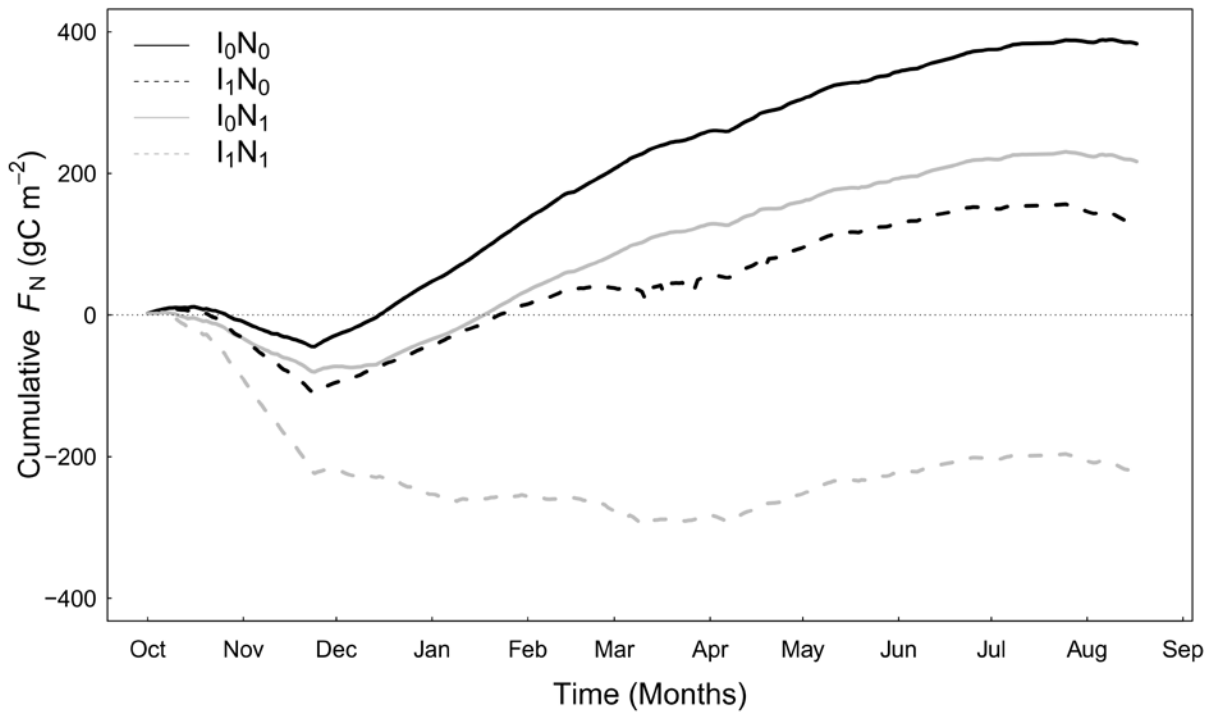


Figure 5.5: Cumulative net ecosystem CO₂ exchange (F_N) for the measurement period from October 2014 to September 2015, for the four treatments: non-irrigated with no nitrogen addition (I_0N_0 , continuous black line), irrigated with no nitrogen addition (I_1N_0 , dashed black line), non-irrigated with added nitrogen (I_0N_1 , continuous grey line) and irrigated with added nitrogen (I_1N_1 , dashed grey line).

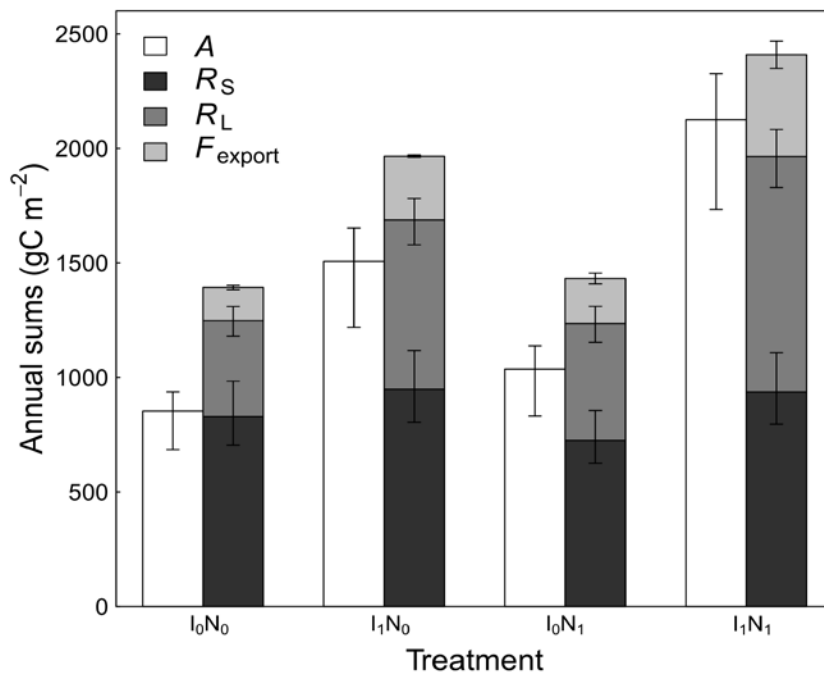


Figure 5.6: Annual estimates of gross canopy photosynthesis (A , white bars), soil respiration (R_S , black bars), leaf respiration (R_L , dark-grey bars) and biomass exported via grazing (F_{export} , light-grey bars), for the four treatments: non-irrigated with no nitrogen addition (I_0N_0), irrigated with no nitrogen addition (I_1N_0), non-irrigated with added nitrogen (I_0N_1) and irrigated with nitrogen addition (I_1N_1). Vertical bars indicate uncertainties calculated as 95% confidence intervals of 1000 Monte Carlo simulations.

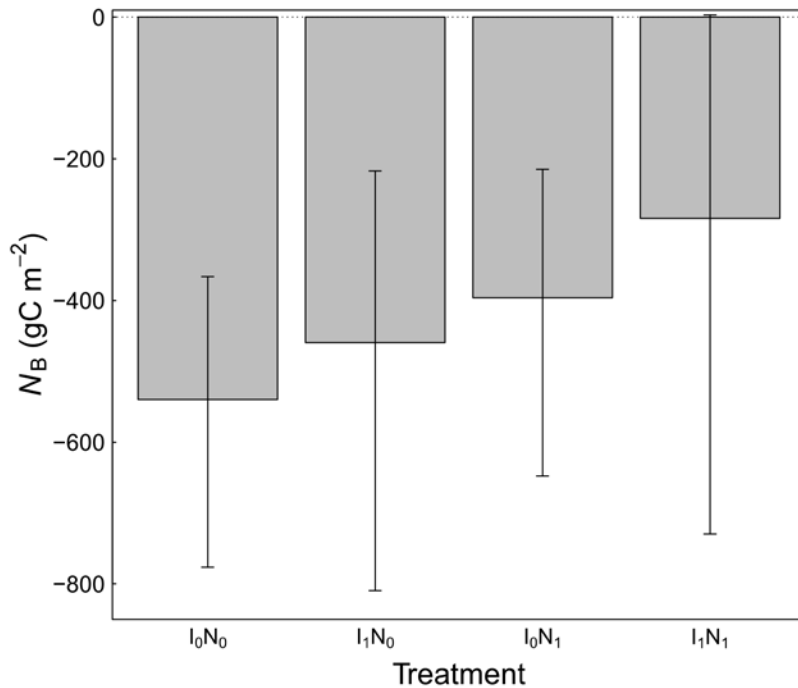


Figure 5.7: Annual estimates of net ecosystem carbon balance (N_B) for the four treatments: non-irrigated with no nitrogen addition (I_0N_0), irrigated with no nitrogen addition (I_1N_0), non-irrigated with nitrogen addition (I_0N_1) and irrigated with nitrogen addition (I_1N_1). Vertical bars indicate uncertainties calculated as 95% confidence intervals of 1000 Monte Carlo simulations.

5.4 Discussion

This study assessed the interactive effects of adding irrigation and nitrogen fertiliser on all the components of ecosystem carbon balance for a grazed grassland. My findings reveal strong differences in the components of carbon balance resulting from irrigation and nitrogen treatments, mediated by seasonal changes in environmental variables. I show that irrigation and nitrogen addition result in significant increases in gross canopy photosynthesis, that are greater than the increases in ecosystem respiration. This results in increased net CO_2 uptake by the ecosystem, and increased productivity. The additional biomass produced is, however, largely exported via grazing. For this first year after irrigation and nitrogen were added, this intensively grazed grassland ecosystem remained a net source of carbon for all treatments.

5.4.1 *Effects of irrigation and nitrogen on seasonal measurements*

Soil temperature is well known to be a dominant factor in regulating rates of soil respiration (Raich and Schlesinger, 1992; Lloyd and Taylor, 1994; Kirschbaum, 1995). Soil water availability is another important factor, with higher rates of R_s resulting from high soil water content near field capacity (Davidson et al., 2000). Water availability may become the predominant limiting factor in dry conditions (Janssens et al., 2003). In my study, seasonal variations in R_s followed variations in soil temperature in the irrigated plots. However, for the non-irrigated plots, water availability became limiting in summer and R_s did not increase with T_s and became very low at the driest time of the year in mid-summer (February). The effect on R_s of adding nitrogen to grasslands is unclear, with studies reporting increases (Jong et al., 1974; Yan et al., 2010; Graham et al., 2012), decreases (Yan et al., 2010) or no effect (Chapter 2). My findings show that R_s is well described by functions incorporating T_s and θ_s , in agreement with previous studies (Janssens et al., 2003; Bahn et al., 2008; Webster et al., 2009; Graham et al., 2012; Chapter 3), but with no effect of the nitrogen treatments on the model parameters.

Temperature, water supply and intercepted irradiance have long been known to influence plant growth (Monteith and Moss, 1977; Monteith, 1981; Myers et al., 1988) and soil water limitations have been found to be the main factor regulating grassland productivity (Flanagan et al., 2002; Hunt et al., 2004; Zhang et al., 2014). Increases in photosynthesis in response to nitrogen addition are also well documented (Evans, 1989; Sinclair and Horie, 1989; Muchow and Sinclair, 1994), attributable to increases in Rubisco activity associated with leaf nitrogen concentration (Friend, 1991). However, above-ground productivity may not increase if water supply is limiting, and nitrogen availability may become a limiting factor for growth only when water deficits are low (Huxman et al., 2004; Bai et al., 2010; Li et al., 2011). My findings support these earlier observations. Biomass production fell almost to zero in the dry summer period when soil water content was low. Canopy nitrogen content and biomass production increased as a result of nitrogen addition only when water availability was not limiting. In early summer (December), before the onset of water limitations, nitrogen contents in the

irrigated and non-irrigated with nitrogen addition treatments were higher than those in plots where there were no additions of nitrogen. In late summer (February), at the driest time of the year, leaf nitrogen content was even greater for the irrigated, non-added nitrogen treatment than that for the non-irrigated with added nitrogen treatment, because growth in the latter had ceased. It is clear that above-ground biomass production at my site was limited dominantly by water availability, and secondarily by nitrogen availability.

Variations in above-ground A and, R_L and F_N are consistent with differences in above-ground biomass. When water was unlimited, I observed increases in R_E resulting from adding nitrogen. As R_S was not affected by nitrogen treatment, this was likely entirely attributable to the concomitant increase in R_L . However, I observed an increase in CO_2 uptake (decrease in F_N) in response to nitrogen addition in well-watered conditions, showing that the increase in R_L was less than the increase in A . Consistent with my findings, an increase in A with leaf nitrogen content has been shown to be greater than increase in R_L (Field and Mooney, 1986). Irrigation alone also resulted in an increase in CO_2 uptake (lower F_N) in summer, consistent with higher canopy nitrogen content. Despite slightly higher canopy nitrogen content for the nitrogen treatments (I_0N_1 and I_1N_1), there were no differences in above-ground biomass production or components in the carbon balance between the treatments during winter. This was likely due to low temperatures limiting CO_2 exchange and plant growth.

When the phytomass index (P_i), representing variations in above-ground biomass, was included in the models for A and R_L , there were no differences in the model parameters between treatments, suggesting that biomass production explained the treatment effects. The model including P_i performed much better in predicting values of A and F_N in the independent data set, confirming the validity of the P_i approach to account for variations in above-ground biomass. Surprisingly, including P_i in the model for R_L did not improve the predictive performance. I attribute this to the variability associated with R_L being calculated from measurements of R_E and R_S measurements being made at different locations within the treatment plots. Increases in R_L shortly after grazing were also

observed and attributed to wounding response of the leaves (Macnicol, 1976; Chapter 2), resulting in a non-linear relationship between R_L and leaf area. Such effects also could have weakened the fit of the model for R_L including P_i .

5.4.2 Annual estimates and net ecosystem carbon balance

Worldwide, annual R_S in grasslands varies from 58 to 1988 gC m⁻² y⁻¹ (Bahn et al., 2008). Focusing on grasslands along a latitudinal transect in Europe, Bahn et al. (2008) found that the range narrowed from 494 to 1 166 gC m⁻² y⁻¹. With annual R_S ranging from 725 to 948 gC m⁻² y⁻¹ between treatments, my findings falls within the range reported in the literature. There are no earlier reports of annual values of R_S in irrigated, intensively-grazed grasslands in New Zealand, but several studies have estimated annual R_E and A using eddy covariance. At a site with higher rainfall and intense grazing management, on a Gley soil, Rutledge et al. (2015) reported mean values over four consecutive years of 2 196 and 2 030 gC m⁻² y⁻¹ for A and R_E , respectively, resulting in the system being a net sink for CO₂ (negative F_N). On a drained peatland with similar management and climate, Campbell et al. (2015) observed a net source of CO₂, with annual A and R_E values of 1 886 and 2 076 gC m⁻² y⁻¹, respectively. Hunt et al. (2016) compared carbon balance components for grasslands used for commercial dairy farm with and without irrigation and nitrogen addition in the same region in New Zealand with similar soil type and conditions as those at my site. After six years from the start of the treatments, they found a significant increase in annual estimates for A and R_E with values of 2 679 and 2 271 gC m⁻² y⁻¹ on the irrigated site and of 1 372 and 1 352 gC m⁻² y⁻¹ on the non-irrigated site, respectively. My estimates were very close to the observations from Hunt et al. (2016) with values of 2 125 and 1 965 gC m⁻² y⁻¹ for A and R_E , respectively, for the treatment with irrigation and nitrogen, and 853 and 1 248 gC m⁻² y⁻¹ for A and R_E , respectively, for my treatment with no irrigation and no added nitrogen.

I showed that irrigation and addition of nitrogen resulted in the grassland becoming a stronger sink for CO₂. However, my grazing regime, representative of intensively managed dairy farms, most

likely resulted in overestimation of the carbon losses from my non-irrigated treatments compared with those for commercial extensive farm management, as shown by my high exports ($145 \text{ gC m}^{-2} \text{ y}^{-1}$ from the I_0N_0 treatment) compared to the non-irrigated site in Hunt et al. (2016) ($45 \text{ gC m}^{-2} \text{ y}^{-1}$). In addition to the fact that grazing also resulted in no uptake of CO_2 from the non-irrigated treatments in summer, this three-fold increase in carbon exports may explain most of the difference in net carbon balance between my non-irrigated and non-fertilised and irrigated and fertilised treatments. Despite nearly identical biomass exported through grazing (F_{export}) in the study of Hunt et al. (2016) ($430 \text{ gC m}^{-2} \text{ y}^{-1}$) and my study ($444 \text{ gC m}^{-2} \text{ y}^{-1}$), I found a contrasting result in terms of the net ecosystem carbon balance, with my site remaining a net carbon source ($N_B = -284 \text{ gC m}^{-2} \text{ y}^{-1}$) while the site with irrigation and added nitrogen in the study by Hunt et al. (2016) was a net sink ($N_B = 103 \text{ gC m}^{-2} \text{ y}^{-1}$). This is possibly attributable to the differences in time since the start of the treatments being six years for the study by Hunt et al. (2006) and the first year at my site. However, direct comparison of my findings with those using eddy covariance is also compromised by the absence of grazing animals at my site. I simulated grazing but did not include the effects of the deposition of animal excreta, a return of up to 29% of the exported biomass in intensively managed dairy farms (Rutledge et al., 2015; Hunt et al., 2016). Such an import of carbon would have moved my plots to be weaker net sources of carbon. It is also noteworthy that the ratio of R_E to A was higher in my study compared to with that for Hunt et al. (2016). Night-time estimation of R_E using the eddy covariance technique is known to include high uncertainty and often leads to underestimated values compared to studies using chamber measurements (Speckman et al., 2015). These observations, as well as the different time-scales after farm conversion, may partly explain the discrepancy between the two studies.

5.4.3 *Implications for changes to soil carbon stocks*

Assuming that I have accounted for changes in carbon accumulation and removal as above-ground biomass in my treatments at my site, I infer that carbon lost from my site must be

attributable to losses from below-ground carbon storage. In an earlier study at my site, Chapter 4 showed that irrigation and nitrogen addition did not change the rate of soil organic matter decomposition six months after the treatments were imposed. My measurements were made in the first year when the treatments were imposed and the amount of carbon lost was statistically similar for all treatments. I conclude that the additional net CO₂ input that resulted from irrigation and nitrogen addition in the present study was rapidly transferred to the leaves for continued rapid growth above-ground, with no net effect on soil organic carbon pool. This does not exclude the possibility of a small increase in carbon transferred from the rhizosphere to the bulk soil, which, in the absence of increased soil organic matter decomposition, would eventually result in an increase in the soil organic carbon pool. However, at a similar site in the same farm, Kelliher et al. (2015) found no significant differences in carbon content at a depth to 0.8 m between non-irrigated extensively sheep-grazed and irrigated, intensively grazed pastures eleven years after conversion. Results from this study and ours converge to the hypothesis that the rate of soil organic matter decomposition will continue to exceed the rate of input of carbon to the soil organic carbon for at least a decade, regardless of differences in above-ground primary production associated with the treatments.

My measurements were made in the first year when the treatments were imposed and contrast with the observations made in a different grassland after six years of irrigation and nitrogen addition (Hunt et al., 2016). Taking together observations from measurements of soil organic matter decomposition at the same site (Chapter 4), long-term chronosequence of soil carbon measurements (Kelliher et al., 2015) and the mechanistic understanding of the changes in CO₂ exchanges from leaves and soil brought in light in the present study, I am able to formulate the hypothesis that soil organic carbon is likely to keep decreasing regardless of whether pastures are converted to intensive dairy management. Such information is not available at the site where the study by Hunt et al. (2016) took place and it is not known whether the benefits from converting the pasture to intensive dairy farming management to the net carbon balance results in increased soil

carbon content. The study by Schipper et al. (2014) showed that long-term gains or losses of soil carbon from grasslands were dependent upon soil types, with no effect of land management. This observation lines up with the emerging theory that soil structure and microbe accessibility to the substrates regulates soil organic matter decomposition, confirmed at my site (Chapter 4). More research is needed to give a mechanistic understanding to the dynamics of soil organic matter decomposition and be able to predict future changes in soil carbon stocks in relation to pasture management, but to conclude, there is yet no evidence that conversion of dryland extensive pastoral farming to intensive management with irrigation and nitrogen addition will result in long-term increases in soil organic carbon stocks.

CHAPTER 6 General discussion

6.1 General results

The research in this thesis investigated the question of whether conversion to intensive dairy farm management with irrigation and addition of nitrogen fertiliser will result in soil carbon sequestration in New Zealand pastures.

Together, the findings have provided consistent evidence that changes in ecosystem carbon dynamics induced by irrigation, addition of nitrogen and grazing are dominated by above-ground processes that result in increased net ecosystem productivity. However, simulating conversion from dryland sheep to intensive dairy farming, Chapter 5 showed little effect on net ecosystem carbon balance. The control treatment was a net source of carbon to the atmosphere and this continued even with the experimental treatments for both irrigation and addition of nitrogen. Chapter 4 revealed that heterotrophic respiration (R_H) was insensitive to the simulated conversion on a seasonal time scale, and changes in the below-ground component of carbon balance were dominated by autotrophic respiration, which has little effect on soil carbon stocks. This grazed grassland ecosystem, newly converted to intensive dairy farming management, will remain a source of carbon if the losses from soil organic matter decomposition continue to exceed the net ecosystem carbon gain. Thus, the answer to the general thesis question *whether conversion from dryland to intensive dairy farm management will result in soil carbon sequestration in New Zealand managed grasslands* strongly depends on my ability to predict how the balance between carbon inputs to and losses from soil organic matter will change under sustained intensive management in the following years after conversion. This is the first study in New Zealand where experimental treatments incorporating irrigation and addition of nitrogen have been used to investigate changes to the components of carbon balance for a grassland. The research has contributed new insights to reveal the nature of the processes regulating carbon exchange in response to driving variables. In particular, the new findings that R_H is independent of changes in soil temperature and soil water content has far reaching implications for the improvement of models of soil carbon dynamics. Further, the data have enabled the development of a model that explains differences between the

treatments and provides ability to forecast the impacts of management practices on annual net changes in carbon storage at ecosystem scales. In particular, the new approach to model changes in biomass production through grazing cycles using the phytomass index (P_i) and development of techniques to overcome problematic estimation of changes in R_H in response to the treatments have contributed new insights.

6.2 Drivers of carbon balance components

6.2.1 Ecosystem carbon uptake

Temperature (Monteith and Moss, 1977; Monteith, 1981), water availability (Myers et al., 1988; Flanagan et al., 2002; Hunt et al., 2004; Zhang et al., 2014) and nitrogen availability (Evans, 1989; Sinclair and Horie, 1989; Muchow and Sinclair, 1994) are known to limit plant growth. In grassland ecosystems, grazing is also known to significantly impact primary production (Ammann et al., 2007; Soussana et al., 2010; McSherry and Ritchie, 2013; Campbell et al., 2015). My studies at Beacon Farm, where conversion to intensive management had occurred six years prior to the measurement period, quantified the significant reductions on A , R_L and the net CO_2 uptake (increased F_N) of repeated defoliation of the canopy by grazing. After each grazing event, temperature and irradiance were the primary factors regulating regrowth, and the rate of regrowth was enhanced by addition of nitrogen. Plant growth was regulated by the same factors at Ashley Dene Farm within the first year of conversion to simulated intensive management. However, water availability was the primary factor, strongly limiting A , R_L and plant growth in the non-irrigated treatments. Annual net productivity at the Ashley Dene site was very similar to that at Beacon Farm, estimated using eddy covariance by Hunt et al. (2016). This confirms that irrigation and nitrogen have immediate effects on above-ground components of the carbon balance and result in rapid and sustained increases in net ecosystem productivity.

6.2.2 Soil organic matter decomposition, R_H

Determining the response of R_H to environmental drivers has largely been confined to measurements using laboratory incubations (Kirschbaum, 1995; Davidson and Janssens, 2006; Manzoni et al., 2012), or from field studies using techniques that disturb the soil environment and remove the autotrophic component (Kuzyakov, 2006). These approaches led to the paradigm that soil water content, and especially soil temperature, are the main drivers of R_H . However, interpretation from other studies suggests that limited substrate availability to micro-organisms in an undisturbed soil may reduce or offset the sensitivity of R_H to soil temperature (Davidson and Janssens., 2006) and soil water content (Moyano et al., 2013). Few studies have used non-disruptive isotopic techniques and showed no effect of soil temperature on R_H in the field (Reviewed by Giardina and Ryan, 2000; Graham et al., 2012). The findings in Chapter 4 are consistent with these studies and also show that R_H is independent of changes in soil water content. Furthermore, Chapter 4 led to new insight to understand the factors regulating soil carbon dynamics, providing additional supporting evidence that microbial access to the substrates, as opposed to chemical recalcitrance, is predominant in regulating soil organic matter decomposition (Schmidt et al., 2011; Dungait et al., 2012; Lehmann and Kleber, 2015).

The physical protection of organic matter into aggregates (frequently referred to as particulate organic matter combined with macro-organic matter defined in Chapter 4) is likely to represent the first and weakest degree of protection and is thus likely to be highly sensitive to disturbance through soil management practices (Six et al., 2002). For example, the particulate organic matter pool of carbon was observed to decrease after 60 years of cultivation (Tiessen and Stewart, 1983), after over 20 years of conventional tillage practices (Cambardella and Elliott, 1992; Six et al., 1999), and after 25 years of application of different mineral fertilisers (Yan et al., 2007). Thus, such changes in aggregate formation are likely to occur slowly over a period of up to 20 years and detecting changes at Beacon Farm (6 years after conversion) and Ashley Dene Farm (first year after conversion) would be problematic. To date, there are no studies revealing the effects of irrigation on aggregate

dynamics in grasslands, and more generally on soil structure. However, it is known that irrigation and nitrogen addition may result in shifts in the composition of plant communities (Lauenroth et al., 1978; Thomas, 1984), leading to differences in root traits (Rillig et al., 2015) and biomass (McNally et al., 2015), potentially resulting in changes in soil aggregate dynamics (Six et al., 2004; Rillig and Mummey, 2006; Rillig et al., 2015). This is particularly relevant to the conversion to intensive farm management practices that involved pasture renewal with ploughing and resowing with ryegrass (*Lolium perenne* L.) and clover (*Trifolium repens* L.), at Beacon Farm. Interestingly, the rates of R_H that I measured on intact mesocosms sampled from Beacon Farm (Chapter 2) and from the irrigated and fertilised treatment at Ashley Dene Farm (Chapter 4) were overall very similar (between 1 and 2 $\mu\text{mol m}^{-2} \text{s}^{-1}$), despite different environmental conditions. I did observe an increase in R_H as a consequence of addition of nitrogen at Beacon Farm, resulting in part from interactions with roots and the rhizosphere (referred to as a rhizosphere priming effect), but this result was not confirmed at Ashley Dene Farm. Differences in root and rhizosphere characteristics between the pasture dominated by Ryegrass at Beacon farm and the mixed sward at Ashley Dene farm could explain partly differences in the priming effect. Further, the significant increase in R_A in response to irrigation at Ashley Dene Farm was not concurrent with changes in R_H , confirming the lack of a rhizosphere priming effects at this site. This suggests that the degree of protection of soil organic matter preventing its degradation was similar at both these sites so time scales of at least a decade are required for this to occur. However, short-term effects of changes in rhizosphere activity on R_H as a consequence of addition of nitrogen cannot be excluded, and further research is needed to confirm the rates of change in field conditions.

6.3 Soil carbon stocks under intensive management

While it seems clear that ecosystem carbon uptake will increase consistently under intensive management practices, the direction and magnitude of changes for soil organic matter decomposition are difficult to predict from current state of knowledge. Thus, predicting changes in

the net carbon balance for grasslands and the resulting long-term effects on soil carbon storage are problematic. Furthermore, available data are contradictory. At an annual time scale, a significant proportion of the carbon uptake by the ecosystem is harvested and exported by grazing. The net balance between increased uptake and export of carbon may result in a net gain (Rutledge et al., 2015; Hunt et al., 2016) or loss (Campbell et al., 2015; Chapter 5) of carbon. These previous studies were undertaken at different sites, and while they are all representative of intensive dairy management practices across New Zealand, inclusion of irrigation and nitrogen addition occurred only at the two sites in this thesis and at Beacon Farm study by Hunt et al. (2016). Interpretation of the consequences of the use of different techniques to estimate net ecosystem carbon balance, and simulated grazing at my site that excluded the presence of the animals, was discussed in Chapter 5. Overall, these effects at least partly cancel each other and I argued that they were unlikely to reconcile my findings and those from Hunt et al. (2016) made at the same site. In addition, they do not explain discrepancies between the other studies elsewhere (Rutledge et al., 2015; Campbell et al., 2015), as these were both conducted using the eddy covariance technique and included grazing animals.

Evidence from sequential core sampling has shown that, for sites across New Zealand, intensive dairy farming management on flat land has resulted in decreases in soil carbon content only for Gley and Allophanic soil orders (Schipper et al., 2014). On the flat stony soils of the Canterbury Region, Kelliher et al. (2012) also found lower soil carbon content in a grassland that had been irrigated for 60 years compared with the carbon content in an adjacent, non-irrigated pasture. However, net ecosystem carbon gains were observed in the study by Rutledge et al. (2015) on Gley soils and the studies by Hunt et al. (2016) and Kelliher et al. (2012) were both on similar Brown soils. Considering that grazed grasslands do not accumulate carbon in above-ground biomass, changes in net ecosystem carbon balance must be attributable to changes in below-ground processes. Without measurements of R_H , changes in the pools of carbon (e.g., heterotrophic or autotrophic) cannot be determined and differences in the observations of the net ecosystem carbon balance may reflect

differences between ecosystem inputs of carbon and losses from either the autotrophic or the heterotrophic pools, leading to different implications for long term soil carbon stocks. It is conceivable that the additional carbon uptake by the ecosystem resulting from a positive net carbon balance resides temporarily in the soil autotrophic pool and is vulnerable to subsequent changes in environmental conditions. My field observations that increased above-ground productivity was concurrent with an increase in soil autotrophic activity and further support this possibility. While additional carbon added to roots will likely result in an eventual transfer to the heterotrophic pool, this will contribute to increasing soil carbon storage only if these increased root inputs are sustained and if the rate of soil organic matter decomposition remains constant or decreases. However, root biomass may eventually decrease as a consequence of irrigation (Scott et al., 2010) and addition of nitrogen (Millard et al., 1990). With changes in root architecture potentially contributing to changes in soil structure, conversion could eventually result in decreased carbon inputs to soil organic matter from the roots and rhizosphere, and increased rate of decomposition. This would explain the discrepancies between studies employing short-term measurements of carbon balance observations in the first decade after conversion to intensive management and those based on long-term direct measurements of soil carbon content.

6.4 Conclusions and future research

The limited evidence from sequential core sampling shows that decades of intensive dairy farm management in New Zealand managed grasslands has resulted in no change or a decrease of soil carbon content, depending on soil type (Schipper et al., 2014). This contrasts with findings from recent carbon balance studies that have reported net uptake of carbon at annual timescales (Rutledge et al., 2015; Hunt et al., 2016). This thesis has provided insights to reconcile these apparent differences by investigating the effects of irrigation, addition of nitrogen fertiliser and grazing, three key management practices, on the components of carbon balance. My findings have confirmed that intensive pasture management resulted in a rapid and sustained increase in

ecosystem productivity that is almost entirely attributable to changes in the above-ground and soil autotrophic components of the carbon balance. These changes may (Rutledge et al., 2015; Hunt et al., 2016) or may not (Campbell et al., 2015; this study Chapter 5) result in a net ecosystem carbon uptake at annual timescales. But these studies cannot simply be extrapolated to infer long-term changes in soil carbon stocks, as annual trends will be sustained only if the balance between ecosystem uptake and losses from soil organic matter decomposition remains balanced. My research has shown that soil organic matter decomposition is regulated by soil characteristics controlling the physical protection of organic matter from microbial degradation, resulting in its stability to changes in environmental conditions induced by conversion to intensive pasture management. Thus, changes in soil organic matter decomposition are dependent on the stability of soil aggregation mechanisms and soil structure and are expected to occur only after decades of sustained intensive management. Such changes are also likely to be specific to different soil types and site conditions.

Overall, pasture conversion to intensive dairy farming practices increases productivity, with a short-term benefit to the net ecosystem carbon balance at some sites. However, only the long-term effect on soil carbon stocks will determine whether intensive dairy production is sustainable economically and environmentally. To date, evidence for a long-term beneficial effect on soil carbon stocks is lacking. Accurate predictions of changes in carbon stocks depend strongly on our ability to develop a mechanistic understanding of the factors regulating soil organic matter decomposition. The findings in Chapter 2 suggest the potential existence of rhizosphere priming mechanisms that result in increased rates of organic matter decomposition under high levels of nitrogen. This is consistent with the suggestions that R_H may increase and offset ecosystem carbon gains under intensive dairy farming, but further research is required to confirm this in field conditions. A mechanistic explanation allowing a generalisation of this observation to other sites and conditions is pending. Future research is needed to identify mechanistic linkages between soil organic matter dynamics and soil structure. Long-term field experiments should be designed to test the hypotheses

that soil organic matter decomposition may change concurrently with the degree of physical protection of organic matter. Measurements of R_H along large spatial gradients, including different soil types and climates, will help us to understand the relationships between soil structure and organic matter decomposition. To assist with this, adoption of the improved natural abundance of ^{13}C technique developed in this thesis will be a useful tool. Furthermore, investigating the rhizosphere priming effect may reveal potential linkages between management practices, soil structure and decomposition of soil organic matter. This may be achieved for example by measuring changes in the structure and organic matter decomposition of similar soils with plant communities exhibiting differences in root characteristics and biomass distribution in the soil profile. Finally, accurate characterisation of the response of soil organic matter decomposition to soil temperature and water content in controlled conditions with minimal disturbance to the soil structure is critical. This will help testing the hypothesis that the physical protection of organic matter in the soil is a predominant driver of its rate of decay as well as directly improving model predictions of the fate of soil carbon under future climatic conditions and management practices.

REFERENCES

- Anderson, D.R., 2007.** Model based inference in the life sciences: a primer on evidence. Springer Science & Business Media.
- Ammann, C., Flechard, C.R., Leifeld, J., Neftel, A., Fuhrer, J., 2007.** The carbon budget of newly established temperate grassland depends on management intensity. *Agriculture, Ecosystems & Environment*, **121**, 5–20.
- Amundson, R., 2001.** The carbon budget in soils. *Annual Review of Earth and Planetary Sciences*, **29**: 535–562.
- Atkinson, C.J., 1986.** The effect of clipping on net photosynthesis and dark respiration rates of plants from an upland grassland, with reference to carbon partitioning in *Festuca ovina*. *Annals of Botany*, **58**: 61–72.
- Baldocchi, D., 2008.** Turner review No. 15. “Breathing” of the terrestrial biosphere: lessons learned from a global network of carbon dioxide flux measurement systems. *Australian Journal of Botany*, **56**: 1–26.
- Bahn, M., Knapp, M., Garajova, Z., Pfahringer, N., and Cernusca, A., 2006.** Root respiration in temperate mountain grasslands differing in land use. *Global Change Biology*, **12**: 995–1006.
- Bahn, M., Rodeghiero, M., Anderson-Dunn, M., Dore, S., Gimeno, C., Drösler, M., Williams, M., Ammann, C., Berninger, F., Flechard, C., Jones, S., Balzarolo, M., Kumar, S., Newesely, C., Priwitzer, T., Raschi, A., Siegwolf, R., Susiluoto, S., Tenhunen, J., Wohlfahrt, G., and Cernusca, A., 2008.** Soil respiration in European grasslands in relation to climate and assimilate supply. *Ecosystems*, **11**: 1352–1367.
- Bai, W., Wan, S., Niu, S., Liu, W., Chen, Q., Wang, Q., Zhang, W., Han, X., Li, L., 2010a.** Increased temperature and precipitation interact to affect root production, mortality, and turnover in a temperate steppe: implications for ecosystem C cycling. *Global Change Biology*, **16**: 1306–1316.
- Bai, Y., Wu, J., Clark, C.M., Naeem, S., Pan, Q., Huang, J., Zhang, L., Han, X., 2010b.** Tradeoffs and thresholds in the effects of nitrogen addition on biodiversity and ecosystem functioning: evidence from Inner Mongolia grasslands: impact of N enrichment on ecosystem functioning. *Global Change Biology*, **16**: 358–372.
- Barthel, M., Cieraad, E., Zakharova, A., Hunt, J.E., 2014.** Sudden cold temperature delays plant carbon transport and shifts allocation from growth to respiratory demand. *Biogeosciences*, **11**: 1425–1433.
- Bottner, P., Pansu, M., Sallih, Z., 1999.** Modelling the effect of active roots on soil organic matter turnover. *Plant and Soil*, **216**: 15–25.

- Boutton, T.W., Archer, S.R., Midwood, A.J., Zitzer, S.F., Bol, R., 1998.** $\delta^{13}\text{C}$ values of soil organic carbon and their use in documenting vegetation change in a subtropical savanna ecosystem. *Geoderma*, **82**: 5–41.
- Bowling, D.R., Pataki, D.E., Randerson, J.T., 2008.** Carbon isotopes in terrestrial ecosystem pools and CO_2 fluxes. *New Phytologist*, **178**: 24–40.
- Bremer, D.J., Ham, J.M., Owensby, C.E., Knapp, A.K., 1998.** Responses of soil respiration to clipping and grazing in a tallgrass prairie. *Journal of Environmental Quality*, **27**: 1539–1548.
- Bronick, C.J., Lal, R., 2005.** Soil structure and management: a review. *Geoderma*, **124**: 3–22.
- Brown, M., Whitehead, D., Hunt, J.E., Clough, T.J., Arnold, G.C., Baisden, W.T., Sherlock, R.R., 2009.** Regulation of soil surface respiration in a grazed pasture in New Zealand. *Agricultural and Forest Meteorology*, **149**: 205–213.
- Buchmann, N., 2000.** Biotic and abiotic factors controlling soil respiration rates in *Picea abies* stands. *Soil Biology & Biochemistry*, **32**: 1625–1635.
- Burnham, K.P., Anderson, D.R., 2002.** Model selection and multimodel inference: a practical information-theoretic approach. Springer Science & Business Media.
- Cambardella, C.A., Elliott, E.T., 1992.** Particulate soil organic-matter changes across a grassland cultivation sequence. *Soil Science Society of America Journal*, **56**: 777–783.
- Campbell, D.I., Wall, A.M., Nieveen, J.P., and Schipper, L.A., 2015.** Variations in CO_2 exchange for dairy farms with year-round rotational grazing on drained peatlands. *Agriculture, Ecosystems & Environment*, **202**: 68–78.
- Chantigny, M.H., 2003.** Dissolved and water-extractable organic matter in soils: a review on the influence of land use and management practices. *Geoderma*, **113**: 357–380.
- Chapin III, F. S., Woodwell, G. M., Randerson, J. T., Rastetter, E. B., Lovett, G. M., Baldocchi, D. D., and Wirth, C. 2006.** Reconciling carbon-cycle concepts, terminology, and methods. *Ecosystems*, **9**: 1041-1050.
- Chen, L., Dick, W.A., Streeter, J.G., Hoitink, H.A.J., 1996.** Ryegrass utilization of nutrients released from composted biosolids and cow manure. *Compost Science & Utilization*, **4**: 73–83.
- Cheng, W., Kuzyakov, Y., 2001.** Photosynthesis controls of rhizosphere respiration and organic matter decomposition. *Soil Biology & Biochemistry*, **33**: 1915–1925.
- Conant, R.T., Paustian, K., Elliott, E.T., 2001.** Grassland Management and conversion into grassland: effects on soil carbon. *Ecological Applications*, **11**: 343–355.
- Condon, L., Black, A., and White, T., 2010.** Effects of long-term inputs of fertiliser and irrigation on soil carbon under grazed pasture. In: R.J. Gilkes and N. Prakongkep, editors, Proceedings of the

19th World Congress of Soil Science, Brisbane, Australia. 1–6 August. Congress Symposium 7 Soil Carbon Sequestration. Brisbane Australia. P. 5–7

Craine, J.M., Wedin, D.A., Iii, F.S.C., 1999. Predominance of ecophysiological controls on soil CO₂ flux in a Minnesota grassland. *Plant and Soil*, **207**: 77–86.

Crawley, M.J., 2007. The R book. Wiley, Chichester, England ; Hoboken.

Davidson, E.A., Verchot, L.V., Cattânio, J.H., Ackerman, I.L., Carvalho, J.E.M., 2000. Effects of soil water content on soil respiration in forests and cattle pastures of eastern Amazonia. *Biogeochemistry*, **48**: 53–69.

Davidson, E.A., Janssens, I.A., and Luo, Y., 2006. On the variability of respiration in terrestrial ecosystems: moving beyond Q₁₀. *Global Change Biology*, **12**: 154–164.

Domanski, G., Kuzyakov, Y., Siniakina, S., Stahr, K., 2001. Carbon flows in the rhizosphere of ryegrass (*Lolium perenne*). *Journal of Plant Nutrition and Soil Science*, **164**: 381.

Detling, J.K., Dyer, M.I., and Winn, D.T., 1979. Net photosynthesis, root respiration, and regrowth of *Bouteloua gracilis* following simulated grazing. *Oecologia*, **41**: 127–134.

Dungait, J.A.J., Kemmitt, S.J., Michallon, L., Guo, S., Wen, Q., Brookes, P.C., Evershed, R.P., 2011. Variable responses of the soil microbial biomass to trace concentrations of ¹³C-labelled glucose, using ¹³C-PLFA analysis. *European Journal of Soil Science*, **62**: 117–126.

Dungait, J.A.J., Hopkins, D.W., Gregory, A.S., Whitmore, A.P., 2012. Soil organic matter turnover is governed by accessibility not recalcitrance. *Global Change Biology*, **18**: 1781–1796.

Ehleringer, J.R., Buchmann, N., Flanagan, L.B., 2000. Carbon isotope ratios in belowground carbon cycle processes. *Ecological Applications*, **10**: 412–422.

Evans, J.R., 1989. Photosynthesis and nitrogen relationships in leaves of C3 plants. *Oecologia*, **78**: 9–19.

FAOSTAT, 2012. <http://faostat3.fao.org/browse/E/EL/E>.

FAO 2014. (Food and Agriculture Organisation of the United Nations): Milk and milk products: price and trade update.

Field, C., Mooney, H.A., 1986. Photosynthesis--nitrogen relationship in wild plants. Econ. Plant Form Funct. Proc. Sixth Maria Moors Cabot Symp. Evol. Constraints Prim. Product. Adapt. Patterns Energy Capture Plants Harv. For. August 1983.

Flanagan, L.B., Wever, L.A., Carlson, P.J., 2002. Seasonal and interannual variation in carbon dioxide exchange and carbon balance in a northern temperate grassland. *Global Change Biology*, **8**: 599–615.

- Flanagan, L.B., Adkinson, A.C., 2011.** Interacting controls on productivity in a northern Great Plains grassland and implications for response to ENSO events: controls on grassland productivity. *Global Change Biology*, **17**: 3293–3311.
- Friend, A.D., 1991.** Use of a model of photosynthesis and leaf microenvironment to predict optimal stomatal conductance and leaf nitrogen partitioning. *Plant, Cell & Environment*, **14**: 895–905.
- Gardner, W.H., 1986.** Water content. Methods of soil analysis. Part 1. Physical and mineralogical methods. 493–544.
- Ghani, A., Dexter, M., Perrott, K.W., 2003.** Hot-water extractable carbon in soils: a sensitive measurement for determining impacts of fertilisation, grazing and cultivation. *Soil Biology & Biochemistry*, **35**: 1231–1243.
- Giardina, C.P., Ryan, M.G., 2000.** Evidence that decomposition rates of organic carbon in mineral soil do not vary with temperature. *Nature*, **404**: 858–861.
- Graham, S.L., Millard, P., Hunt, J.E., Rogers, G.N.D., Whitehead, D., 2012.** Roots affect the response of heterotrophic soil respiration to temperature in tussock grass microcosms. *Annals of botany*, **110**: 253–258.
- Gramig, G.G., and Stoltenberg, D.E., 2007.** Leaf appearance base temperature and phyllochron for common grass and broadleaf weed species. *Weed Technology*, **21**: 249–254.
- Green, J.J., Dawson, L.A., Proctor, J., Duff, E.I., Elston, D.A., 2005.** Fine root dynamics in a tropical rain forest is influenced by rainfall. *Plant and Soil*, **276**: 23–32.
- Gregorich, E., Beare, M., Stoklas, U., St-Georges, P., 2003.** Biodegradability of soluble organic matter in maize-cropped soils. *Geoderma*, **113**: 237–252.
- Gregorich, E.G., Beare, M.H., McKim, U.F., Skjemstad, J.O., 2006.** Chemical and biological characteristics of physically uncomplexed organic matter. *Soil Science Society of America Journal*, **70**: 975–985.
- Hanson, P.J., Edwards, N.T., Garten, C.T., Andrews, J.A., 2000.** Separating root and soil microbial contributions to soil respiration: A review of methods and observations. *Biogeochemistry*, **48**: 115–146.
- Hart, P.B.S., Rayner, J.H., Jenkinson, D.S., 1986.** Influence of pool substitution on the interpretation of fertilizer experiments with ¹⁵N. *Journal of Soil Science*, **37**: 389–403.
- Högberg, P., and Read, D.J., 2006.** Towards a more plant physiological perspective on soil ecology. *Trends in Ecology & Evolution*, **21**: 548–554.
- Hunt, J.E., Kelliher, F.M., McSeveny, T.M., Ross, D.J., and Whitehead, D., 2004.** Long-term carbon exchange in a sparse, seasonally dry tussock grassland. *Global Change Biology*, **10**: 1785–1800.

- Hunt, J.E., Laubach, J., Barthel, M., Fraser, A., and Phillips, R.L. (2016).** Carbon budgets for an irrigated intensively-grazed dairy pasture and an unirrigated winter-grazed pasture. *Biogeosciences Discussion*. 1–38.
- Hutchinson, G.L., Livingston, G.P., 2001.** Vents and seals in non-steady-state chambers used for measuring gas exchange between soil and the atmosphere. *European Journal of Soil Science*, **52**: 675–682.
- Huxman, T.E., Smith, M.D., Fay, P.A., Knapp, A.K., Shaw, Mr., Loik, M.E., Smith, S.D., Tissue, D.T., Zak, J.C., Weltzin, J.F., Pockman, W.T., Sala, O.E., Haddad, B.M., Harte, J., Koch, G.W., Schwinning, S., Small, E.E., Williams, D.G., 2004.** Convergence across biomes to a common rain-use efficiency. *Nature*, **429**: 651–654.
- Janssens, I.A., Dore, S., Epron, D., Lankreijer, H., Buchmann, N., Longdoz, B., Brossaud, J., and Montagnani, L., 2003.** Climatic influences on seasonal and spatial differences in soil CO₂ efflux. In fluxes of carbon, water and energy of European forests, P.D.R. Valentini ed. Springer Berlin Heidelberg, pp. 233–253.
- Janssens, I.A., Dieleman, W., Luysaert, S., Subke, J.-A., Reichstein, M., Ceulemans, R., Ciais, P., Dolman, A.J., Grace, J., Matteucci, G., Papale, D., Piao, S.L., Schulze, E.-D., Tang, J., Law, B.E., 2010.** Reduction of forest soil respiration in response to nitrogen deposition. *Nature Geoscience*, **3**: 315–322.
- Jia, X., Shao, M., and Wei, X., 2012.** Responses of soil respiration to N addition, burning and clipping in temperate semiarid grassland in northern China. *Agricultural and forest meteorology*, **166**: 32–40.
- Jenny, H., 1941.** Factors of soil formation: a system of quantitative pedology. Dover, New York.
- Jiang, L., Shi, F., Li, B., Luo, Y., Chen, J., Chen, J., 2005.** Separating rhizosphere respiration from total soil respiration in two larch plantations in northeastern China. *Tree Physiology*, **25**: 1187–1195.
- Jingguo, W., Bakken, L.R., 1997.** Competition for nitrogen during mineralization of plant residues in soil: Microbial response to C and N availability. *Soil Biology & Biochemistry*, **29**: 163–170.
- Jong, E. de, Schappert, H.J.V., MacDonald, K.B., 1974.** Carbon dioxide evolution from virgin and cultivated soil as affected by management practices and climate. *Canadian Journal of Soil Science*, **54**: 299–307.
- Kahle, M., Kleber, M., Jahn, R., 2002.** Carbon storage in loess derived surface soils from Central Germany: Influence of mineral phase variables. *Journal of Plant Nutrition and Soil Science*, **165**: 141–149.
- Kelliher, F.M., Condon, L.M., Cook, F.J., and Black, A., 2012.** Sixty years of seasonal irrigation affects carbon storage in soils beneath pasture grazed by sheep. *Agriculture, Ecosystems & Environment*, **148**: 29–36.

- Kelliher, F., West, P., Moir, J., 2015.** Soil carbon stock beneath an established irrigated pasture grazed by dairy cattle. *New Zealand Journal of Agricultural Research*, **58**: 78–83.
- Kirschbaum, M.U.F., 1995.** The temperature dependence of soil organic matter decomposition, and the effect of global warming on soil organic C storage. *Soil Biology & Biochemistry*, **27**: 753–760.
- Kleber, M., and Johnson, M.G., 2010.** Chapter 3 - Advances in understanding the molecular structure of soil organic matter: implications for interactions in the environment. In *Advances in Agronomy*, Donald L. Sparks, ed. (Academic Press), pp. 77–142.
- Kuzyakov, Y., 2006.** Sources of CO₂ efflux from soil and review of partitioning methods. *Soil Biology & Biochemistry*, **38**: 425–448.
- Kuzyakov, Y., 2002.** Review: factors affecting rhizosphere priming effects. *Journal of Plant Nutrition and Soil Science*, **165**: 382.
- Kuzyakov, Y., Biryukova, O., Kuznetzova, T., Mölter, K., Kandeler, E., Stahr, K., 2002.** Carbon partitioning in plant and soil, carbon dioxide fluxes and enzyme activities as affected by cutting ryegrass. *Biology and Fertility of Soils*, **35**: 348–358.
- Kuzyakov, Y., and Gavrichkova, O., 2010.** Review: Time lag between photosynthesis and carbon dioxide efflux from soil: a review of mechanisms and controls. *Global Change Biology*, **16**: 3386–3406.
- Lal, R., 2004.** Soil carbon sequestration impacts on global climate change and food security. *Science*, **304**: 1623–1627.
- Lal, R., 2009.** Challenges and opportunities in soil organic matter research. *European Journal of Soil Science*, **60**: 158–169.
- Laubach, J., Barthel, M., Fraser, A., Hunt, J.E., and Griffith, D.W.T., 2015.** Combining two complementary micrometeorological methods to measure CH₄ and N₂O fluxes over pasture. *Biogeosciences Discussion*, **12**: 15245–15299.
- Lauenroth, W.K., Dodd, J.L., and Sims, P.L. (1978).** The effects of water- and nitrogen-induced stresses on plant community structure in a semiarid grassland. *Oecologia*, **36**: 211–222.
- Lee, M., Nakane, K., Nakatsubo, T., Koizumi, H., 2003.** Seasonal changes in the contribution of root respiration to total soil respiration in a cool-temperate deciduous forest. In: Abe, J. (Ed.), *Roots: The dynamic interface between plants and the earth*. Springer, Netherlands, pp. 311–318.
- Lehmann, J., and Kleber, M., 2015.** The contentious nature of soil organic matter. *Nature*, **528**: 60–68.
- Li, J., Lin, S., Taube, F., Pan, Q., and Dittert, K., 2011.** Above and belowground net primary productivity of grassland influenced by supplemental water and nitrogen in Inner Mongolia. *Plant and Soil*, **340**: 253–264.

- Lin, G., Ehleringer, J.R., Rygielwicz, P., Johnson, M.G., Tingey, D.T., 1999.** Elevated CO₂ and temperature impacts on different components of soil CO₂ efflux in Douglas-fir terracosms. *Global Change Biology*, **5**, 157–168.
- Lloyd, J., Taylor, J.A., 1994.** On the Temperature dependence of soil respiration. *Functional ecology*, **8**: 315–323.
- Lohila, A., Aurela, M., Tuovinen, J.-P., and Laurila, T., 2004.** Annual CO₂ exchange of a peat field growing spring barley or perennial forage grass. *Journal of Geophysical Research: Atmospheres*, **109**, D18116.
- Longdoz, B., Yernaux, M., Aubinet, M., 2000.** Soil CO₂ efflux measurements in a mixed forest: impact of chamber disturbances, spatial variability and seasonal evolution. *Global Change Biology*, **6**: 907–917.
- Luo, Y., Hui, D., Cheng, W., Coleman, J.S., Johnson, D.W., Sims, D.A., 2000.** Canopy quantum yield in a mesocosm study. *Agricultural and Forest Meteorology*, **100**, 35–48.
- MacLeod, C.J., Moller, H., 2006.** Intensification and diversification of New Zealand agriculture since 1960: an evaluation of current indicators of land use change. *Agriculture, Ecosystems & Environment*, **115**, 201–218.
- Magid, J., Kjærgaard, C., 2001.** Recovering decomposing plant residues from the particulate soil organic matter fraction: size versus density separation. *Biology and Fertility of Soils*, **33**: 252–257.
- Macnicol, P.K., 1976.** Rapid metabolic changes in the wounding response of leaf discs following excision. *Plant Physiology*, **57**: 80–84.
- Manzoni, S., Schimel, J.P., Porporato, A., 2012.** Responses of soil microbial communities to water stress: results from a meta-analysis. *Ecology*, **93**: 930–938.
- Marschner, B., Brodowski, S., Dreves, A., Gleixner, G., Gude, A., Grootes, P.M., Hamer, U., Heim, A., Jandl, G., Ji, R., Kaiser, K., Kalbitz, K., Kramer, C., Leinweber, P., Rethemeyer, J., Schäffer, A., Schmidt, M.W.I., Schwark, L., and Wiesenberg, G.L.B., 2008.** How relevant is recalcitrance for the stabilization of organic matter in soils? *Journal of plant nutrition and soil science*, **171**: 91–110.
- McLauchlan, K.K., Hobbie, S.E., 2004.** Comparison of labile soil organic matter fractionation techniques. *Soil Science Society of America Journal*, **68**: 16161625.
- McSherry, M.E., and Ritchie, M.E., 2013.** Effects of grazing on grassland soil carbon: a global review. *Global Change Biology*, **19**: 1347–1357.
- McTiernan, K.B., Jarvis, S.C., Scholefield, D., Hayes, M.H.B., 2001.** Dissolved organic carbon losses from grazed grasslands under different management regimes. *Water Research*, **35**: 2565–2569.

- Meier, I.C., Leuschner, C., 2008.** Belowground drought response of European beech: fine root biomass and carbon partitioning in 14 mature stands across a precipitation gradient. *Global Change Biology*, **14**: 2081–2095.
- Midwood, A.J., Gebbing, T., Wendler, R., Sommerkorn, M., Hunt, J.E., Millard, P., 2006.** Collection and storage of CO₂ for ¹³C analysis: an application to separate soil CO₂ efflux into root- and soil-derived components. *Rapid Communications in Mass Spectrometry*, **20**: 3379–3384.
- Midwood, A.J., Thornton, B., Millard, P., 2008.** Measuring the ¹³C content of soil-respired CO₂ using a novel open chamber system. *Rapid Communications in Mass Spectrometry*, **22**: 2073–2081.
- Millard, P., Thomas, R.J., Buckland, S.T., 1990.** Nitrogen supply affects the remobilization of nitrogen for the regrowth of defoliated *Lolium perenne* L. *Journal of Experimental Botany*, **41**: 941–947.
- Millard, P., Midwood, A.J., Hunt, J.E., Whitehead, D., Boutton, T.W., 2008.** Partitioning soil surface CO₂ efflux into autotrophic and heterotrophic components, using natural gradients in soil δ¹³C in an undisturbed savannah soil. *Soil Biology & Biochemistry*, **40**: 1575–1582.
- Millard, P., Midwood, A.J., Hunt, J.E., Barbour, M.M., Whitehead, D., 2010.** Quantifying the contribution of soil organic matter turnover to forest soil respiration, using natural abundance δ¹³C. *Soil Biology & Biochemistry*, **42**: 935–943.
- Miller, R.W., Donahue, R.L., 1990.** Soils: an introduction to soils and plant growth. xiv + 768 pp.
- Moinet, G.Y.K., Cieraad, E., Rogers, G.N.D., Hunt, J.E., Millard, P., Turnbull, M.H., and Whitehead, D., 2016a.** Addition of nitrogen fertiliser increases net ecosystem carbon dioxide uptake and the loss of soil organic carbon in grassland growing in mesocosms. *Geoderma*, **266**: 75–83.
- Moinet, G.Y.K., Cieraad, E., Fraser, A., Turnbull, M.H., and Whitehead, D., 2016b.** Soil heterotrophic respiration is insensitive to changes in soil water content but related to microbial accessibility. *Geoderma* (In press).
- Monteith, J.L., 1981.** Climatic variation and the growth of crops. *Quarterly Journal of the Royal Meteorological Society*, **107**: 749–774.
- Monteith, J.L., and Moss, C.J., 1977.** Climate and the efficiency of crop production in Britain [and Discussion]. *Philosophical Transactions of the Royal Society of London B: Biological Sciences*, **281**: 277–294.
- Moyano, F.E., Manzoni, S., Chenu, C., 2013.** Responses of soil heterotrophic respiration to moisture availability: An exploration of processes and models. *Soil Biology & Biochemistry*, **59**: 72–85.
- Muchow, R.C., Sinclair, T.R., 1994.** Nitrogen response of leaf photosynthesis and canopy radiation use efficiency in field-grown maize and sorghum. *Crop Science*, **34**: 721–727.
- Mudge, P.L., Wallace, D.F., Rutledge, S., Campbell, D.I., Schipper, L.A., Hosking, C.L., 2011.** Carbon balance of an intensively grazed temperate pasture in two climatically contrasting years. *Agriculture, Ecosystems & Environment*, **144**: 271–280.

- Myers, B.J. (1988).** Water stress integral - a link between short-term stress and long-term growth. *Tree Physiology*, **4**: 315-324.
- Nakane, K., Kohno, T., Horikoshi, T., 1996.** Root respiration rate before and just after clear-felling in a mature, deciduous, broad-leaved forest. *Ecological Research*, **11**: 111–119.
- Nieveen, J.P., Campbell, D.I., Schipper, L.A., and Blair, I.J., 2005.** Carbon exchange of grazed pasture on a drained peat soil. *Global Change Biology*, **11**: 607–618.
- Ourry, A., Boucaud, J., Salette, J., 1988.** Nitrogen mobilization from stubble and roots during re-growth of defoliated Perennial Ryegrass. *Journal of Experimental Botany*, **39**: 803–809.
- Pachauri, R.K., Allen, M.R., Barros, V.R., Broome, J., Cramer, W., Christ, R., Church, J.A., Clarke, L., Dahe, Q., Dasgupta, P., others, 2014.** Climate Change 2014: Synthesis Report. Contribution of Working Groups I, II and III to the Fifth Assessment Report of the Intergovernmental Panel on Climate Change.
- Parfitt, R.L., Whitton, J.S., Theng, B.K.G., 2001.** Surface reactivity of A horizons towards polar compounds estimated from water adsorption and water content. *Australian Journal of Soil Research*, **39**: 1105–1110.
- Parsons, A.J., Leafe, E.L., Collett, B., and Stiles, W., 1983.** The physiology of grass production under grazing. i. characteristics of leaf and canopy photosynthesis of continuously-grazed swards. *Journal of applied ecology*, **20**: 117.
- Parsons, A.J., Penning, P.D., 1988.** The effect of the duration of regrowth on photosynthesis, leaf death and the average rate of growth in a rotationally grazed sward. *Grass and forage science*, **43**: 15–27.
- Paterson, E., Midwood, A.J., Millard, P., 2009.** Through the eye of the needle: a review of isotope approaches to quantify microbial processes mediating soil carbon balance. *New Phytologist*, **184**: 19–33.
- Pinheiro, J., Bates, D., DebRoy, S., Sarkar, D., 2014.** R Core Team. Nlme: linear and nonlinear mixed effects models. R package version 3.1–117 URL: <http://cran.r-project.org/web/packages/nlme/index.html>.
- Powlson, D.S., Gregory, P.J., Whalley, W.R., Quinton, J.N., Hopkins, D.W., Whitmore, A.P., Hirsch, P.R., Goulding, K.W.T., 2011.** Soil management in relation to sustainable agriculture and ecosystem services. *Food Policy*, **36**: S72–S87.
- Raun, W.R., Johnson, G.V., Phillips, S.B., Westerman, R.L., 1998.** Effect of long-term N fertilization on soil organic C and total N in continuous wheat under conventional tillage in Oklahoma. *Soil & Tillage Research*, **47**: 323–330.
- Raich, J.W., and Schlesinger, W.H., 1992.** The global carbon dioxide flux in soil respiration and its relationship to vegetation and climate. *Tellus B*, **44**: 81–99.

- Reich, P.B., Tjoelker, M.G., Pregitzer, K.S., Wright, I.J., Oleksyn, J., Machado, J.-L., 2008.** Scaling of respiration to nitrogen in leaves, stems and roots of higher land plants. *Ecological Letters*, **11**: 793–801.
- Rillig, M.C., and Mummey, D.L., 2006.** Mycorrhizas and soil structure. *New Phytologist*, **171**: 41–53.
- Rillig, M.C., Aguilar-Trigueros, C.A., Bergmann, J., Verbruggen, E., Veresoglou, S.D., and Lehmann, A., 2015.** Plant root and mycorrhizal fungal traits for understanding soil aggregation. *New Phytologist*, **205**: 1385–1388.
- Ritchie, J.T., and Nesmith, D.S., 1991.** Temperature and crop development. *Modeling plant and soil systems*, modelingplantan, 5–29.
- Rochette, P., Hutchinson, G., 2005.** Measurement of Soil Respiration in situ: Chamber techniques. Publ. USDA-ARS UNL Fac.
- Rogiers, N., Eugster, W., Furger, M., and Siegwolf, R., 2004.** Effect of land management on ecosystem carbon fluxes at a subalpine grassland site in the Swiss Alps. *Theoretical and Applied Climatology*, **80**: 187–203.
- Ross, K.A., 2009.** Cache-conscious query processing. In *Encyclopedia of Database Systems*, Springer, US, pp. 301–304.
- Rutledge, S., Mudge, P.L., Campbell, D.I., Woodward, S.L., Goodrich, J.P., Wall, A.M., Kirschbaum, M.U.F., and Schipper, L.A., 2015.** Carbon balance of an intensively grazed temperate dairy pasture over four years. *Agriculture, Ecosystems & Environment*, **206**: 10–20.
- Pinheiro J, Bates D, DebRoy S, Sarkar D and R Core Team, 2015.** nlme: Linear and nonlinear mixed effects models. R package version 3.1-122.
- Saggar, S., Parshotam, A., Hedley, C., and Salt, G., 1999.** ¹⁴C-labelled glucose turnover in New Zealand soils. *Soil Biology & Biochemistry*, **31**: 2025–2037.
- Saggar, S., and Hedley, C.B., 2001.** Estimating seasonal and annual carbon inputs, and root decomposition rates in a temperate pasture following field ¹⁴C pulse-labelling. *Plant and Soil*, **236**: 91–103.
- Schimel, D.S., House, J.I., Hibbard, K.A., Bousquet, P., Ciais, P., Peylin, P., Braswell, B.H., Apps, M.J., Baker, D., Bondeau, A., Canadell, J., Churkina, G., Cramer, W., Denning, A.S., Field, C.B., Friedlingstein, P., Goodale, C., Heimann, M., Houghton, R.A., Melillo, J.M., Moore, B., Murdiyarso, D., Noble, I., Pacala, S.W., Prentice, I.C., Raupach, M.R., Rayner, P.J., Scholes, R.J., Steffen, W.L., Wirth, C., 2001.** Recent patterns and mechanisms of carbon exchange by terrestrial ecosystems. *Nature*, **414**: 169–172.
- Schipper, Baisden, W.T., Parfitt, R.L., Ross, C., Claydon, J.J., Arnold, G., 2007.** Large losses of soil C and N from soil profiles under pasture in New Zealand during the past 20 years. *Global Change Biology*, **13**: 1138–1144.

- Schipper, Parfitt, R.L., Ross, C., Baisden, W.T., Claydon, J.J., Fraser, S., 2010.** Gains and losses in C and N stocks of New Zealand pasture soils depend on land use. *Agriculture, Ecosystems & Environment*, **139**: 611–617.
- Schipper, Dodd, M.B., Pronger, J., Mudge, P.L., Upsdell, M., and Moss, R.A., 2013.** Decadal changes in soil carbon and nitrogen under a range of irrigation and phosphorus fertilizer treatments. *Soil Science Society of America Journal*, **77**: 246256.
- Schipper, L.A., Parfitt, R.L., Fraser, S., Littler, R.A., Baisden, W.T., and Ross, C., 2014.** Soil order and grazing management effects on changes in soil C and N in New Zealand pastures. *Agriculture, Ecosystems & Environment*, **184**: 67–75.
- Schlesinger, W.H. 1977.** Carbon balance in terrestrial detritus. *Annual review of ecology and systematics*, 51–81.
- Schmidt, M.W.I., Torn, M.S., Abiven, S., Dittmar, T., Guggenberger, G., Janssens, I.A., Kleber, M., Kögel-Knabner, I., Lehmann, J., Manning, D.A.C., Nannipieri, P., Rasse, D.P., Weiner, S., and Trumbore, E.S., 2011.** Persistence of soil organic matter as an ecosystem property. *Nature*, **478**: 49–56.
- Semiring, H., Raun, W.R., Johnson, G.V., 1998.** Nitrogen accumulation efficiency: Relationship between excess fertilizer and soil-plant biological activity in winter wheat. *Journal of plant nutrition*, **21**: 1235–1252.
- Sinclair, T.R., Horie, T., 1989.** Leaf nitrogen, photosynthesis, and crop radiation use efficiency: A review. *Crop Science*, **29**: 9098.
- Six, J., Elliott, E.T., and Paustian, K., 1999.** Aggregate and Soil Organic Matter Dynamics under Conventional and No-Tillage Systems. *Soil Science Society of America Journal*, **63**: 13501358.
- Six, J., Elliott, E.T., Paustian, K., 2000.** Soil macroaggregate turnover and microaggregate formation: a mechanism for C sequestration under no-tillage agriculture. *Soil Biology & Biochemistry*, **32**: 2099–2103.
- Six, J., Conant, R.T., Paul, E.A., Paustian, K., 2002.** Stabilization mechanisms of soil organic matter: Implications for C-saturation of soils. *Plant and Soil*, **241**: 155–176.
- Six, J., Bossuyt, H., Degryze, S., and Deneff, K., 2004.** A history of research on the link between (micro)aggregates, soil biota, and soil organic matter dynamics. *Soil Tillage Research*, **79**: 7–31.
- Smith, P., Smith, J.U., Powlson, D.S., McGill, W.B., Arah, J.R.M., Chertov, O.G., Coleman, K., Franko, U., Frolking, S., Jenkinson, D.S., others, 1997.** A comparison of the performance of nine soil organic matter models using datasets from seven long-term experiments. *Geoderma*, **81**: 153–225.
- Snell, H.S.K., Robinson, D., Midwood, A.J., 2014.** Minimising methodological biases to improve the accuracy of partitioning soil respiration using natural abundance ¹³C. *Rapid Communications in Mass Spectrometry*, **28**: 2341–2351.

- Soussana, J.F., Allard, V., Pilegaard, K., Ambus, P., Amman, C., Campbell, C., Ceschia, E., Clifton-Brown, J., Czobel, S., Domingues, R., Flechard, C., Fuhrer, J., Hensen, A., Horvath, L., Jones, M., Kasper, G., Martin, C., Nagy, Z., Neftel, A., Raschi, A., Baronti, S., Rees, R.M., Skiba, U., Stefani, P., Manca, G., Sutton, M., Tuba, Z., Valentini, R., 2007.** Full accounting of the greenhouse gas (CO₂, N₂O, CH₄) budget of nine European grassland sites. *Agriculture, Ecosystems & Environment*, **121**: 121–134.
- Soussana, J.F., Tallec, T., and Blanfort, V., 2010.** Mitigating the greenhouse gas balance of ruminant production systems through carbon sequestration in grasslands. *Animal*, **4**: 334–350.
- Speckman, H.N., Frank, J.M., Bradford, J.B., Miles, B.L., Massman, W.J., Parton, W.J., and Ryan, M.G., 2015.** Forest ecosystem respiration estimated from eddy covariance and chamber measurements under high turbulence and substantial tree mortality from bark beetles. *Global Change Biology*, **21**: 708–721.
- Steinfeld, H., Gerber, P., Wassenaar, T., Castel, V., Rosales, M., Haan, C. de, 2006.** Livestock's long shadow: environmental issues and options. Food and Agriculture Organisation (xxiv + 390 pp).
- Stockmann, U., Adams, M.A., Crawford, J.W., Field, D.J., Henakaarchchi, N., Jenkins, M., Minasny, B., McBratney, A.B., Courcelles, V. de R. de, Singh, K., Wheeler, I., Abbott, L., Angers, D.A., Baldock, J., Bird, M., Brookes, P.C., Chenu, C., Jastrow, J.D., Lal, R., Lehmann, J., O'Donnell, A.G., Parton, W.J., Whitehead, D., Zimmermann, M., 2013.** The knowns, known unknowns and unknowns of sequestration of soil organic carbon. *Agriculture, Ecosystems & Environment*, **164**: 80–99.
- Subke, J.-A., Inglima, I., Francesca Cotrufo, M., 2006.** Trends and methodological impacts in soil CO₂ efflux partitioning: A metaanalytical review. *Global Change Biology*, **12**: 921–943.
- Thomas, H., 1984.** Effects of drought on growth and competitive ability of perennial ryegrass and white clover. *Journal of Applied Ecology*, **21**: 591–602.
- Thomsen, I.K., Hansen, E.M., 2014.** Cover crop growth and impact on N leaching as affected by pre- and postharvest sowing and time of incorporation. *Soil Use and Management*, **30**: 48–57.
- Tiessen, H., and Stewart, J.W.B., 1983.** Particle-size fractions and their use in studies of soil organic matter: II. Cultivation Effects on Organic Matter Composition in Size Fractions¹. *Soil Science Society of America Journal*, **47**: 509514.
- Tjoelker, M.G., Oleksyn, J., and Reich, P.B., 2001.** Modelling respiration of vegetation: evidence for a general temperature-dependent Q₁₀. *Global Change Biology*, **7**: 223–230.
- Trotter, C.M., Tate, K.R., Saggarr, S., Scott, N.A., Sutherland, M.A., 2004.** A multi-scale analysis of a national terrestrial carbon budget and the effects of land-use change. Global Environmental Change in the Ocean and Lands. TERRAPUB, Tokyo, pp. 311–341.
- Trumbore, S., 2000.** Age of soil organic matter and soil respiration: radiocarbon constraints on belowground C dynamics. *Ecological Applications*, **10**: 399–411.

- Valkama, E., Lemola, R., Känkänen, H., Turtola, E., 2015.** Meta-analysis of the effects of undersown catch crops on nitrogen leaching loss and grain yields in the Nordic countries. *Agriculture, Ecosystems & Environment*, **203**: 93–101.
- Vargas, R., Detto, M., Baldocchi, D.D., and Allen, M.F., 2010.** Multiscale analysis of temporal variability of soil CO₂ production as influenced by weather and vegetation. *Global Change Biology*, **16**: 1589–1605.
- Vargas, R., Baldocchi, D.D., Bahn, M., Hanson, P.J., Hosman, K.P., Kulmala, L., Pumpanen, J., and Yang, B. 2011.** On the multi-temporal correlation between photosynthesis and soil CO₂ efflux: reconciling lags and observations. *New Phytologist*, **191**: 1006–1017.
- Venables, W. N. & Ripley, B. D., 2002.** Modern applied statistics with S. Fourth Edition. Springer, New York.
- Von Lützw, M., Kögel-Knabner, I., Ekschmitt, K., Flessa, H., Guggenberger, G., Matzner, E., Marschner, B., 2007.** SOM fractionation methods: Relevance to functional pools and to stabilization mechanisms. *Soil Biology & Biochemistry*, **39**: 2183–2207.
- Wander, M., 2004.** **Soil organic matter fractions and their relevance to soil function.** Soil Organic Matter in Sustainable Agriculture. CRC Press, Boca Raton, FL 67–102.
- Wang, W., Fang, J., 2009.** Soil respiration and human effects on global grasslands. *Global and Planetary Change*, **67**: 20–28.
- Watt, M.S., Whitehead, D., Richardson, B., Mason, E.G., and Leckie, A.C., 2003.** Modelling the influence of weed competition on the growth of young *Pinus radiata* at a dryland site. *Forest Ecology and Management*, **178**: 271–286.
- Webster, K.L., Creed, I.F., Skowronski, M.D., and Kaheil, Y.H., 2009.** Comparison of the performance of statistical models that predict soil respiration from forests. *Soil Science Society of America Journal*, **73**: 1157.
- Willson, T.C., Paul, E.A., Harwood, R.R., 2001.** Biologically active soil organic matter fractions in sustainable cropping systems. *Applied Soil Ecology*, **16**: 63–76.
- Yan, D., Wang, D., and Yang, L., 2007.** Long-term effect of chemical fertilizer, straw, and manure on labile organic matter fractions in a paddy soil. *Biology and Fertility of Soils*, **44**: 93–101.
- Yan, L., Chen, S., Huang, J., and Lin, G., 2010.** Differential responses of auto- and heterotrophic soil respiration to water and nitrogen addition in a semiarid temperate steppe. *Global Change Biology*, **16**: 2345–2357.
- Zakharova, A., Beare, M.H., Cieraad, E., Curtin, D., Turnbull, M.H., Millard, P., 2015.** Factors controlling labile soil organic matter vulnerability to loss following disturbance as assessed by measurement of soil-respired $\delta^{13}\text{C}\text{O}_2$: Factors controlling labile SOM vulnerability to loss. *European Journal of Soil Science*, **66**: 135–144.

- Zakharova, A., Midwood, A.J., Hunt, J.E., Graham, S.L., Artz, R.R.E., Turnbull, M.H., Whitehead, D., Millard, P., 2014.** Loss of labile carbon following soil disturbance determined by measurement of respired $\delta^{13}\text{CO}_2$. *Soil Biology and Biochemistry*, **68**: 125–132.
- Zhang, L., Guo, H., Jia, G., Wylie, B., Gilmanov, T., Howard, D., Ji, L., Xiao, J., Li, J., Yuan, W., Zhao, T., Chen, S., Zhou, G., Kato, T., 2014.** Net ecosystem productivity of temperate grasslands in northern China: an upscaling study. *Agricultural and Forest Meteorology*, **184**: 71–81.
- Zhou, X., Fei, S., Sherry, R., Luo, Y., 2012.** Root biomass dynamics under experimental warming and doubled precipitation in a tallgrass prairie. *Ecosystems*, **15**: 542–554.
- Zsolnay, Á., 2003.** Dissolved organic matter: artefacts, definitions, and functions. *Geoderma*, **113**: 187–209.

APPENDIX A Back extrapolation approach to estimate $\delta^{13}CR_H$

During the study presented in chapter 4, in the summer measurement campaign, soil cores were excavated for analysis of $\delta^{13}CR_H$ as described by Zakharova et al. (2014). A of 100 mm diameter steel tube was hammered into the soil to a depth of 200 mm and the core removed. The soil from the core was broken up loosely and roots and stones were removed by hand and discarded. The root-free soil was placed into air tight bags (Tedlar® Keika Ventures, Chapel Hill, NC, USA). The bags were sealed then flushed quickly three times and filled with approximately 500 ml of CO₂ free air. An aliquot of gas was removed and the CO₂ partial pressure checked to make sure it fell within the range 250-750 $\mu\text{mol mol}^{-1}$ for analysis. Two sets of 12 cores were incubated and compared. The first set was sampled at 4, 7.5 and 10 min and the second set at 5, 7.5 and 10 min. This allowed testing for potential differences in the kinetics of the exponential decrease in $\delta^{13}CR_H$ between treatments, as well as comparing values of $\delta^{13}CR_H$ sampled at 4 and 5 min. If the CO₂ partial pressure in the bag was lower than 250 $\mu\text{mol mol}^{-1}$ when it was first measured at either 4 or 5 min, another core was excavated from the same plot and the operation repeated.

The decrease in $\delta^{13}CR_H$ during the incubation of root-free soil was modelled as an exponential decay function using non-linear, mixed-effect models in the 'nlme' package (Pinheiro and Bates, 2014) using R version 3.2.1 (R Development Core Team, 2014) as:

$$\delta^{13}CR_H = a + be^{-ct} \quad (\text{A1})$$

where a is the steady-state value of $\delta^{13}CR_H$, b is the difference between a and the value of $\delta^{13}CR_H$ at incubation time zero, c characterises the shape of the curve and t is the incubation time. To account for non-independence of repeated measurements through time, the replicate number was included as a random effect and an autocorrelation function was included in each model. To determine whether one or a combination of the coefficients differed between replicates, the best random structure for the model was determined based on comparison of Akaike's Information Criterion corrected for small sample size (AICc), the model with the lowest AICc being the most strongly

supported. The initial incubation time, t_i , was then introduced to separate the group of replicates measured from 4 min from the group measured from 5 min. Models with different and the same coefficients for the two groups where t_i was different were compared using AICc. The same procedure was repeated for the irrigation (I_0 or I_1) and nitrogen addition (N_0 or N_1) treatments.

The best random structure in the exponential decrease model describing the changes in $\delta^{13}CR_H$ with time during the incubation period showed that only parameter a was different between the replicates, confirming that the form of the curve was the same for all replicates. There were no significant differences between the parameters describing the changes in $\delta^{13}CR_H$ for different nitrogen or irrigation treatments or for different plots. Further, there were no significant differences between the parameters describing the changes in $\delta^{13}CR_H$ from samples incubated from 4 min onwards, compared with the samples incubated from 5 min onwards (Fig. 1). This showed that the average value at 4 min was more enriched than the average value at 5 min. This confirmed that back extrapolation of the $\delta^{13}CR_H$ values to 4 min was valid. It was possible to estimate the parameter a_j for each replicate j from the measured value of $\delta^{13}CR_H$ at time q (5 min or more) and the parameters b and c , common to all replicates, from

$$a_j = \delta^{13}CR_{H,qmin} - be^{-cq} \quad (A2)$$

The set of parameters for the exponential decay of $\delta^{13}CR_H$ is, however, site specific and likely to depend on soil structure (Zakharova et al., 2014) and could vary with season (Snell et al., 2014). While these parameters did not differ between treatments in my study, they will need to be assessed for individual site and experimental conditions in future studies.

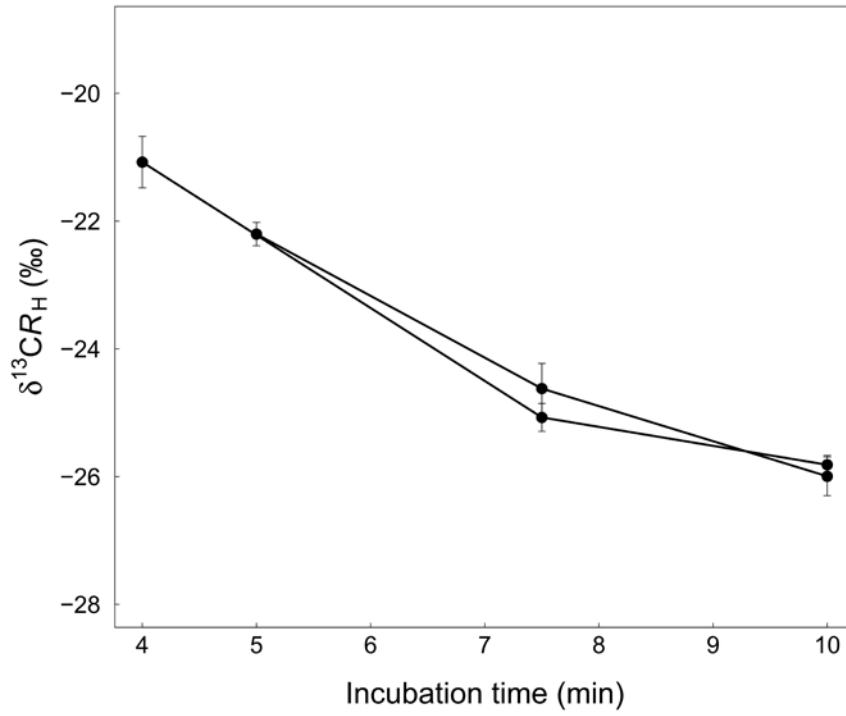


Figure A: Isotopic signature of respired CO₂ from root-free soil, $\delta^{13}CR_H$, in response to time for root-free soils incubated at 4, 7.5 and 10 min and at 5, 7.5 and 10 min. The vertical bars indicate standard errors of the mean.